A black carbon source apportionment study in central Stockholm with special attention to road traffic emissions

by Jennie Hurkmans

Master's Degree Project in Environmental Science, 45 HTC

Department of Environmental Science and Analytical Chemistry (ACES), Stockholm University

June 2015

Supervisor:
Christer Johansson
Assistant supervisor:
Michael Norman

Abstract

Residential biomass combustion may be an important source of particulate matter in urban areas; even in centers of large cities with dense traffic. For the first time in Sweden, the contributions of fossil fuel (FF) and wood burning (WB) emissions to black carbon (BC) have been investigated using data from a multi-wavelength aethalometer (model AE31). It measures the light attenuation of seven wavelengths simultaneously allowing studying aerosols with abundant organic materials which also absorb light, but mainly at shorter wavelengths, so called brown carbon. The fact that brown carbon absorbs light more efficiently in the short wavelengths while BC show weak spectral dependence, leads to the possibility to separate sources of carbonaceous aerosols. This study utilizes the wavelength dependence to separate the contribution to BC from the major sources in Stockholm; traffic and residential biomass combustion, assuming that the brown carbon is mainly associated with biomass combustion. We used data from the urban sites Hornsgatan (urban street canyon) and Torkel (urban background) during Nov 2012 to June 2014. The contribution of FF and WB to BC was determined from the aerosol absorption coefficients of FF and WB aerosols, calculated using Ångström exponents and site specific mass absorption cross sections, determined by separation between organic carbon (OC) and elemental carbon (EC) using a thermal optical transmission (TOT) method. The results indicate that BC from WB contributes on average 34 ± 6 % and 16 ± 6 % to total BC at Torkel and Hornsgatan, respectively. The WB contribution showed a clear annual trend increasing in winter and decreasing in summer. Highest contributions to PM2.5 were found for BC from FF during daytime at Hornsgatan reaching a value of 17 %, while the contribution from WB was highest at Torkel during winter (Dec – Feb) with 5 %. Generally, the contribution of BC from WB to PM2.5 was twice as high at Torkel compared to Hornsgatan. The used approach was supported by high correlation (R = 0.82) between FF contributions to BC and NOx (good marker of vehicle exhaust), while WB contributions to BC showed lower correlations with NOx (R = 0.44). Known biomass fire events like the bonfire on April 30 showed a dominating contribution from WB and illustrated a nicely separation between the two sources.

Correlation between local BC and particle size at Hornsgatan reached a peak at about 80 nm (R = 0.66). The correlation with particles below 80 nm were lower and decreased drastically for particle sizes above 150 nm, indicating that most traffic related BC particles at Hornsgatan are in the size interval of 50 – 150 nm, where 64 % (53 – 80 %) of the total mass of exhaust particles in this size range would be BC particles. In the past, NOx or particle number concentrations have been used as an indicator of the contribution from combustion particle emissions from road traffic vehicles, but now measurements indicate that the trends are very different. In recent years the number of diesel vehicles in traffic in Sweden has increased rapidly and this raises concerns as diesel engine exhaust has been classified as carcinogenic to humans. A possibility is that BC can be used as a good marker for combustion sources, especially for diesel exhaust. In this study four different approaches were used to evaluate the possibilities for estimation of BC EF's for local road traffic in Stockholm. The measurements of NOx concentration in ambient local air at Hornsgatan was found to decrease much less than expected from the calculated vehicle-km weighted HBEFA NOx EF, indicating an underestimation of the NOx EF. The NOx based BC EF showed result highly in line with the trend in local BC concentration giving a potential to be a reliable way of estimating BC EF's from local air measurements of BC and NOx, combined with HBEFA NOx EF. The measured concentration of NOx and BC in ambient local air indicated that BC is decreasing much faster than NOx, and more in line with both the NOx based BC EF and the TRANSPHORM fraction BC EF, than the TRANSPHORM absolute BC EF.

Table of content

1 Introduction

1.1 Background

An abundant constituent of atmospheric aerosols is carbonaceous matter (CM) that consists of elemental carbon (EC) and organic carbon (OC). Black carbon (BC) is the light absorbing part of CM and commonly referred to as soot (EEA, 2013).

Exposure to BC has negative effects on human health (Grahame et al, 2014), contributes to climate change and poor air quality (WHO, 2012a). BC is a fraction of $PM_{2.5}$ (particulate matter with diameter smaller than 2.5 µm) that has often been considered as among the most harmful air pollutants. A broad range of human health impacts are related to both short-term (24h) and long-term (annual) exposure to PM, inter alia respiratory and cardiovascular effects and premature death (EEA, 2013). Today evidence is indisputable for a link between adverse health effects and $PM_{2.5}$ in ambient air (Pope et al., 2002; Jerret et al., 2005; WHO, 2013). In 2011, EU researchers also found that life expectancy could be extended four to nine times by reducing a unit of BC, vs reducing a unit of $PM_{2.5}$ (Grahame et al, 2014). The main route of exposure to air pollution is by breathing and BC aerosols are usually small enough to be transported into the human lungs and can therefore act as transporters of much more harmful compounds into the body's´ pulmonary system (WHO, 2012a; Kristensson et al., 2013).

BC has been estimated to be the second most important contributor to global warming, after CO_2 (Ramanathan et al., 2008; UNEP/WMO, 2011; Bond et al., 2013). The particles have a large optical absorption cross section and can absorb both infrared and visible light, which increases the net absorption optical depth leading to disruption in the solar radiation balance (warming of the Earth's atmosphere) (EEA, 2013). The size of BC particles is an important factor for the climate forcing potential effect of BC (Ramanathan et al., 2008). Changes in the climate system leads to impacts on humans, plants and ecosystems (EEA, 2013). Current air quality standards for PM in the EU and those recommended by WHO use the PM mass concentration as a metric, but the Directive 2008/50/EC of the European Parliament and of the Council of 21 May 2008 on ambient air quality and cleaner air for Europe (AQ Directive; EC, 2008) sets a minimum requirement for background monitoring of PM that includes a chemical speciation of $PM_{2.5}$ mass (i.e. analysing the amount of EC and OC content of the particles).

BC is a particulate pollutant species emitted from the combustion of any carbonaceous fuel and has two major emission sources; diesel engines and biomass burning (EEA, 2013). Especially in winter, wood combustion from residential heating has been found to be a major contributor to total BC, even in large cities like Zürich (Herich et al., 2011). Residential wood combustion has been associated with adverse health effects in epidemiological studies (Barregard et al., 2006; Sehlstedt et al., 2010) but there is insufficient evidence available to decide whether particles from wood combustion are more or less harmful than diesel derived particles. However, BC particles from vehicle exhaust has been found to be smaller than those from combustion of biomass (Gramsch et al., 2014; Schwarz et al., 2008) and the breathable dose of particles are often not linearly related to particle concentration since the deposition in the

respiratory tract can vary substantially depending on the particle source. Deposition is a function of several parameters; concentration, particle size distribution, hygroscopic growth ability, density, breathing pattern and lung morphology (Kristensson et al., 2013). However, the current practice is to treat fine particles ($PM_{2.5}$) as equally harmful irrespective of origin (WHO, 2013).

The physical and chemical characteristics of BC aerosols close to the emission source can vary a lot in size and surface, especially between traffic and wood burning sources, but also between different vehicles and different wood stoves. The emission factor (EF), grams of BC emitted per gram of carbon consumed in the fuel, varies depending on the combustion process and makes it hard to predict the emissions of BC. Once BC has been emitted from the source it undergoes physical changes (Giechaskiel et al., 2014) but is still considered to be chemically stable. BC in diesel exhaust is in the form of small spherules with a radius of 15 – 30 nm. Once they are released from tailpipe they agglomerate and form chain structures of soot particles that consist of primary carbonaceous particles together with volatile organic and inorganic constituents (Ning et al., 2013). BC aerosols have a great porosity and the ability to absorb other species from the vapour phase, especially organics. Different combustion processes generates different size distributions. The mean size of atmospheric BC aerosols has been found to increase with the distance from the traffic emission source (Chakrabarty et al., 2006) due to the agglomeration, condensation of hydrocarbons and mixing with larger BC particles generated from other sources than traffic (residential wood combustion) (Gramsch et al., 2014). BC in urbanized areas originates from both local emissions sources and is a part of the regional background pollution due to transportation from more distant sources (Jönsson et al., 2013; Targino et al., 2012). Ning et al. (2013) showed differences in the characteristics of fresh and aged BC particles that confirmed the evolution of these particles going from source emission to atmosphere with internal or external mixing by for example sulfate, nitrate and organics. At Hornsgatan diesel vehicles represents a large share of the total emissions of particles in the size range for vehicle exhaust. Nearly all diesel particulates have sizes of significantly less than 1 µm and represent a mixture of fine, ultrafine and nanoparticles and includes both solids (e.g. EC and ash) and liquids (e.g. condensed hydrocarbons, water, sulphuric acid). Gasoline engine particles are characterized by generally smaller sizes than those from diesel engines (TRANSPHORM, 2013).

Although vehicles have become cleaner, as a result of more efficient after treatment of exhausts and improved fuel efficiency, there are still several mechanisms that are hard to control. An additional problem is the growing number of vehicles. In Stockholm, the growth rate in registered vehicles is about 2 % per year (Transport Analysis Vehicle Statistics, 2005-2014, figure A19 in Appendix), and this growth is accompanied with a fuel shift for passenger cars from gasoline to diesel (diesel vehicles emitting more NOx than gasoline vehicles) (SLB 7:2010, fig. 21 and 22). Nitrogen oxides species (NOx) is sometimes used as an indicator of health effects due to exposure to vehicle exhaust particles. This is due to the lack of PM-exhaust measurements and less known EF's for PM-exhaust as compared to NOx. But trends in concentrations measured at traffic influenced sites indicate that the relation between NOx and PM-exhaust is changing drastically. This is due to the changing vehicle fleet, with different

NOx and PM-exhaust emissions due to different technologies applied, largely depending on fuel. BC has the potential to be an excellent marker for combustion sources, especially for diesel exhaust that has been classified as a human carcinogen by World Health Organisation (WHO, 2012b), but still there are no regulations for BC (even though WHO in 2012 suggested creating a public health standard for airborne BC). EF's for unregulated pollutants is connected with larger uncertainties than the regulated pollutants since both emission measurements and ambient concentration measurements of these pollutants are not as common as for the regulated pollutants.

In recent years the number of diesel vehicles in traffic in Sweden has increased rapidly and this raises concerns as diesel engine exhaust has been classified as carcinogenic to humans (IARC, 2012). Even though there is legislation that regulates total exhaust particle emissions, there are no limit values for the concentrations in ambient air. In addition, there are no methods for measuring ambient combustion particles (PM-exhaust); $PM_{2.5}$ and PM_{10} include many other source contributions, not only combustion particles. In the past, NOx or particle number (PN) concentrations has been used as an indicator of the contribution from combustion particle emissions from road traffic vehicles, but now measurements indicate that the trends are very different; NOx concentrations at e.g. Hornsgatan in Stockholm tend to increase while PN is decreasing. For BC trends are less clear with an increase in the urban background and decrease at Hornsgatan (SLB, 2015).

1.2 Aim

To be able to distinguish BC aerosols from different sources is a prerequisite for decision-makers to take the optimal actions to reduce human exposure and adverse health effects. The overall objective of this thesis work is therefore to assess the importance of road traffic and residential wood combustion on the BC concentrations by a source apportionment study, but also to further analyse the importance of the increasing diesel vehicle fleet for BC concentrations in Stockholm (Hornsgatan). The hope is that this work will contribute to the knowledge of the importance of BC particle sources in Stockholm and how the vehicle shift with increased diesel vehicles may affect the emissions of BC from local road traffic at Hornsgatan.

Specific aims of this study are

- to quantify the contribution to BC from wood burning and fossil fuel sources in central Stockholm, using multi-wavelength AE data at two sites together with the aethalometer model. The approach will be to utilize the aerosol spectral dependence to determine the contribution of wood burning (WB) and fossil fuel (FF) emissions to total BC (Herich et al., 2011).
- to assess the importance of the increasing diesel vehicle fleet for BC concentrations in Stockholm (Hornsgatan).
- to determine the size of the BC particles,
- to investigate how emissions of BC from local road traffic has changed due to the fuel shift from gasoline to diesel and finally,
- to compare different ways of estimating EF's for BC.

2 Method

2.1 Spectral dependence

There are several commercial instruments that can be used to determine BC in PM. One of them is the aethalometer (AE, Hansen et al., 1984), where the contributions of fossil fuel (FF) and wood burning (WB) emissions to BC can be investigated by analysis of multi-wavelength aethalometer data. The reason why it is possible to do a BC source apportionment is due to the difference in spectral dependence between combustion related aerosols. This in turn depends on the ratio between organic materials (OM) and BC in the combusted aerosols. Wood smoke contains a high fraction of OM such as polycyclic aromatic hydrocarbons (PAHs), aromatics and humic-like substances (HULIS) (Kochbach et al., 2006), so called brown carbon which also absorbs light. The brown carbon has a high spectral dependence and absorbs light more efficiently at shorter wavelengths compared to longer. Traffic emission aerosols contain less OM and have instead a higher fraction of BC and the absorption is therefore more evenly distributed over the spectra. This leads to a much higher spectral dependence for WB aerosols (depending on the amount of brown carbon) compared to the weaker spectral dependence for FF related aerosols and therefore give a possibility to distinguish between carbonaceous aerosols from different sources. It is also important to clarify that the aethalometer measures the amount of light absorbing material (BC and OC (i.e. brown carbon)) but it is all classified as BC. This means that the spectral dependence can vary even though the amount of BC is the same. A limitation of using the spectral dependence for source apportionment might be the presence of particles, except OM, having the ability to absorb strongly in the UV-spectra, e.g. mineral dust particles (EEA, 2013), giving rise to an enhanced UV-spectra absorption that is not created by BC particles.

2.2 Sampling sites

Measurements were conducted at the sites Torkel Knutssonsgatan (Torkel) and Hornsgatan at Södermalm in central Stockholm. Torkel is an urban background site located at a roof top 20 m above ground level (figure 1) while Hornsgatan (figure 2) is an urban street canyon site which is densely trafficked with an average traffic volume of about 20 000 vehicles/weekday. Hornsgatan is located about 450 m north-west of Torkel. The difference between the two sites is expected to be contributions mainly from the traffic at Hornsgatan.

Fig. 1. *Urban background site Torkel.*

Fig. 2. *Urban street canyon site Hornsgatan.*

2.3 Time periods and instrumentation specifications

Depending on the different parts of this study the time period and instrumentation differ:

- **BC source apportionment (using the optical attenuation method)**
  Simultaneous measurements at Hornsgatan and Torkel from Nov 2012 to June 2014 by the use of an aethalometer (model AE31, Magee Scientific, Berkeley, California, USA, figure A13 in appendix).
- **OC/EC sampling and analysis**
  Field study campaign at Torkel from Oct 7 to Oct 24 2014 by the use of a low volume sampler (Comde - Derenda, type PNS 16T-3.1, Germany, figure A2 and A3 in appendix). The analysis was carried out in the laboratory at ACES, Stockholm University using a Thermal/Optical Carbon Aerosol Analyzer (Sunset Laboratory Inc., Forest Grove, USA, figure A12 in appendix).
- **Investigation of the particle number size distribution**
  Measurements at Hornsgatan from Oct 2007 to Dec 2014 using a Differential Mobility Particle Sizer (DMPS) (made by ACES, Stockholm University, Sweden, according to a European standard, EUSAAR).
- **Investigation of the BC particle size distribution**
  Done for the same time period as the BC source apportionment, Nov 1012 to June 2014. For this investigation the aethalometer AE31 was used together with the DMPS used for the particle number distribution.

- **BC emission factors for local traffic at Hornsgatan**
  Measurements of CO_2 at Hornsgatan and Torkel from 2014 Oct 14 to 2015 May 11 using a Carbon Dioxide Probe (model GMP343, Vaisala CARBOCAP, Helsinki, Finland, figure A15). The CO_2 probe is linked to an aethalometer (model AE33, Magee Scientific, Slovenia, figure A14 in appendix) giving the data for the BC mass concentration used for the CO_2 approach. NOx is continuously measured at both Hornsgatan and Torkel and data has been taken from 2006 to present. These measurements are done using a Chemiluminescence Analyser (model AC 32 M (Torkel), model AC 31 M (Hornsgatan), Environment S.A, France, figure A16 and A17 in appendix). For the NOx approach BC mass concentrations are given by the AE31.

2.4 Instrumentation principles and measurement procedures

2.4.1 The optical attenuation method

The aethalometer (AE) was first described by Hansen et al. (1984). The AE is an instrument for measurement of aerosol particles and the name itself are derived from the Greek word "aethaloun" which means "to blacken with soot". The principle of the AE is to measure the attenuation of a beam of light transmitted through a filter while the filter is continuously collecting an aerosol particulate matter (PM) sample. The filter gets loaded with particles through an air flow with constant velocity. The deposition rate of BC on the filter is linearly proportional to its concentration within the aerosol and therefore the optical attenuation will increase as the aerosol load of the filter increases. The optical attenuation through the filter is defined as

$$\mathrm{ATN} \equiv \ln\left(\frac{I_0}{I}\right) \qquad (1)$$

where I_0 is the intensity of the incoming light and I is the remaining light intensity when transmitted through the filter while its loaded with aerosol particles.

An aethalometer (model AE31 and older) measure the light attenuation through a quartz filter collecting the light-absorbing particles. Two detectors monitor the light transmission through the filter where one measures the light passing through the sample spot while the other measures the light passing through a spot that is kept free from particles (reference part) (Weingartner et al., 2003). This procedure corrects for variations in incident light intensity and drift in electronics (Sandradewi et al., 2008b). Using an AE31 model the aerosols are deposited on a 1.67 cm^2 collection area of a quartz filter tape (organic and inorganic fibers, Q250F, Pall Corporation). AE31 has a $PM_{2.5}$ sample inlet and a sample flow rate of 3.9 L min^{-1}. The particles are collected on such a fiber tape whose deep mat of optically-scattering fibers ensures that the instrument responds only to optically-absorbing particles, not to optically-scattering particles (Magee Aethalometer handbook AE31, 2005).

The attenuation coefficient of the particles collected on the filter (b_{ATN}) is calculated as

$$b_{ATN} = \frac{A}{Q}\frac{\Delta ATN}{\Delta t} \qquad (2)$$

where A is the filter collection area, Q is the air flow rate, Δt is the time interval, and ΔATN is the change in attenuation during Δt. Particles loaded on a filter has some different properties compared to particles in ambient air. Therefore b_{ATN} need to be corrected for instrumental artefacts to be converted into the absorption coefficient of particles in airborne state (b_{abs} (λ)).

In this study a seven wavelength AE has been collecting data at two measuring sites since Oct 2012 until June 2014. The AE continuously detects and gives as an output the wavelength dependent aerosol attenuation coefficient of the collected aerosol particles, b_{ATN} (λ) at given wavelengths (370, 470, 520, 590, 660, 880 and 950 nm). The time resolution is 15 min averaged into 1 hour mean values.

In order to calculate the aerosol light absorption coefficient, b_{abs} (λ) (unit of m^{-1}), b_{ATN} (λ) needs to be corrected for sampling artefacts (Weingartner et al., 2003; Sandradewi et al., 2008a). The first artefact occurs when the filter is relatively clean and unloaded with particles. This allows for the light beam to be scattered within the filter fibers (multiple scattering) and affect the intensity I which leads to enhanced light absorption (Liousse et al., 1993). The second artefact occurs when the filter gets highly loaded with particles and the light absorbing particles in the filter starts to absorb a higher fraction of the scattered light, which is called shadowing effect. Correcting for these artifacts the optical properties that the particles have in the airborne state is restored.

One method to correct for these artefacts was developed by Weingartner et al. (2003) (used by Sandradewi et al., 2008a; Sandradewi et al., 2008b; Herich et al., 2011) who calculated b_{abs} (λ) using

$$b_{abs}(\lambda) = \frac{b_{ATN}(\lambda)}{C \times R\,(ATN_{\lambda})} \qquad (3)$$

A constant factor of C = 2.14 was empirically determined using Palas soot, diesel soot and diesel soot mixed with $(NH_4)_2SO_4$ particles with known absorption coefficient in AIDA aerosol chamber experiments (Weingartner et al., 2003).

The correction of the shadowing effect is somewhat more difficult. Weingartner et al. (2003) used an empirical function R of the measured light ATN at the different wavelengths according to

$$R\,(ATN_{\lambda}) = \left(\frac{1}{f_{\lambda}} - 1\right)\frac{\ln(ATN_{\lambda}) - \ln(10\%)}{\ln(50\%) - \ln(10\%)} + 1 \qquad (4)$$

that varies with the amount of aerosol particles collected on the filter and the optical properties of these particles. In eq. (4) R (ATN_{λ}) is a linear function of ln (ATN) and f_{λ} is a free parameter that relates to the slope. By variation in f_{λ} it is possible to do an estimation of the instrumental error occurring when the shadowing effect is disregarded.

Sandradewi et al. (2008b) calculated f_{λ} values by minimizing the difference between the b_{ATN} values before and after a filter spot change. The calculated median f_{λ} values were then plotted as a function of λ and fitted with a linear equation. One approach is to use the same f values as Sandradewi et al. (2008b) (done by e.g. Herich et al. (2011)) but in this study site specific f_{λ}

values were calculated for Hornsgatan and Torkel using the mean values of the two b_{ATN} values before and after a filter spot change. Table 1 summarizes the linearized f_λ values that were applied for the calculation of b_{abs} (λ).

Table 1. *f_λ values used for calculating R (ATN_λ) – correction of the shadowing effect. Values calculated for Hornsgatan and Torkel using the mean values of the two b_{ATN} values before and after a filter spot change.*

Wavelength λ (nm)	**370**	**470**	**520**	**590**	**660**	**880**	**950**
f_λ value Hornsgatan	1.37	1.30	1.26	1.23	1.21	1.15	1.14
f_λ value Torkel	1.37	1.23	1.16	1.11	1.06	0.99	0.97

The fitting parameter f_λ has been found to vary depending on aerosol type and mixing state. Weingartner et al. (2003) found the highest f_λ values for fresh pallas and diesel soot (1.6 to 1.93) and lower values for aged and internally mixed aerosols.

Newer AEs (model AE33) has an in-built technique which automatically corrects for the shadowing effect (Aethalometer Model AE33 User Manual, 2014). The exact knowledge of empirical calibration values C and R is of high importance for the derivation of correct values of b_{abs} (λ) (Weingartner et al., 2003). However, there are also studies that shows that the optical attenuation method provides an accurate measure of the variation in aerosol absorption with wavelength and that the above artefacts only have a minor impact on the measured spectral dependence of aerosol light absorption (Bond, 2001; Horvath et al., 1997)

The wavelength dependence in light absorption is commonly given by a power law relationship

$$b_{abs}(\lambda) \propto \lambda^{-\alpha} \qquad (5)$$

where λ is the wavelength and α the absorption Ångström exponent (Kirchstetter et al., 2004). For a constant $\alpha > 1$, b_{abs} (λ) increases with shorter wavelengths and that is the basis for the possibility to separate the sources for particles containing light absorbing material (BC and OC).

By using the relationship (5), equations relating b_{abs}, λ and α can be set up for conditions of pure fossil fuel (FF) and pure wood burning (WB) conditions (Sandradewi et al., 2008a).

$$\frac{b_{abs}(470nm)_{FF}}{b_{abs}(950nm)_{FF}} = \left(\frac{470nm}{950nm}\right)^{-\alpha_{FF}} \qquad (6)$$

$$\frac{b_{abs}(470nm)_{WB}}{b_{abs}(950nm)_{WB}} = \left(\frac{470nm}{950nm}\right)^{-\alpha_{WB}} \qquad (7)$$

$$b_{abs}(\lambda) = b_{abs}(\lambda)_{FF} + b_{abs}(\lambda)_{WB} \qquad (8)$$

For given values of α_{FF} and α_{WB} together with the field data of the light absorption measurements at 470 and 950 nm, values for $b_{abs}(470nm)_{FF}$, $b_{abs}(950nm)_{FF}$, $b_{abs}(470nm)_{WB}$, and $b_{abs}(950nm)_{WB}$ can be computed using eq. 6-8. The approach is to use one low and one high wavelength to be able to capture the spectral dependence in light absorption to the fullest. In this study 470 and 950 nm were used due to uncertain data for the 370 nm wavelength.

According to Sandradewi et al. (2008a) there should be no difference using any of the three lowest wavelengths. The equation for computing $b_{abs}(470nm)_{WB}$ is

$$b_{abs}(470nm)_{WB} = \frac{b_{abs}(470nm) - (\frac{470}{950})^{-\alpha_{FF}} \, x \, b_{abs}(950nm)}{1 - \frac{(\frac{470}{950})^{-\alpha^{FF}}}{(\frac{470}{950})^{-\alpha^{WB}}}} \qquad (9)$$

and $b_{abs}(950nm)_{WB}$, $b_{abs}(470nm)_{FF}$ and $b_{abs}(950nm)_{FF}$ can be computed in the same way.

Aerosols from combustion of biomass have been found to have a strong spectral dependence ($\alpha > 2$) while aerosols from fossil fuel combustion show less spectral dependence ($\alpha \sim 1$) (e.g. Sandradewi et al., 2008a; Kirchstetter et al., 2004; Day et al., 2006; Schnaiter et al., 2005). The α value for pure traffic conditions has been found to be close to 1 (according to previous studies (Herich et al., 2011; Kirchstetter et al., 2004; Sandradewi et al., 2008a), while the difference in spectral dependence for wood burning depends on the wood type and combustion process resulting in a much wider range. Table 2 show α values, used in or derived by previous studies, which are found to be representative for general reported values of α_{FF} or α_{WB}.

Table 2. *Representative α values found in the literature.*

Reference	**α value**		
	FF	**WB**	
Herich et al., 2011	0.9	1.9	
Sandradewi et al., 2008a	1.1	1.86	
Favez et al., 2010	1.0	2.0	
	Content	**Spectral range (nm)**	**α value**
Kirchstetter et al., 2004	Auto exhaust	300-1000	1.0
	Biomass burning	300-1000	2.0
Schnaiter et al., 2006	Soot OC < 20%	200-1000	1.0
Schnaiter et al., 2003	Diesel soot	450-700	1.1
Schnaiter et al., 2006	Soot OC ≈ 50%	200-1000	2.2-3.5
Clarke et al., 2007	Biomass smoke	467-660	2.1
Day et al., 2006	Cotton wood	370-950	2.1
	Oak	370-950	1.8

The absorption Ångström exponent α was calculated by linear regression over all seven wavelengths. In this study the value for α_{FF} were determined by the difference between Hornsgatan and Torkel, which is assumed to be a pure traffic signal. A mean value of 0.86 ± 0.03 was calculated for α_{FF} with a monthly variation according to figure A1 in appendix. This calculation together with values of α_{FF} in previous studies resulted in $\alpha_{FF} = 0.9$ for this study.

The calculation approach of equation 9 resulted in some percentage of negative values of the aerosol absorption coefficient for $b_{abs}(\lambda)_{WB}$ and $b_{abs}(\lambda)_{FF}$. A sensitivity analysis of α_{FF} (0.9 – 1.1) and α_{WB} (1.7 – 2.3) showed the amount of negative values resulting from equation 9 (table T1 in appendix) at Hornsgatan and Torkel. According to previous studies in table 2, α_{WB} is assumed to be around 2. This, together with the sensitivity analysis, were the base for the determination of $\alpha_{WB} = 2.0$ for this study.

In the final step, the BC mass concentration (µg m^{-3}) is determined by division of b_{abs} (λ) (m^{-1}) by σ_{abs} (λ) (m^2 g^{-1}). Assuming that σ_{abs} (λ) from FF and WB combustion ($\sigma_{abs,FF}$ (λ) and $\sigma_{abs,WB}$ (λ)) can be represented by the average site specific σ_{abs} (λ), the contributions of FF and WB to total BC (BC_{FF} and BC_{WB}) can be directly calculated according to equation 10 and 11. This is the approach used in this study, former used with good results by Herich et al. (2011).

$$BC_{FF} = b_{abs,FF}\,(950nm) / \alpha_{abs}\,(950nm) \quad (10)$$

$$BC_{WB} = b_{abs,WB}\,(470nm) / \alpha_{abs}\,(470nm) \quad (11)$$

Average site specific σ_{abs} (λ) were determined by separate OC/EC sampling and analysis.

2.4.2 OC/EC sampling and analysis

A field study campaign at Torkel was conducted to separate EC from OC in the collected aerosols to be able to derive average site specific σ_{abs} (λ) used for the calculations of BC_{FF} and BC_{WB}. The calculated BC_{FF} and BC_{WB} will then be consistent with EC concentrations during the time period of the OC/EC campaign and the average site specific σ_{abs} (λ) can be used for retroactive corrections in the time series.

Twelve-hour integrated samples for analysis of organic carbon (OC) and elemental carbon (EC) were collected by the Derenda low volume sampler from 7 October at 07:00 local time (LT) to 24 October at 07:00 LT, with a gap in the sampling period between 14 October 07:00 LT to 17 October 07:00 LT due to problems in the filter change mechanism (table T2 in appendix). The sampler was equipped with an impactor inlet of 10 µm cut-off size (figure A4 in appendix) and the aerosol particles were sampled on quartz fiber filters (Munktell T293, 47mm, Pall Corporation, figure A7 in appendix) at a flow rate of 2.3 m^3 h^{-1}. The filters were pre-baked in a furnace at 800°C for 12 hours and placed in filter holders (figure A8 in appendix) that were placed in a magazine that could store 16 filter holders in total (figure A6 in appendix). The magazine was stored in a protective specially designed container until deposit to the sampler. After aerosol collection, the magazine holding the loaded filters was placed back in the protective container until analyzed. Before sampling start the PM_{10} inlet was treated with gel on the inside to prevent particles >10 µm to reach the sampling filters (figure A5 in appendix).

Possible artifacts that may occur during filter sampling is both positive and negative (Krecl et al., 2007), and involves the adsorption and desorption, respectively, of organic gases onto the sampling filters or on particles already collected on it. The negative artifacts are believed to be low since a Peltier cooling unit ensures low temperature of the enclosure with the un-sampled and sampled filters.

The OC/EC analysis was carried out in the laboratory at ACES, Stockholm University, applying a thermal optical transmission method (TOT) (Birch and Cary, 1996) using a Thermal/Optical Carbon Aerosol Analyzer operating with the EUSAAR2 temperature protocol (Cavalli et al., 2010). Before analyzing the loaded filters (punches of 1.5 cm^2, figure A10 in appendix), two unloaded filter punches from the laboratory were analyzed for control of the TOT Analyzer.

It is important to remember that the amount of EC will vary with the method used, since it cannot be definitely separated from OC. It is the method used for analysis of carbonaceous

aerosols that defines the terms elemental carbon or black carbon (BC). For EC a thermal optical method is used, whereas for BC optical transmission is measured. The TOT method uses both the thermal refractory and the light absorption properties, and was derived from thermal methods while the term EC is retained for the refractory component. The method separates between original EC in the sample, and Pyrolytic Carbon (PC) that is EC formed from OC during the analysis (Wallén, 2011). Unfortunately no widely accepted standard measurement method exists for the determination of light-absorbing carbon (EEA Technical report, 2013), which complicates comparisons between different studies. Different thermal evolution protocols in use can result in an EC/total carbon (TC) variation up to a factor of five. The EUSAAR2 protocol is an optimized thermal evolution protocol defined by the framework of the EU-project EUSAAR (European Supersites for Atmospheric Aerosol Research). The major biases affecting thermal-optical analysis have been minimized to define a protocol that is optimized for European aerosols. One major improvement is the reduction of pyrolysis to a minimum. In other protocols PC is considered to evolve completely before native EC throughout the analysis, resulting in overestimation of EC. Further improvements include inter alia minimization of early evolution of light absorbing carbon species at higher temperatures in the He-mode (Cavalli et al., 2010).

During analysis the loaded filter was heated stepwise following the EUSAAR2 protocol. The first part of the analysis was conducted in helium to volatilize/pyrolyse the sample while in the second part oxygen was added for carbon combustion. Carbon dioxide formed was converted to methane for detection by a flame ionization detector. By monitoring the filter transmittance separation between OC and EC can be determined. In the helium part, OC that pyrolyses decreases the transmission. All carbon detected before the transmittance returns to its initial value (split point) is termed OC, while EC is the carbon detected after the transmittance has reached the split point and increases further (Wallén, 2011). According to EMEPs Manual for OC/EC sampling and analysis (Standard Operating Procedures for thermal-optical analysis of atmospheric particulate organic and elemental carbon, SOP), the carbon (OC and EC) amount per surface area of the filter should not be corrected for field blank values.

The formula used to calculate the OC and EC mass concentration in air (C) from the aerosol mass loading on the filter is

$$C = g\ A / V \qquad (12)$$

where g is the result from the TOT analysis (µg cm^{-2}), A is the filter sampling area (11.521 cm^2) and V is the volume (27.62 m^3).

The equation for calculation of site specific σ_{abs} (λ) is

$$\sigma_{abs}\ (\lambda)\ (m^2\ g^{-1}) = b_{abs}\ (\lambda)\ (Mm^{-1}) / EC\ (\mu g\ m^{-3}) \qquad (13)$$

In equation 13 the assumption of EC = BC is made allowing for determination of the site specific σ_{abs} (λ), used both for Torkel and Hornsgatan.

2.4.3 Particle number size distribution

Particle number size is continuously measured at the north side of Hornsgatan using a Differential Mobility Particle Sizer (DMPS), a standard instrument in atmospheric science used to measure the particle size distribution in the sub-micron size range. A DMPS consists of a Differential Mobility Analyzer (DMA) and a Condensation Particle Counter (CPC). In the DMA the particles move through an electrical charged field and gets separated according to their electrical mobility, which is different depending on the particle size and electrical charge. The smaller the particle and/or the higher the electrical charge the higher is the electrical mobility. By increasing the DMA voltage, the selected particle diameter can be changed. The CPC counts the aerosol particles that pass through the DMA. Incoming particles needs to be enlarged for the CPC to be able to detect them, which is done by vapour condensation of n-butanol causing the particles to grow into droplets that is detected by a laser beam (Knutson et al., 1975; TSI Incorporated, 2002). The CPC detects particles between 10 nm and 337 nm, where the sizes are separated into 14 intervals. The DMPS at Hornsgatan is made by ACES, Stockholm University, according to a European standard, EUSAAR (Asmi et al., 2011).

2.4.4 BC emission factors for local traffic at Hornsgatan

Road vehicle emissions depend on many parameters such as vehicle type and age, fuel, engine load, after treatment devices fitted, travel speed, driving conditions, road type, slope of the road and local meteorological conditions. Emission factors (EF) predict the quantity of a pollutant that is emitted per distance driven, energy consumed or amount of fuel used. EF's mostly refer to the distance travelled (task-based EF's) but can also refer to the fuel burned (mass-based EF's) (TRANSPHORM, 2013). For the purpose of providing appropriate EF's either direct measurements (from vehicles placed on a dynamometer and run through certain driving cycles) or indirect estimation through measurements of concentrations close to a road (Franco et al., 2013). Both methods have advantages and limitations. Direct measurements provides EF's of relatively small number of vehicles but for very well controlled conditions, which on the other hand may not be representative for vehicles on a road. The use of indirect estimations does not enable control of either meteorological or traffic conditions and requires models to calculate EF's from measured concentrations. However, the big advantage is that EF's for a whole vehicle fleet travelling on a specific road or in an area can be derived for real world conditions.

Since BC is an unregulated pollutant measurement of BC in vehicle emissions are few and the EF's come with higher uncertainties than the regulated pollutants. To make BC more useful as a widely used marker for vehicle emissions in health assessment studies, it is of great importance to evaluate different ways to calculate EF's for BC and decrease the uncertainties to a minimum.

2.3.4.1 Handbook on Emission Factors for Road Transport (HBEFA)

HBEFA is a database for vehicular EF's in Europe that provides EF's in g/vehicle km for all current vehicle categories of road transport (for all Euro standards and for a wide variety of traffic situations). EF's are given for all regulated and the most important non-regulated air pollutants, unfortunately not including BC. The first version was published in December 1995 and newest version is from July 2014. The HBEFA EF's are based on real world driving patterns that are representative for local traffic. Typical traffic situations (categorized by areas,

road type, speed limit and level of service) are based on the measured driving patterns and measurements of real world emissions are done to generate reliable emission factors. Unfortunately emission measurements cannot be done for all possible traffic situations (too costly and time-consuming) so the HBEFA approach is to use parameterizations for the most important influencing factors based on the real world emission measurements in real world driving cycles in order to derive emission factors for all traffic situations (http://www.hbefa.net). EF development from real-world techniques, such as HBEFA, is more limited than laboratory techniques (engine and chassis dynamometer studies) due to the presence of additional sources of variability that makes them less precise and repeatable. However, real-world emission measurements are essential for the validation of EF's derived from laboratory testing (Franco et al., 2013). On the other hand, the controlled environment of laboratory techniques has the disadvantage of not always reflecting the field conditions (e.g. driver behavior and traffic conditions) in a truthful manner. HBEFA EF's are derived using four levels of traffic service; free flow, heavy, saturated, and stop and go. At Hornsgatan the distribution is 16, 52, 28 and 4 %, respectively. Implementation of the different Euro classes (pre-Euro to Euro 6) are divided into subgroups trying to reflect the real-world techniques in the best way there is.

2.3.4.2 TRANSPHORM emission factors

To improve the knowledge of transport related pollution and its impact on human health the EU founded project TRANSPHORM has been formed, today consisting of 21 partners from 14 European countries, bringing together internationally leading air quality and health researchers. The project is organized into five subprojects (SP) where SP1 (Transport and emission sources) focuses on improving the emission estimates from transport sources and consist of a work package which has an objective to deliver EF's from road transport, including EF's for BC (TRANSPHORM, 2013). TRANSPHORM EF's are derived using three levels of traffic service; highway, urban peak-off, and urban peak. For Hornsgatan the distribution is estimated to be 75 % urban peak and 25 % urban peak-off. Different Euro classes is not divided into sub groups. TRANSPHORM EF's is considered having higher uncertainty compared to HBEFA due to the more coarse division in the level of traffic service and Euro classes. However, TRANSPHORM has EF's for BC which is not given by HBEFA.

2.3.4.3 Calculations of emission factors for BC

Four different approaches were used to calculate and evaluate EF's for BC:

1. Using TRANSPHORM absolute BC emission factors.
2. Using TRANSPHORM fraction BC emission factors (absolute BC emission factors calculated from the ratio BC/PM-exhaust, where PM-exhaust emission factors are from HBEFA).
3. Using the emission factor for NOx from HBEFA and scaling of the measured ratio in ambient air concentrations of local BC and local NOx at Hornsgatan (urban background at Torkel subtracted from the measurements at Hornsgatan).
4. Using local CO_2 measurements and emission factors for CO_2 from HBEFA and scaling according to the ratio of local BC/local CO_2.

Measurements of CO_2 at Hornsgatan and Torkel were done using a CO_2 probe designed for high accuracy CO_2 measurements with a measuring range between 0 and 1000 ppm, linked to an aethalometer model AE33. For this measurement the flow-through model was used. Principle of operation is that a pulsed light is reflected and re-focused back to an IR detector placed behind a silicon-based Fabry-Perot Interferometer (FPI), which is tuned electrically so the measurement wavelength is changed between the CO_2 absorption band and a reference band. When the passband of the FPI match the CO_2 absorption wavelength the IR detector register a decrease in the light transmission. The measurement wavelength of the FPI is then changed to the reference band and a full light transmission is registered by the IR sensor. The ratio of the two signals indicates the degree of light absorption in the gas and is proportional to the gas concentration.

Measurements of NOx has been performed for several years at both Hornsgatan and Torkel by a Chemiluminescence Analyser. The instrument has two chambers measuring NO and NOx, respectively. The incoming gas is divided into two currents, where half of the incoming gas goes directly to the NO reaction chamber and the other haft passes through a molybdenum converter which converts NO_2 to NO before the gas reaches the NOx reaction chamber. The instrument also has an ozone generator generating ozone from the ambient air. In the reaction chambers NO, which is a relatively unstable molecule, reacts with ozone and is oxidized to NO_2. A quantity of the oxidized NO_2 (~10 – 20 %) will be in the exited state (NO_2^*) producing light (*hv*) when it returns to ground state. The light intensity is proportional to the concentration of NO in the gas sample. The light is in the interval 600 – 3000 nm and detected by a photomultiplier tube that convert the light signal into an electrical signal. The NO_2 concentration is obtained by subtracting the NO concentration from the NOx concentration.

The chemiluminescence reaction of NO to NO_2 is

$NO + O_3 \rightarrow NO_2 + O_2$

$NO_2^* \rightarrow NO_2 + hv$

At Torkel the NOx measurements are performed using a single chamber Chemiluminescence Analyser that in cycles of 5 seconds measure zero air, NO and NOx. The Analyser at Hornsgatan has a dual chamber system, which continuously measure NO and NOx. The site has a switching system that covers three measuring points (street level south side, street level north side and roof level), and simultaneous forms average values every fifteen minutes.

3 Results and Discussion

3.1 OC/EC analysis

3.1.1 Comparison with PM_{10} and $PM_{2.5}$

PM_{10} is considered as one of the main problems regarding the air quality in central Stockholm, with values above the Swedish environmental quality objective for both the annual mean limit and the limit for the number of days exceeding the diurnal mean concentration at e.g. Hornsgatan (SLB, 2015). $PM_{2.5}$ is considered among the most harmful pollutants in ambient air due to its ability to penetrate deep into the human lungs. Therefore it is of great importance to map the components that contributes to the high amount of PM_{10} and $PM_{2.5}$.

Fifteen-minute PM_{10} and $PM_{2.5}$ mass concentrations were averaged into 12-hour values to match the integrated OC and EC mass concentrations obtained from the TOT analysis. Descriptive statistics of OC, EC, total carbon (TC), PM_{10} and $PM_{2.5}$ mass concentrations are given in table 3 for the sampling period. All data from the OC/EC campaign period can be found in appendix table T2 – T5.

Table 3. *Descriptive statistics (mean day, mean night, mean, percentiles and standard deviation (std) of the mean value) of 12-h average values of OC, EC, TC, PM_{10} and $PM_{2.5}$ mass concentrations, together with OC/EC ratios, measured at the site Torkel, 7 October to 24 October 2014.*

Statistics	OC (µg m^{-3})	EC (µg m^{-3})	TC (µg m^{-3})	OC/EC	PM_{10} (µg m^{-3})	$PM_{2.5}$ (µg m^{-3})
Mean day	2.46	0.50	2.91	6.09	11.16	8.31
Mean night	2.07	0.35	2.42	6.10	9.91	8.47
Mean	2.27	0.40	2.67	6.10	10.53	8.39
25th percentile	1.51	0.24	1.76	5.10	5.63	4.58
75th percentile	2.86	0.46	3.38	6.80	13.82	10.72
Std	1.17	0.25	1.39	2.00	6.43	5.20

A large variation in OC, EC and PM_{10} mass concentrations were observed with the highest OC and EC values during the first 24 hours of the sampling period with concentrations exceeding 5.6 µg m^{-3} and 1.0 µg m^{-3}, respectively. The mean and standard deviation mass concentrations are 2.27 ± 1.17 µg m^{-3} for OC, and 0.40 ± 0.25 for EC. The half-day sampling interval was chosen to give maximum difference in carbon mass concentration between day and night. The day/night ratio showed that OC and EC mass concentrations were 19 % respectively 29 % higher during day time. On the average, OC and EC accounted for 21.6 % and 3.8 % of total PM_{10}, respectively (27.1 % and 4.8 % of total $PM_{2.5}$). This means that TC (OC+EC) accounted for 25.3 % of PM_{10} (31.9 % of $PM_{2.5}$) and can be considered as a major component of the total PM_{10} and $PM_{2.5}$ mass concentration.

Another study in Sweden by Krecl et al. (2007) reported 12-h maximum concentration values of 17 µg m^{-3} and 5 µg m^{-3} for OC and EC at a northern situated site in the town of Lycksele where residential wood combustion (RWC) was frequently occurring during the sampling

period. Their measurements were performed using the same technique as in this study, but the sampling period was during the colder winter months January to March. The difference in sampling period and the experimental site location further north could have had an important contribution to the carbon mass concentration resulting in higher values compared to this study.

Organic matter (OM) is matter composed of organic compounds (i.e. not only carbon) and the ratio OM/OC is sometimes used as an estimate of the degree of chemical processing in the atmosphere. The literature suggests shifting values of OM/OC ranging from 1.2 to 2.2, due to differences in primary emissions and secondary formations (Chan et al., 2010 and references therein). Applying a value of 1.8 (used by e.g. Favez et al., 2010; Harrison et al., 2013) OM will account for 38.8 % of total PM_{10} (48.7 % of total $PM_{2.5}$) and is indeed a major component contributing to the high amount of PM_{10} and $PM_{2.5}$.

During this campaign the OC/EC ratio ranged from 3.8 to 14.7 with a mean value of 6.1. The mean distribution of TC was 85.1 % OC and 14.8 % EC. The OC/EC ratio remained close to the mean value except for a single occasion with a ratio of 14.7. The ratio of OC to EC in ambient aerosols varies due to different emission sources and can be increased by secondary processes (Chan et al., 2010). OC/EC ratios for urban sites are usually reported in the interval 2.0 - 3.0 (Lin and Tai, 2001 and references therein). Significant local sources, like biomass combustion, can explain higher OC/EC ratios (Na et al., 2004). The OC/EC ratios in Lycksele (Krecl et al., 2007) ranged from 1.9 to 64.0 with a median value of 3.6. In this study the ratios had a low variation (5.1 – 6.8 for the 25th and 75th percentile), indicating the air mass of the sampled air not changing properties to a high extent during the sampling period, while Krecl et al. (2007) had a much longer sampling period allowing air masses from different sources and with different properties affecting the samples. High ratios indicates clean atmosphere with periods of low EC concentrations while low ratios means that the air is more polluted. However, one expects higher OC/EC ratios near biomass combustion sources compared to fossil fuel sources which is not the case comparing Torkel and Lycksele.

Linear correlations between OC, EC, PM_{10} and $PM_{2.5}$ mass concentrations are illustrated by figure 3 and 4.

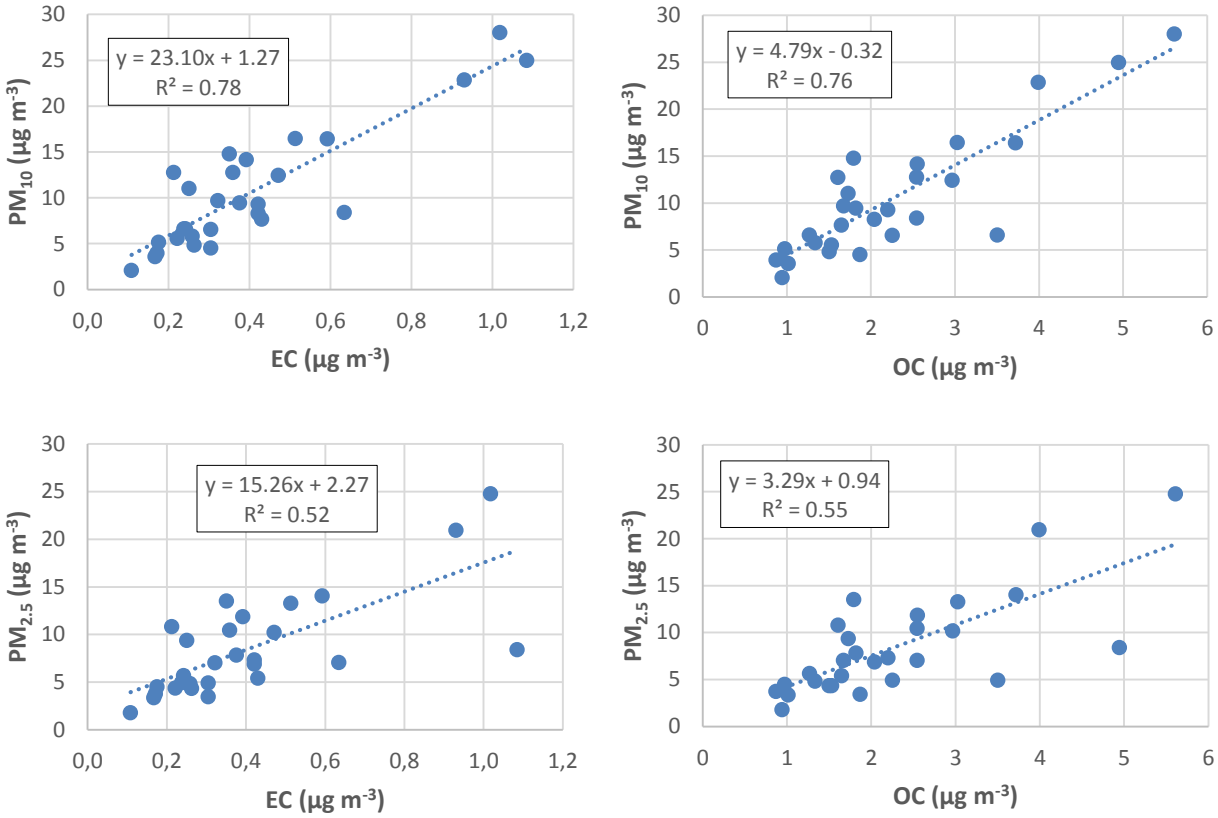

Fig. 3. *Linear correlations of 12-hour integrated values of OC, EC, PM_{10} and $PM_{2.5}$ mass concentrations, 7 October at 07:00 LT to 24 October at 07:00 LT. The line represents the least squares line regression. The coefficient of determination R^2 is also shown.*

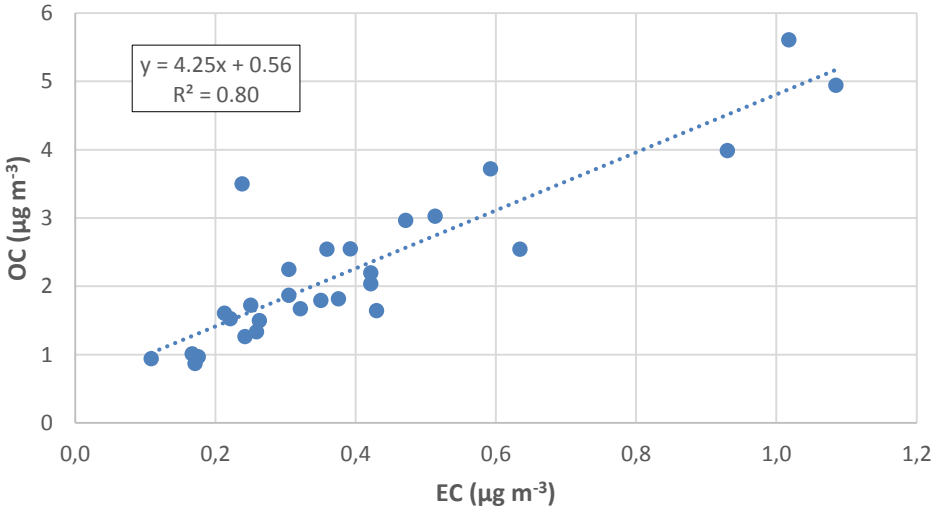

Fig. 4. *Linear correlations of 12-hour integrated values of OC and EC mass concentrations, 7 October at 07:00 LT to 24 October at 07:00 LT. The line represents the least squares line regression. The coefficient of determination R^2 is also shown.*

The linear correlation between OC and EC has an R^2-value of 0.80 which means that the linear model explains 80 % of the data variability. This may serve as an indication for the major fraction of OC and EC being emitted by a dominant primary source (Turpin and Huntzicker, 1995). Linear correlations between PM_{10} and OC and EC showed R^2-values of 0.76 and 0.78, respectively, indicating that the processes generating PM_{10} and OC and EC particles (fuel combustion) are largely the same during this period. The concentrations of PM_{10} are highest during spring when the roads are dry and many vehicles still uses studded tires. During these months, especially Feb – April, the correlation between PM_{10} and exhaust particles are very low (see figure A19 in Appendix). However, during the time of the year when studded tires are not used the correlation is found to be relatively good. The OC/EC campaign was conducted in October which can explain the high correlation. Linear correlations between $PM_{2.5}$ and OC and EC were found to be lower with R^2-values of 0.55 and 0.52, respectively. The correlation is still high indicating common sources but the model cannot explain about half of the variation, indicating other sources affecting the concentration of $PM_{2.5}$ compared to PM_{10}, OC and EC mass concentrations. A possible reason might be accumulation mode particles (0.1 µm < particle size < 2.5 µm) that has been long range transported from non-local sources.

3.1.2 Site specific mass absorption cross sections σ_{abs} (λ)

σ_{abs} (λ) values reported in the literature vary between 1 and 30 $m^2\ g^{-1}$ for λ = 880 nm (Andreae et al., 2006), depending on aerosol properties such as chemical composition, age, particle size and shape, and mixing state of the aerosols (Liousse et al., 1993). To make it even more complicated, σ_{abs} (λ) values also depend on the method used to determine EC mass concentrations. In practice, this leads to the fact that different σ_{abs} (λ) values can be derived from the same instrument and site, but calibrated with different reference methods. As one can understand this leads to difficulties comparing results between different studies and sites using different methods. A way to establish σ_{abs} (λ) values that are most representative is to determine values that are site specific for the location of interest. Using eq. 13 site specific mass absorption cross sections σ_{abs} (λ) were calculated, displayed in table 4 (details in appendix table T4). The variation in the mean value is given by the 75th and 25th percentile.

Table 4. *Site specific mass absorption cross sections (MAC) σ_{abs} (λ) ($m^2\ g^{-1}$), mean value together with the 75th and 25th percentile.*

Wavelength λ (nm)	370	470	520	590	660	880	950
Mean	48.0	27.4	22.9	20.0	17.4	12.3	11.0
75th percentile	54.5	30.5	25.0	21.8	19.1	13.2	11.8
25th percentile	39.2	23.1	19.3	16.8	14.6	10.5	9.4

These values were then used to calibrate the AE31 by forcing the calculated b_{abs} (λ) (table T3 in appendix) to be consistent with the EC mass concentration (table T2 in appendix). If no site specific TOT analysis is performed general σ_{abs} (λ) values given by the manufacturer (Magee Scientific, USA) can be used (deriving method explained in the Magee Aethalometer handbook). Table 5 shows a comparison of σ_{abs} (λ) values obtained in this study and the values provided by the manufacturer for the AE31.

Table 5. *Wavelength dependent σ_{abs} (λ) values reported for the AE31 by the manufacturer (Magee Scientific) and site specific σ_{abs} (λ) values obtained by using the reported EC mass concentration from the TOT analysis.*

λ (nm)	**Manufacturer's values**		**Site specific values**
	σ_{abs} (λ) (m^2 g^{-1}) "Magee BC"	**σ_{abs} (λ) (m^2 g^{-1}) "Harvard TOR-EC"**	**σ_{abs} (λ) (m^2 g^{-1}) TOT**
370	39.5	30.0	48.0
470	31.1	23.6	27.4
520	28.1	21.3	22.9
590	24.8	18.8	20.0
660	22.1	16.8	17.4
880	16.6	12.6	12.3
950	15.4	11.7	11.0

The "Magee BC" factor was originally derived in the early 1980's and converts optical ATN to a mass of BC. Harvard School of Public Health found that the Thermo-Optical Reflectance (TOR) method gave EC data that tracked the Aethalometer BC data very well, but with numbers that were higher than BC. This difference was explained by BC being a subset of EC or that the TOR method had a systematic property that resulted in higher EC values. The TOT method has been found to often differ markedly from the TOR result on the same samples giving rise to the conclusion that the Thermo-Optical Analysis (TOA) methods (TOR and TOT) do not offer an absolute determination of EC content. According to this Magee Scientific (Magee aethalometer handbook) argues that "the aethalometer optical measurement of BC can be as method dependent as that of thermal analyses of EC, provided it is consistent and reproducible". Therefore two values are given from the manufacturer for the absorption cross section calibration. In this study the AE31 is calibrated with the site specific values from the TOT method, with the hope that this will result in the most correct absolute values of aethalometer BC at this specific location.

σ_{abs} (λ) values from this TOT analysis seems to be more consistent with σ_{abs} (λ) according to the "Harvard TOR-EC" calibration method than the "Magee BC" method. Most deviation is seen for 370 nm while longer wavelengths shows very similar values.

During the period of the OC/EC campaign EC mass concentration is considered to be the most representative value of the amount of BC. However, it is important to note that this rather short period give an average value that is applied on the whole time period. The value of σ_{abs} (λ) is however not a constant and therefore the simplification of using a constant value will result in some uncertainty in the BC mass concentrations before and after the OC/EC campaign period. When the conditions are similar to those during the OC/EC campaign period one can assume that the derived σ_{abs} (λ) values have a lower uncertainty than during very different conditions. To get a better understanding about the variation in the site specific σ_{abs} (λ) it would be of importance to do more and longer OC/EC campaigns.

The mean value of EC and BC is exactly the same, but the individual 12-h values will differ more or less depending on σ_{abs} (λ) being a constant and not a variable. Table 6 show descriptive statistics of EC and BC mass concentrations.

Table 6. *Descriptive statistics (mean day, mean night, mean, percentiles and standard deviation (std) of the mean value) of 12-h average values of EC and aethalometer BC mass concentrations (µg m^{-3}), measured at the site Torkel in central Stockholm, 7 October to 24 October 2014. The wavelength 880 nm has been used for all statistic values.*

Statistics	EC (µg m^{-3})	BC (µg m^{-3})
Mean day	0.50	0.44
Mean night	0.35	0.34
Mean	0.40	0.40
25th percentile	0.24	0.24
75th percentile	0.46	0.43
Std	0.25	0.22

A scatter plot for the OC/EC campaign period (figure 5) illustrate the linear correlation between EC (from the TOT analysis) and BC (calculated using the average site specific σ_{abs} (880 nm)). AE31 operates with 7 wavelengths and therefore the BC mass concentration will be different for different wavelengths. For this purpose the wavelength λ = 880 nm has been chosen for comparison with earlier studies.

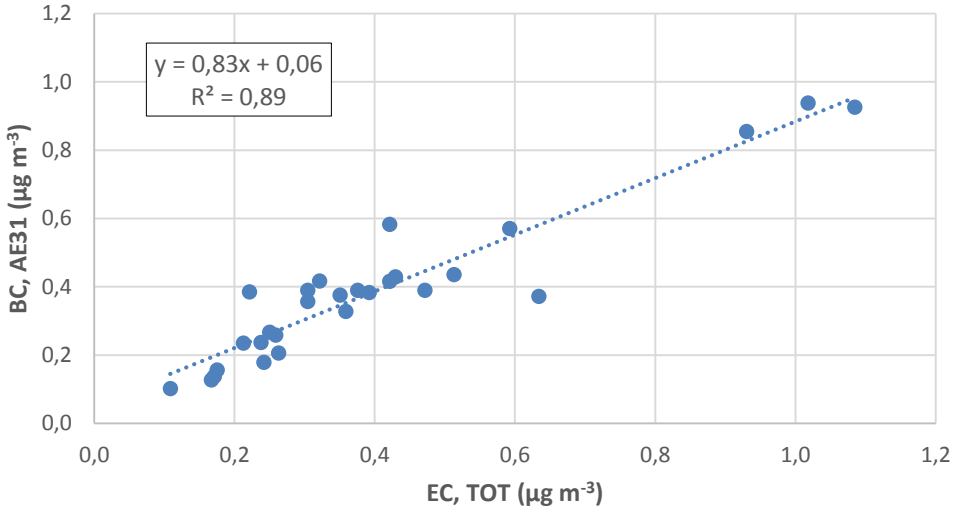

Fig. 5. *Linear correlation between EC (from the TOT analysis) and BC (measured with AE31 and calibrated with EC) (µg m^{-3}). The slope of the line represents the least square line regression. The coefficient of determination R^2 is also shown.*

The site specific σ_{abs} (880 nm) derived from the TOT method was 12.3 m^2 g^{-1}, with a 25th and 75th percentile of 10.5 and 13.2 m^2 g^{-1}, respectively. Using a site specific σ_{abs} (880 nm) resulted in a good linear fit between EC and BC (R^2 = 0.89) but due to the constant site specific σ_{abs} (880 nm) the mean value will not give perfect correlation in every point. A slope < 1 (0.83 ± 0.12 with 95 % confidence interval) means that BC is underestimated with respect to EC.

3.2 BC mass calculations

In the final step, the BC mass concentration (µg m^{-3}), from fossil fuel combustion (BC_{FF}) and biomass combustion (BC_{WB}) was determined according to eq. 10 and 11.

3.2.1 Total BC mass and source apportionment

Table 7 shows the mean BC mass concentration (µg m^{-3}) at Hornsgatan, in total and from biomass burning and fossil fuel combustion, respectively, for the whole campaign period (total) and divided into winter (Dec, Jan, Feb) and summer periods (June, July, Aug). The percentage of WB and FF related BC are also shown. In appendix table T6 and T7 shows monthly mean values in detail. The variation in the mean values were obtained by a sensitivity analysis of BC mass concentration from the two sources, changing α_{WB} and α_{FF} ± 0.2 and ± 0.1, respectively (Torkel table T8 and Hornsgatan table T9 in appendix).

At Hornsgatan, for the whole campaign period the average BC mass concentration was 1.44 ± 0.05 µg/m^3 where 84 ± 6 % came from FF and 16 ± 6 % from WB. In winter the contribution from WB increases to 20 ± 6 % while in summer it is half of that in winter (11 ± 7 %). At Torkel, the average BC mass concentration was 0.52 ± 0.01 µg/m^3 where 66 ± 6 % came from FF and 34 ± 6 % from WB. The contribution from WB during winter was 39 ± 6 % and during summer 25 ± 5 %. The total amount of BC are about three times higher at Hornsgatan compared to Torkel. However, the absolute values of BC_{WB} are relatively similar at Hornsgatan and Torkel while BC_{FF} are 3.6, 4.1 and 2.8 times higher in total, in summer and in winter, respectively, at Hornsgatan compared to Torkel.

Herich et al. (2011) found in their long term study in Switzerland the contribution from WB to be 10 ± 8 % in summer and 24 ± 11% in winter, for the urban background site located in a courtyard in the city centre of Zurich (ZUE). The total BC concentration was 1.19 ± 0.37 µg/m^3 in summer and 1.54 ± 0.48 µg/m^3 in winter. The contribution to BC at Hornsgatan is found to be similar to ZUE both in summer and winter, while Torkel show higher contributions from WB. In 2006/2007 Andersson et al. (2011) conducted aerosol sampling both at Torkel and at the rural background site Aspvreten for source apportionment of soot carbon (SC) using a radiocarbon methodology. They found the fraction biomass at Torkel to be 35 ± 18 % in the campaign conducted 25 Aug – 2 Oct 2006, and 43 ± 23 % in a second campaign 21 Dec – 14 Mar 2007. Aspvreten had similar biomass contributions. These findings are highly in line with the contributions from WB at Torkel from this study. However, the differences in methodology and campaign period are important factors that must be taken into consideration comparing these studies.

Table 7. *Mean BC mass concentrations (total, from biomass burning and from fossil fuel combustion), for the whole campaign period (total) and divided into winter (Dec, Jan, Feb) and summer periods (June, July, Aug) at Hornsgatan and Torkel. The percentage of BC_{WB} and BC_{FF} of total BC are also given. The variation in the mean values were obtained by a sensitivity analysis of BC mass concentration from the two sources, changing α_{WB} and α_{FF} ± 0.2 and ± 0.1, respectively.*

HORNSGATAN					
Time	**Total BC (µg/m^3)**	**BC_{WB} (µg/m^3)**	**BC_{FF} (µg/m^3)**	**BC_{WB} (%)**	**BC_{FF} (%)**
Winter (DJF)	1.38 ± 0.04	0.28	1.10	20 ± 6	80 ± 6
Summer (JJA)	1.54 ± 0.08	0.17	1.38	11 ± 7	89 ± 7
Total	1.44 ± 0.05	0.23	1.21	16 ± 6	84 ± 6
TORKEL					
Winter (DJF)	0.64 ± 0.02	0.25	0.39	39 ± 6	61 ± 6
Summer (JJA)	0.45 ± 0.01	0.11	0.34	25 ± 5	75 ± 5
Total	0.52 ± 0.01	0.18	0.34	34 ± 6	66 ± 6

Time series of the contribution of BC_{WB} to total BC at Hornsgatan and Torkel during the campaign period are displayed in fig. 6 and 7. The time series shows an annual pattern with higher contributions from WB during colder periods while warmer periods are characterized by higher contributions of FF. The pattern are similar at Hornsgatan and Torkel but the absolute values differ with a contribution from WB that are about 2 times higher at Torkel compared to Hornsgatan.

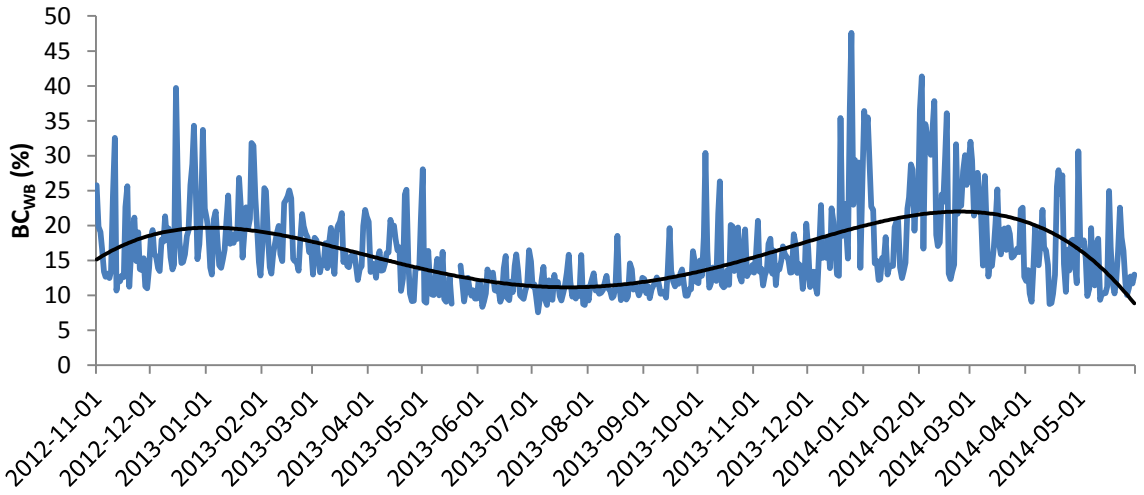

Fig. 6. *Time series of BC mass concentration generated from biomass combustion (% of total BC) at Hornsgatan.*

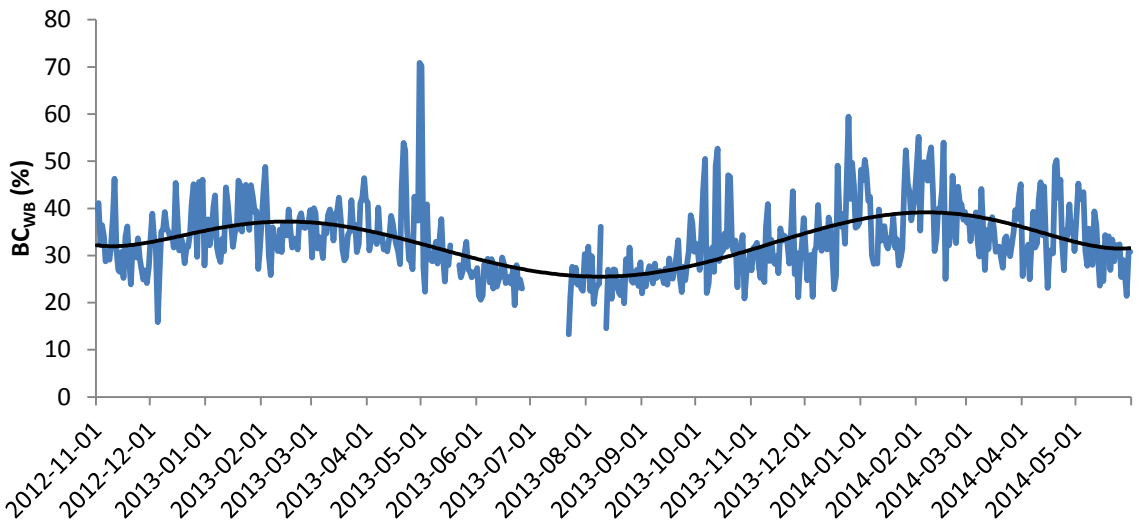

Fig. 7. *Time series of BC mass concentration generated from biomass combustion (% of total BC) at Torkel.*

3.2.2 Share of PM2.5

BC is a fraction of $PM_{2.5}$, which is continuously measured at both Torkel and Hornsgatan since it is important to monitor the levels of these particles in ambient air due to its harmful effects on human health. To get a better understanding of the BC contribution to the mass concentration of $PM_{2.5}$, at Hornsgatan and Torkel, the share of BC to $PM_{2.5}$ has been calculated for different time periods displayed in table 8.

Table 8. *Mass concentrations of $PM_{2.5}$, total BC, BC_{FF} and BC_{WB} ($\mu g\ m^{-3}$) at Hornsgatan and Torkel for different time periods.*

		$PM_{2.5}$	**BC**	**BC_{FF}**	**BC_{WB}**
HORNSGATAN					
Whole week (Mon-Sun)	Whole year	10.83	1.29	1.06	0.23
Weekends (Sat-Sun)	Whole year	10.39	0.92	0.71	0.21
Daytime (Mon-Thu 06-18)	Whole year	11.58	1.92	1.64	0.28
Winter	Dec – Feb	11.63	1.24	0.96	0.28
TORKEL					
Whole week (Mon-Sun)	Whole year	5.91	0.49	0.31	0.18
Weekends (Sat-Sun)	Whole year	5.26	0.44	0.25	0.19
Daytime (Mon-Thu 06-18)	Whole year	6.92	0.75	0.55	0.20
Winter	Dec – Feb	7.04	0.59	0.34	0.25

The mass concentration of $PM_{2.5}$ varies moderately between the different time periods. A large fraction of these particles have been long range transported from distant sources, which is evident by comparison between urban and rural sites (ITM-report 110, 2004). However, the absolute values are about two times higher at Hornsgatan compared to Torkel which showing a significant local contribution of particles in this size range.

The BC mass concentration is highest during daytime at both Hornsgatan and Torkel and lowest at weekends. The increase in BC between weekends and daytime is 109 % at Hornsgatan and 70 % at Torkel (with dominating contribution from increase in BC_{FF}). At Torkel an increase in BC mass concentration in winter is seen (17 % higher than for the whole week scenario) while Hornsgatan has a decrease in BC (4 %) comparing the winter period with the whole week.

The highest concentrations of BC_{WB} is during winter and daytime at Hornsgatan and during winter at Torkel. Absolute values are somewhat higher at Hornsgatan, indicating that the traffic related particles contain material with absorbing properties in the UV spectra. Low variation in BC_{WB} but high variation in total BC means that BC_{FF} is the variable that is changing between the different scenarios. At both Hornsgatan and Torkel the highest concentrations for BC_{FF} is found during daytime and lowest concentrations during weekends. The values at Hornsgatan are about three times higher compared to Torkel (four times higher during daytime), which then can be used as a good indication of the local contribution of BC from traffic (diesel vehicles).

The total BC contribution and contributions from FF and WB to total $PM_{2.5}$ (%) are shown in figure 8 (Hornsgatan) and figure 9 (Torkel) divided into four groups.

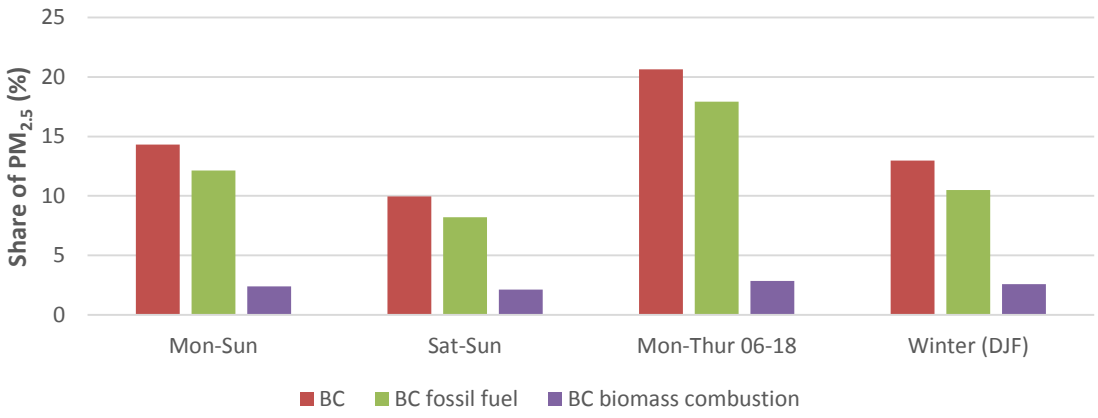

Fig. 8. *The share of BC to $PM_{2.5}$ (total BC, BC_{FF} and BC_{WB}) for different time periods at Hornsgatan.*

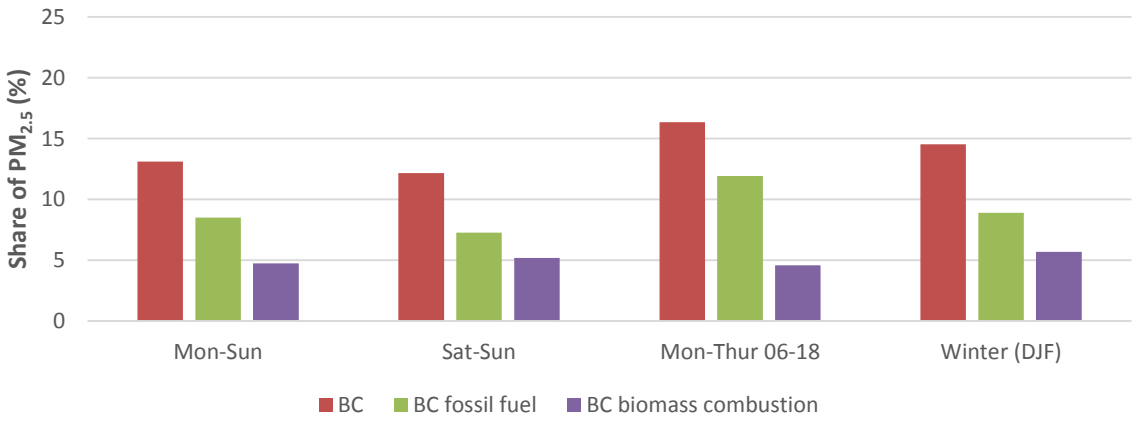

Fig. 9. *The share of BC to $PM_{2.5}$ (total BC, BC_{FF} and BC_{WB}) for different time periods at Torkel.*

During daytime (Mon-Thu 06-18) more than 20 % of the total concentration of $PM_{2.5}$ at Hornsgatan consists of BC particles that are mostly formed during fossil fuel combustion (18 %). During weekends (Sat-Sun) the contribution is 10 %. The general pattern for Hornsgatan is high contribution of BC to $PM_{2.5}$, mainly from BC_{FF}, during times of high traffic load and lower contribution at weekends. The contribution from BC_{WB} is less than 3 % for all periods. Also at Torkel the highest contribution of BC to $PM_{2.5}$ is during daytime (16 %) but the difference between the different periods is smaller than at Hornsgatan. In general the contribution from BC_{WB} are about two times higher at Torkel compared to Hornsgatan and around 4.5 % (highest during winter with 5.7 %).

3.3 Diurnal variation

A good indicator of the separation between the two sources is by using NOx as a tracer. NOx has largely the same source as BC_{FF} (mostly diesel vehicles) and therefore the diurnal variation of NOx and BC_{FF} shall follow the same pattern if the model manages to separate BC_{FF} and BC_{WB}.

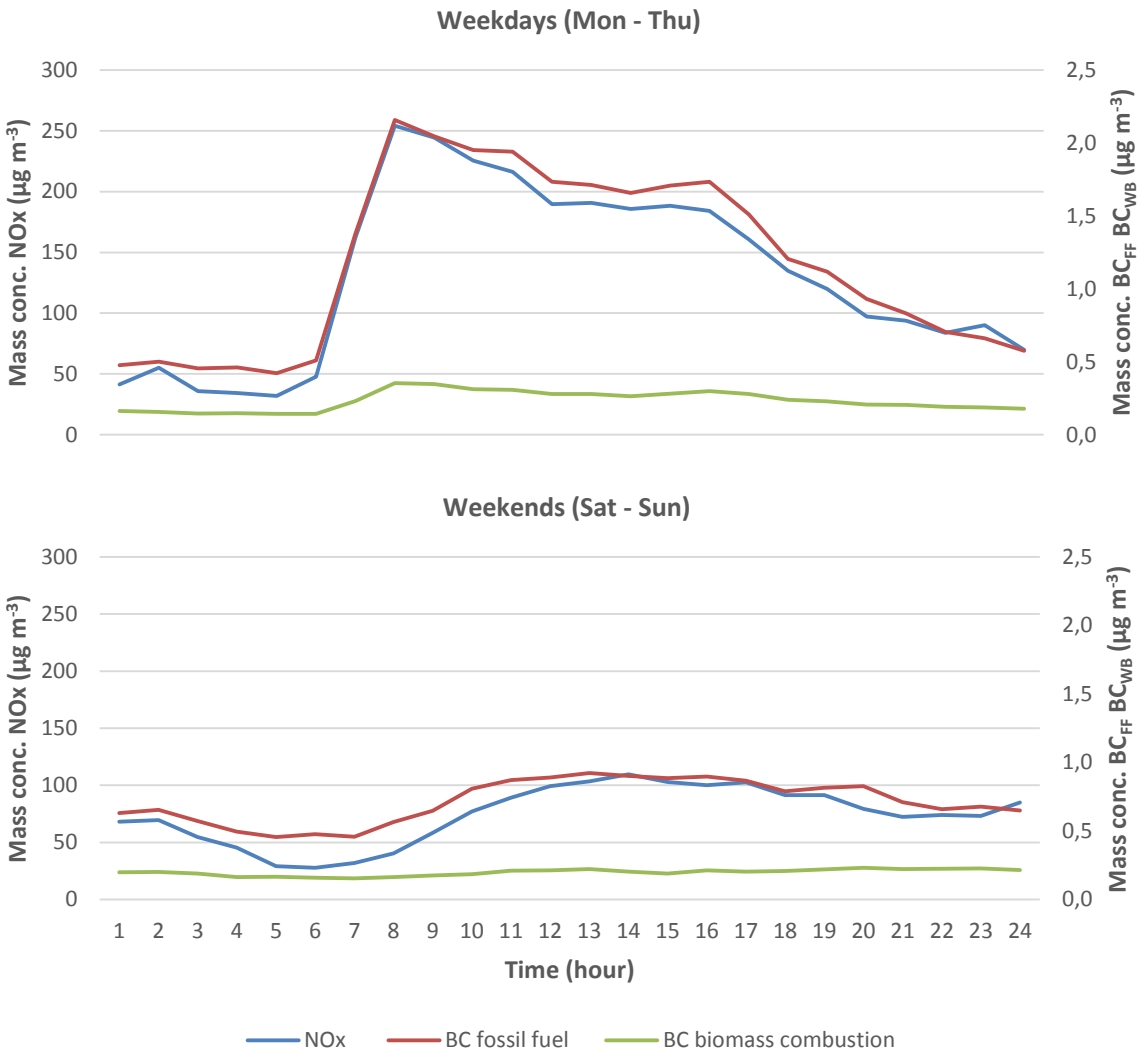

Fig. 10. *Diurnal variation for BC_{FF}, BC_{WB} (right axis) and NOx (left axis) at Hornsgatan during weekdays (Mon-Thu) (top) and weekends (Sat-Sun) (bottom) for the whole campaign period.*

The diurnal variation show a separation between BC_{FF} and BC_{WB} with clear differences between the two sources. The blue line show the diurnal pattern for NOx which is almost identical to BC_{FF} but differ from BC_{WB}, showing a successful separation between the two sources of BC.

The diurnal variation of BC_{FF} (red line) during weekdays (figure 10 top) at Hornsgatan has a rapid increase of more than 4 times the concentration between 6 and 8 AM, probably caused by the traffic morning rush and meteorological stable conditions favouring high concentrations of pollutants. The highest concentration is seen around 8 AM and slowly decreasing until around 4 PM where a small increase is seen (probably caused by the traffic afternoon rush). The concentration of BC_{FF} remain at a much higher level than BC_{WB} throughout the whole day and night. BC_{WB} (blue line) has a much weaker diurnal variation with only small changes in concentration. The pattern is similar to BC_{FF} with an increase due to the morning traffic rush but much smaller and less distinct. During weekends (figure 10 bottom) the pattern for BC_{FF} is much flatter with no distinct peak. BC_{WB} is more or less constant at weekends.

The same pattern is seen for Torkel (figure 11) but with much lower concentrations and a smaller morning peak (an increase in concentration of about 2 times). The general pattern for Torkel compared to Hornsgatan is in general smaller differences between BC_{FF} and BC_{WB} concentrations due to less traffic impact. The correlation between NOx and BC_{FF} is somewhat lower at Torkel compared to Hornsgatan (especially at weekends) which might be explained by an increased distance from the source of NOx and BC_{FF} allowing for internal and external mixing changing the chemical composition and optical properties of the BC particles and dilution of NOx. It is also possible that the further away from the source BC_{FF} can be affected by other sources than the local traffic, e.g. long range transport (not affecting NOx), which can explain the difference seen in the diurnal variations of BC_{FF} and NOx at Torkel.

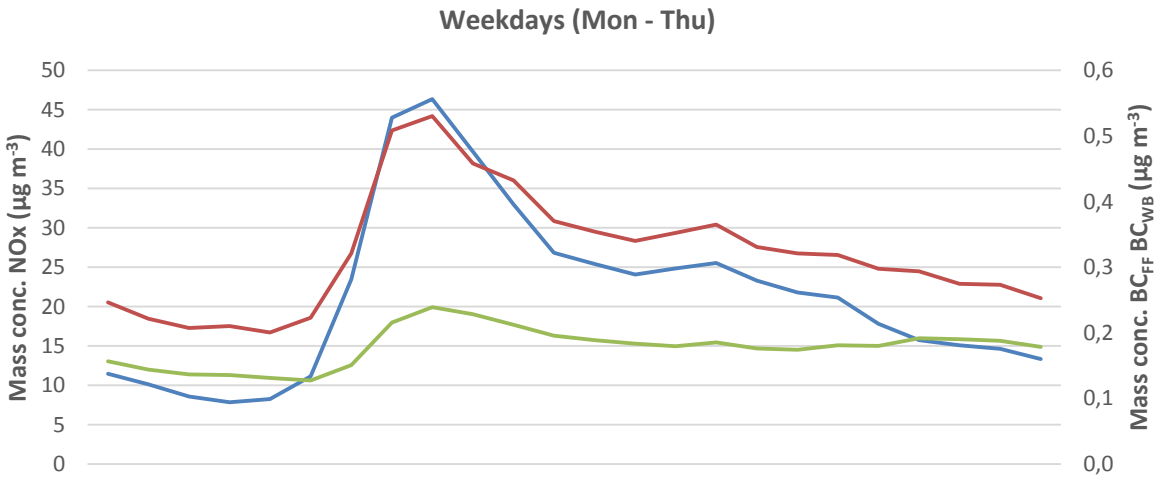

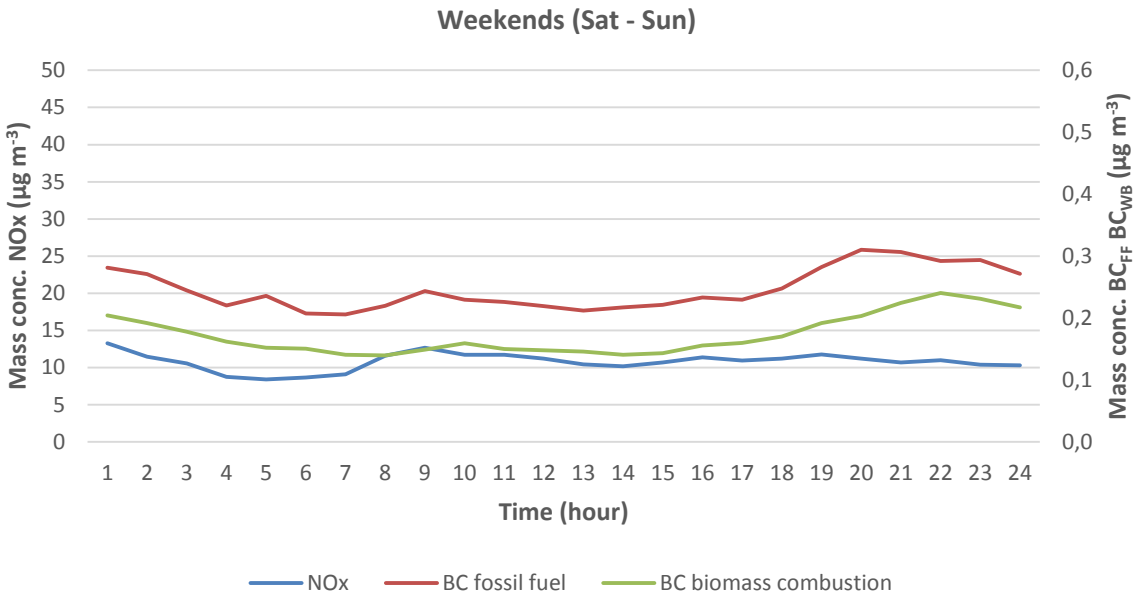

Fig. 11. *Diurnal variation for BC_{FF}, BC_{WB} and NOx at Torkel during weekdays (Mon-Thu) (top) and weekends (Sat-Sun) (bottom) for the whole campaign period.*

3.4 Correlations

Figure 12 shows the correlation (R-value) between parameters of interest at Hornsgatan and Torkel. At Hornsgatan a high correlation is seen between BC_{FF} and NOx (R = 0.82) while BC_{WB} and NOx have a lower correlation for the whole period (blue bars) (R = 0.44). The correlation is also high between BC_{FF} and traffic (number of vehicles) at Hornsgatan (R = 0.61) while BC_{WB} and traffic show a weaker correlation (R = 0.24). High correlation is also seen between BC_{FF} and particle number at Hornsgatan while BC_{WB} correlates more with $PM_{2.5}$ at both Hornsgatan and Torkel. Lowest correlation is found between BC_{WB} at Torkel and Hornsgatan and traffic at Hornsgatan. The winter period (red bars) show similar results with some small deviations e.g. higher correlation between BC_{WB} and $PM_{2.5}$.

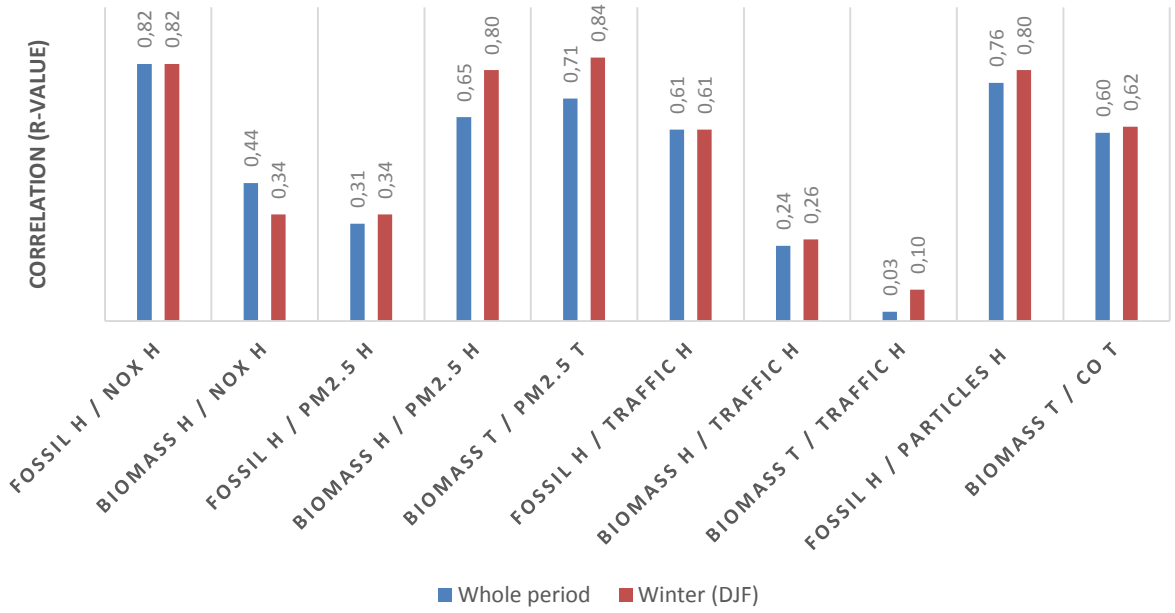

Fig. 12. *Correlation (R-value) between BC_{FF}, BC_{WB} and different parameters at Hornsgatan and Torkel. Blue bars indicating the whole campaign period and red bars are for winter month (Dec – Feb) only.*

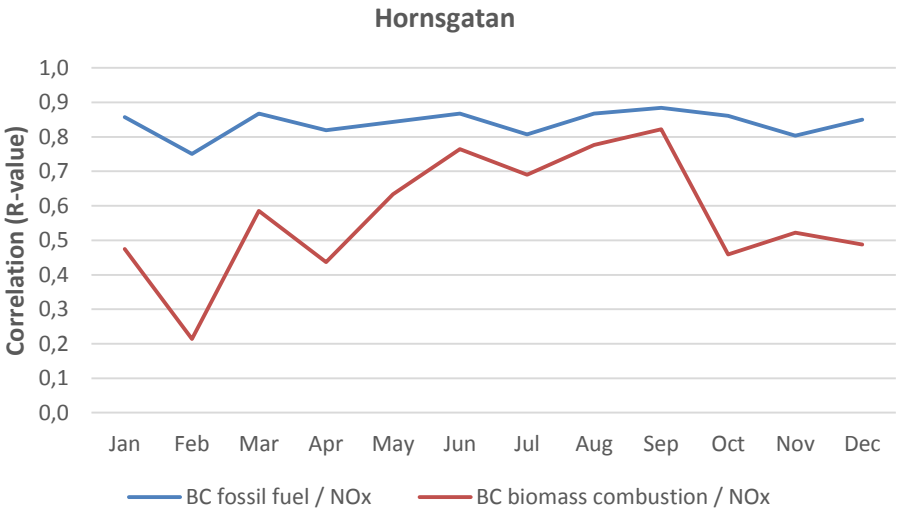

Fig. 13. *Annual variation of the correlation (R-value) between NOx and BC_{FF} (blue line) and BC_{WB} (red line), respectively, at Hornsgatan.*

The correlation between BC_{FF} and NOx (blue line in figure 13) show only small seasonal changes with an R-value > 0.80 during the whole year with only one exception in Feb (R = 0.75). An explanation to the small decrease in Feb might be a higher share of BC_{WB} due to more residential biomass combustion during this month when the temperature usually is low. The correlation between BC_{WB} and NOx (red line in figure 13) is lower during the whole year and has a much stronger annual trend with R-values ranging from 0.21 to 0.82. The correlation is highest during the warmer summer months and decreases during winter. The lowest correlation between BC_{WB} and NOx is seen in Feb (R = 0.21). The minimum correlation can be that BC_{WB} and NOx have different sources. If the temperature decreases it is possible that the share of

residential biomass combustion will increase (temperature and BC_{WB} at Hornsgatan were found to be anti-correlated with an R-value of -0.20 while BC_{FF} and temperature had an R-value of 0.04). However, the emissions of NOx will remain fairly constant which will result in a decrease in the correlation between BC_{WB} and NOx.

3.5 Application of the apportionment model to episodes

The apportionment model is, like all models, a simplification of the reality and therefore it is of great importance to test the model to look shortcomings and needs for improvements. The model has been evaluated by using known episodes of increased wood burning activities or events of air pollution long range transport or increased emissions from local sources. The variation in the diurnal cycle during different special occasions (e.g. the Christmas holiday) can also give good insight on how the model manage to separate BC from fossil fuel and biomass combustion.

3.5.1 Variations in the diurnal cycle

BC_{FF} at Hornsgatan (blue line in figure 14) has a strong diurnal cycle with five clear peaks at weekdays following the traffic rhythm. At Torkel (red line in figure 14) BC_{FF} has a weaker diurnal cycle but there is still a clear signal from the traffic. However, the difference between the amount of BC from fossil fuel (due to local road traffic) at Hornsgatan and Torkel is obvious. The diurnal cycle at the weekend is much weaker and the difference between Hornsgatan and Torkel comes to a minimum when the traffic impact are low. Advantageous conditions (e.g. strong winds that flavours dilution and effective mixing of the pollutants) can also play a significant role for the low levels of BC_{FF} that are seen but there is a clear difference between weekdays and weekends (also seen in table 8 in section 3.3.2). On the contrary, conditions that creates strong inversions will give the opposite effect and increase the difference between Hornsgatan and Torkel. During Sunday afternoon and evening a small increase is seen again. This is a typical example of the diurnal variation for most regular weeks during the year.

During a special holiday like Christmas the diurnal cycle is changed; the total amount of BC_{FF} is decreasing and the difference between Hornsgatan and Torkel is reduced.

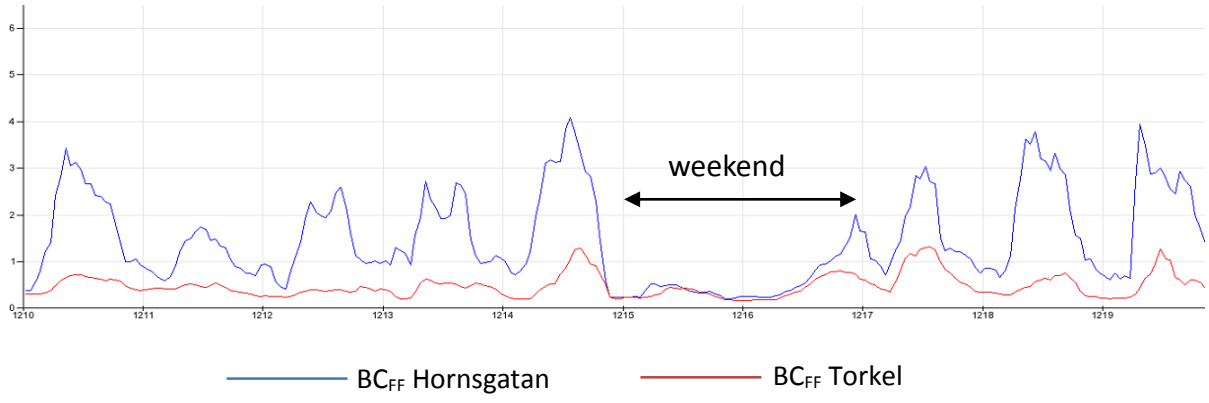

Fig. 14. *Diurnal cycle of BC_{FF} at Hornsgatan and Torkel with a time series of a typical week pattern.*

3.5.2 Episodes

The model was further evaluated using known episodes of increased wood burning activities, events of air pollution long range transport and increased emissions from local sources.

3.5.2.1 Local source

Figure 15 shows an example where the source to the increased amount of BC very likely is to be local with particles exhibit an increased absorption for shortwave radiation. A strong proof of a local source is that the BC mass concentration at the rural background site Aspvreten (red line), located south of Stockholm, is unchanged. Also $PM_{2.5}$ at Aspvreten (turquois line) is constant, a fraction that will be effected if there is a case of long range transport of particles. BC_{WB} at Torkel (blue line) and BC_{FF} at Torkel (purple line) is both increased but the amount of BC_{WB} is considerably higher. The difference in temperature between 2 and 20m (green dotted line) show that there was a strong inversion during this episode which largely can explain the increased amounts of BC. However, the normal case is not higher amounts of BC_{WB} than BC_{FF} when there are meteorological conditions like an inversion explaining increase concentrations of pollutants. There is probably also some kind of local emissions of biomass combustion that causes the increased contributions of BC_{WB} contra BC_{FF}. The wind during this period was westerly and weak, 1-2 m/s. An additional motive to a source that is not traffic related is the time for this event, as it occurs on a Sunday (Oct 13th) with little traffic, where the concentrations started to increase in the afternoon and the highest peak was reached at midnight.

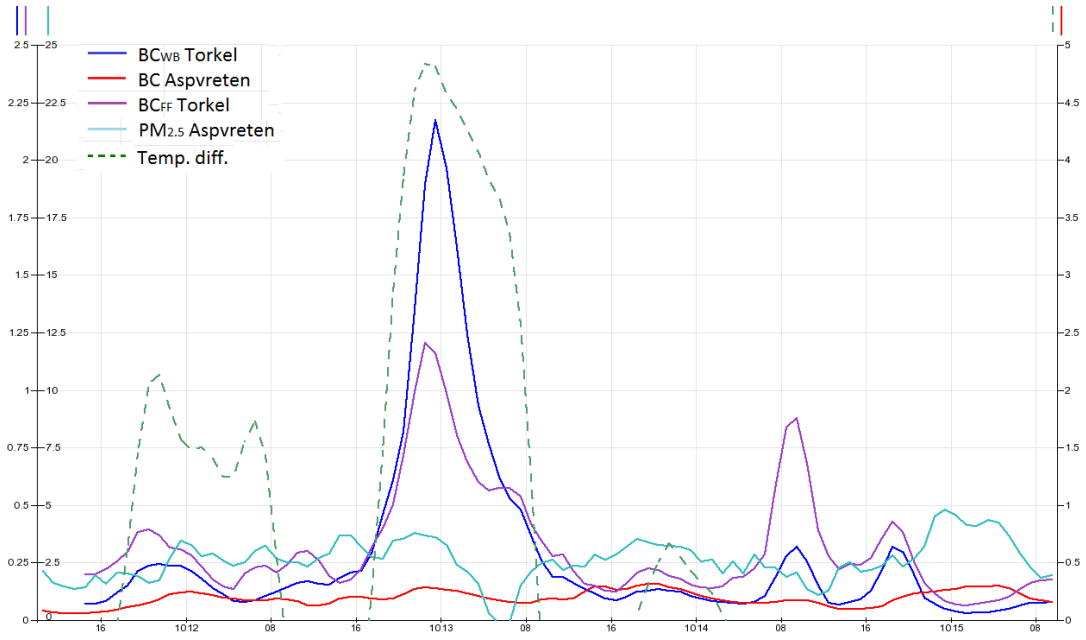

Fig. 15. *Local source episode at 13 Oct 2013.*

3.5.2.2 Long range transport

During the episode at 19 December 2013 there is a simultaneous increase for the observed concentrations of BC_{FF} and BC_{WB} at Torkel together with BC and $PM_{2.5}$ at Aspvreten (figure 16), which indicates a case of long range transport of polluted air, probably from the south since Aspvreten is located south of Torkel. Aspvreten is a rural background site and has no local sources nearby. This massive increase in both $PM_{2.5}$ (turquoise line) and BC (red line) concentration is not seen unless there is polluted air coming from sources located further away. The level of $PM_{2.5}$ is often most affected by long range transport due to a secondary formation of PM, of e.g. sulphates and nitrates, during the transport from source to measuring site. On the contrary, BC is not created during the transport and therefore decreases successively due to dilution and deposition (Johansson and Hansson, ITM-rapport 165, 2007). BC_{WB} (blue line) and BC_{FF} (purple line) at Torkel is also affected by the incoming polluted air, with increased concentrations that are in the same order of magnitude. This strengthens the assumption that this episode is not caused by a local source of either increased traffic emissions or local biomass combustion. A more likely explanation to the increased levels are to be found in the long range transported air mass containing particles both from traffic emissions and combustion of biomass. The wind direction (yellow line) can also play a significant role for the determining of long range particle transportation. During this episode there was a wind shift from westerly to southerly wind during the time of increased concentrations. The wind speed was 4-6 m/s.

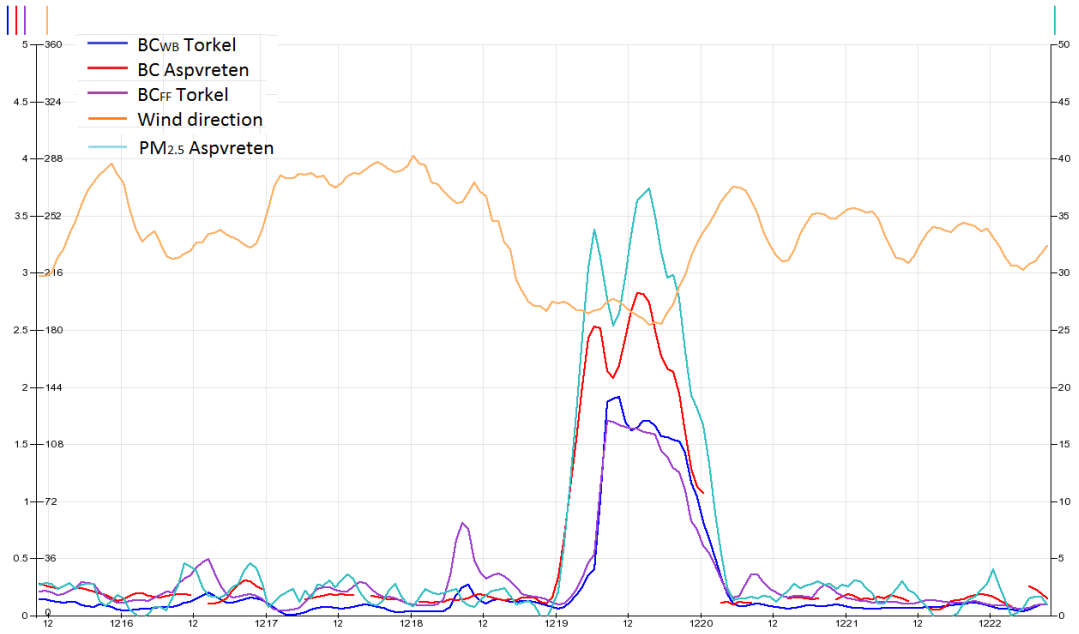

Fig. 16. *Long range transport episode at 19 Dec 2013.*

To be able to determine the origin of the polluted air mass a backward trajectory analyses can be made. This reveal how the air mass has been transported before reaching the measuring sites in Aspvreten and Torkel. If the air mass has been transported over areas known to have high emissions of pollution it is likely that the source to the increased concentrations in Aspvreten and Torkel is to be found somewhere along the way.

Fig. 17. *Backward trajectory of the air mass over Aspvreten and Torkel during the episode at Dec 19 2013. A red arrow corresponds to 6 h backwards in time from the end time at 12 UTC 131219.*

Figure 17 displays that the air mass over Aspvreten and Torkel during this episode has come from the south and travelled over areas known to have high emission rates. This further strengthens the assumption of long range transport of polluted air where the source is located abroad.

3.5.2.3 April 30

One occasion where the model really can be tested is when there is an episode of known increased biomass combustion. In Sweden, every April 30 people light bond fires to keep away evil forces (mostly withes and wild beasts) which creates an excellent opportunity for source apportionment studies of BC since bond fires only creates BC_{WB} (i.e. the particles contain a lot of brown carbon). During April 30 in 2013 (figure 18) a massive increase of BC_{WB} at Torkel (blue line) is seen while the concentration of BC_{FF} (purple line) stays unaffected. This is a really nice prove of a successful separation between the two sources of BC. BC at Aspvreten (red line) also increases but since there is so separation between FF and WB for this BC content it is hard to draw any conclusions for this increase. The wind was moderate, 3-5 m/s, temperature 6-9 degrees, no precipitation or inversion conditions. The wind (yellow line) was steady westerly until 4 AM the next day.

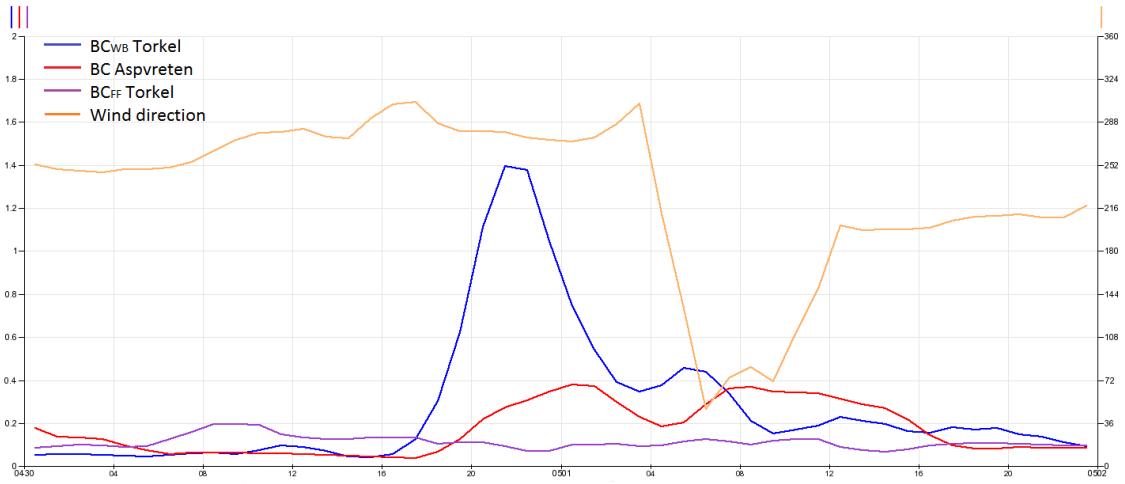

Fig. 18. *Biomass combustion episode at April 30 in 2013 due to local bonfire events.*

However, during the same occasion 2014 the pattern is different (figure 19). The increase in BC_{WB} is only minor and BC at Aspvreten is not showing any increased levels of BC particles at all. The wind was weak to moderate, 2-6 m/s, temperature 4-6 degrees dropping to 0 at midnight, no precipitation or inversion conditions. The only meteorological difference to be found as an explanation to this difference between 2013 and 2014 is found in the wind direction. During 2013 the wind was steady coming from the west, while 2014 showed a more diverse wind (yellow line) that was southerly during the day but shifted rapidly during the evening and became northerly instead. Since the separation between BC_{FF} and BC_{WB} was so successful for April 30 2013 it is unlikely that the explanation to the different pattern in 2014 is an error in the model. It is more likely to find explanations in the meteorological conditions which was present during this two occasions, e.g. the difference in wind direction.

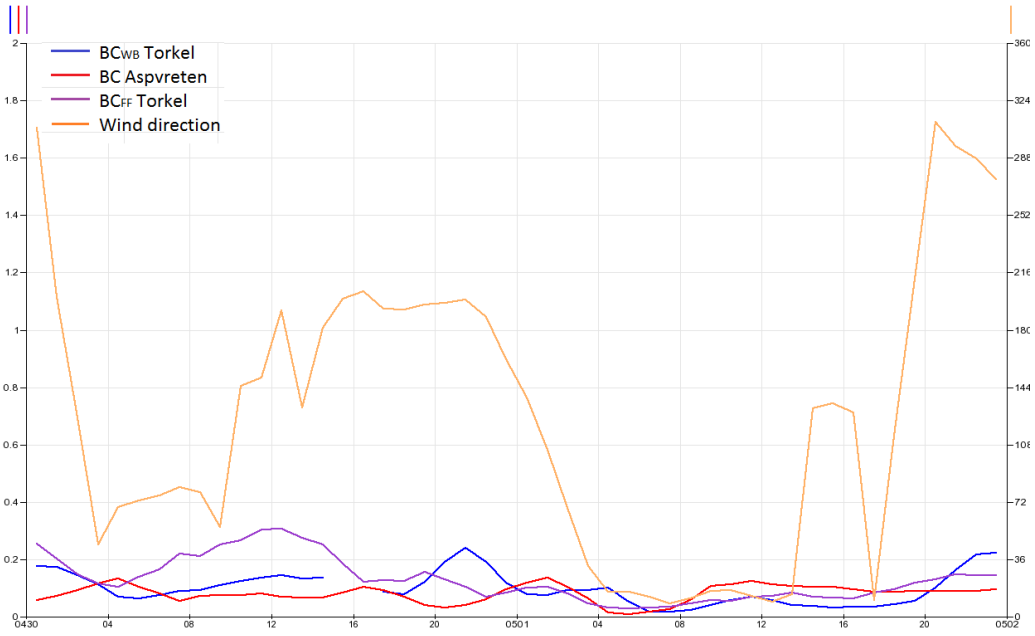

Fig. 19. *Biomass combustion episode at April 30 in 2014 due to local bonfire events.*

3.6 Uncertainties of the source apportionment

The apportionment model used to separate BC contributions from fossil fuel and biomass combustion used in this study is, like all models, associated with uncertainties.

The Aethalometer model (the optical attenuation method), relies on two assumptions; FF and WB emissions are the only sources of BC and the total ambient BC can be modelled by the light absorption of aerosols emitted by these two sources. However, there might be other sources contributing at certain occasions (e.g. long range transport) and impacts of other substances than BC and OC, holding enhanced absorbing properties in the UV-spectra giving rise to a "biomass signal" even though we know that there are only local traffic emissions contributing to the mass of BC. This might be one of the most difficult problems, trying to determine the amount of these substances and how much they effect the source apportionment. We know that traffic emissions contain OC and that traffic give rise to enhanced concentrations of PM containing for example mineral dust particles that can absorb strongly in the UV-spectra.

The artefact corrections for multiple scattering and shadowing effect is also associated with uncertainties. The amount of these artefacts and how much they affect the measurement result depend e.g. on the quartz filter used and the BC concentration at the measurement site. A site where the air is highly polluted will be much more affected by the shadowing effect while a site with clean air might experience a higher impact of multiple scattering. The best is to correct for these artefacts by site specific measurements since this phenomenon's depend on the site location. One instrument that automatically corrects for light scattering is the Multi-Angle Absorption Photometer (MAAP). The MAAP has multiple detectors to simultaneously measure transmitted and scattered light. Therefore BC content can be corrected with respect to the reflection and scattering of light in multiple directions due to particle size and shape. These measurements can then be used for comparison and quantifying of this uncertainty.

The choice of the Ångström exponent, α_{FF} and α_{WB}, is what has been pointed out as the largest uncertainty factor by earlier studies and it was obvious how sensitive this parameter was for the creation of negative b_{abs} (λ) values performing sensitivity analysis (table T7 and T8 in appendix).

Another important uncertainty lies in the derived site specific mass absorption cross sections from the OC/EC campaign. Using a calculated constant mean value from a more or less variable σ_{abs} (λ) can create deviations from the "true" σ_{abs} (λ) which leads to uncertainties in the source apportionment. An additional limitation is the assumption that σ_{abs} (λ) from FF and WB combustion ($\sigma_{abs,FF}$ (λ) and $\sigma_{abs,WB}$ (λ)) can be represented by the average site specific σ_{abs} (λ). This simplification can be justified by an absence of a seasonal cycle in the average site specific σ_{abs} (λ), something that can be supported (or disproved) by a longer OC/EC sampling period. The site specific σ_{abs} (λ) value is also used to retroactively change the BC mass concentration time series while the possibility that the site specific σ_{abs} (λ) can have changed during the years (due to the development of Stockholm). The same site specific σ_{abs} (λ) is used for both Torkel and Hornsgatan while the OC/EC campaign was only performed at Torkel. Herich et al. (2011) also used site specific σ_{abs} (λ) for three different sites and found differences in σ_{abs} (λ) between urban background and rural environment sites. The urban background site had higher σ_{abs} (λ)

values for longer wavelengths while the rural sites showed enhanced σ_{abs} (λ) values for shorter wavelengths. However, even though the two rural sites were similarly positioned regarding traffic impact and industry emissions, the σ_{abs} (λ) differed systematic for all wavelengths. This indicates that there is a large risk of differences in σ_{abs} (λ) between Torkel and Hornsgatan.

A final uncertainty lies in the different methods available for source apportionment studies, which make it difficult to compare results and do appropriate estimates of the overall uncertainties. For example, even though the same method is used there can still be differences in the choice of deriving site specific σ_{abs} (λ) or using the manufacturer σ_{abs} (λ) values, different ways of correcting for the artefacts (or not correcting for them at all) or the choice of α_{FF} and α_{WB}. Additional, different methods are available, e.g. linear regression of CM against $b_{abs,FF}$ (950 nm) and $b_{abs,WB}$ (470 nm) (Sandradewi et al., 2008a) are used in several studies (but only for shorter campaign periods).

The purpose of the above argumentation is both to point out the most important uncertainties and difficulties performing a source apportionment study, but also to illustrate the real world complexity and created limitations trying to explain real world events by the use of simplifications and parameterisations. In this study NOx was used as a tracer for fossil fuel combustion, but it is also possible to use tracers for biomass combustion, e.g. potassium or levoglucosan, that only come from the combustion of cellulose.

3.7 Further investigation of BC emissions at Hornsgatan

The source apportionment show the dominating contribution from traffic to the total BC concentration in ambient air at the two sites, especially at Hornsgatan. Therefore a further investigation was of interest that could contribute with deeper understanding about BC particles from traffic and perhaps further verification of the results from the source apportionment. The trends in measured BC concentrations should reflect the trends in emissions from local road traffic at Hornsgatan.

3.7.1 Particle size distribution

Particle number size distribution data are from Hornsgatan between Oct 7 2010 and Dec 16 2014. Fifteen minutes values have been averaged into hourly means. Figure 20 shows the particle number size distribution data for Hornsgatan during day time (6:00 AM – 18:00 PM) at weekdays Monday to Thursday.

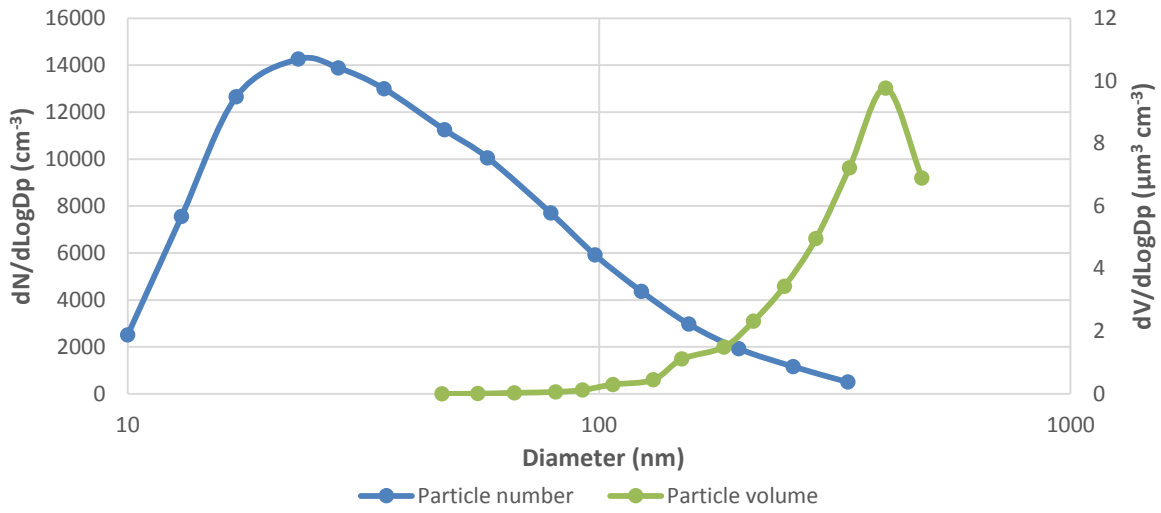

Fig. 20. *Particle number size distribution (blue line, left axis) and particle volume size distribution (green line, right axis) at Hornsgatan during daytime (6:00 AM to 18:00 PM) at weekdays (Mon – Thu) for the time period 101007 to 141216.*

The particle number (blue line) show a distribution shifted toward nucleation mode particles with a peak at 25 nm. The location of this peak in the size distribution is similar to the study by Gramsch et al. (2014) in Santiago de Chile but is slightly higher than in the study by Kittelson et al. (2004) and Wåhlin et al. (2001), which found a size distribution centered around 10 nm (near a highway) and 20 nm (in streets of Copenhagen). At Hornsgatan diesel vehicles represents a large share of the total emissions of particles in the size range for vehicle exhaust and nearly all diesel particulates have sizes of significantly less than 1 um (TRANSPHORM, 2013).

Figure 20 also displays the particle volume size distribution (based on the assumption of spherical particles) (green line) where instead the coarse mode particles are dominating giving rise to a peak around 250 nm. The small particles of the nucleation mode do not contribute much to the total volume. Instead the fewer, but larger, particles are more important.

The density for fresh BC exhaust particles have been found to be around 1.8 g/cm^3 (Eriksson, 2015). With the assumption of spherical particles a mass concentration could be derived for different size intervals and compared with measured mass concentration of local BC in ambient air. Unfortunately the background particle number concentration cannot be subtracted since there are no measurements of particle number at Torkel, but a comparison with particle number at Hornsgatan and Aspvreten (background site located south of Stockholm) showed almost no contribution of background particles to the local concentration of particles smaller than 100 nm. Based on traffic measurements and fuel share (high contribution from diesel LDTs and HDTs at day time) at Hornsgatan during 2009 (SLB 7:2010), the shift from gasoline to diesel from 2009 until present, and the amount of BC particles in exhaust from gasoline and diesel vehicles (EMEP/EEA, table A4-0-2, 2013), a mean density of 1.5 g/cm^3 for exhaust particles were assumed and multiplied with the particle volume distribution.

Table 9. *Total mass (µg m^{-3}) for different particle size intervals measured at Hornsgatan during daytime (6:00 AM to 18:00 PM) at weekdays (Monday to Thursday) for the time period 101007 to 141216. The total mass of BC (µg m^{-3}) is also showed together with the share of BC of total mass (%) in the different particle size intervals. The interval given for the percentage BC of total mass was obtained by letting the density for exhaust particles to vary with ± 0.3 g/cm^3 (from 1.2 to 1.8 g/cm^3).*

Particle size	Total PM-exhaust mass (µg m^{-3})	BC of total mass (%)
< 155 nm	2.42	59 (50 – 74)
47-155 nm	2.26	64 (53 – 80)
155-337 nm	4.26	34 (28 – 42)
< 337 nm	6.68	22 (18 – 27)
BC	1.44	

Using this approach 64 % of the total mass of exhaust particles in the size range 47-155 nm would be BC particles, which is in line with the amount of BC particles in exhaust from a vehicle fleet still containing a large percentage of gasoline and diesel vehicles. However, the uncertainties regarding the vehicle fleet in 2012 – 2015 compared to the measurements in 2009 and the amount of vehicles in different Euro classes is relatively high. For example the shift from Euro 4 to Euro 5 for diesel LDTs can decrease the amount of BC in the exhaust from 87 % to 10 % (with an uncertainty in this number increasing from 5 to 50 %) (EMEP/EEA, table A4-0-2, 2013). On the other hand, if the density for exhaust particles is allowed to vary with ± 0.3 g/cm^3 (from 1.2 to 1.8 g/cm^3) the BC amount would be 80 % and 53 %, respectively, in the BC size range 47-155 nm. The lower density assumed for the exhaust particles the higher influence the BC particles will have on the total mass concentration. Funasaka et al. (1998) found that EC concentration increased linearly with increase in diesel traffic (measurements in a highway tunnel in Osaka, Japan, with dense traffic of diesel vehicles) and that EC accounted for 71 % of PM with a diameter < 2 µm. Another study by Weingartner et al. (1997) in the same tunnel reported average BC contributions to PM_3 of 0.5 at the entrance and 0.3 at the exit. The founding's of the contribution of BC to PM-exhaust in this study is a little lower than found by these studies, with a possible explanation of a higher impact of diesel emissions in the tunnel compared to Hornsgatan. Table 9 show the total mass (µg m^{-3}) for different particle size intervals measured at Hornsgatan during daytime (6:00 AM to 18:00 PM) at weekdays (Monday to Thursday) for the time period 101007 to 141216.

3.7.2 Correlation between BC and particle size

A correlation between the time series for BC and different particle sizes at Hornsgatan during the time period of November 2012 to June 2014, indicates the size of the traffic generated BC particles. Figure 21 shows the correlation coefficient (R-value) between BC mass concentration during daytime (6:00 AM to 18:00 PM, Monday to Thursday) and particle number size at Hornsgatan. Traffic is supposed to be the only source to this BC fraction (local BC) since the blue line represents BC measurements at Torkel (background BC) subtracted from the BC measurements at Hornsgatan.

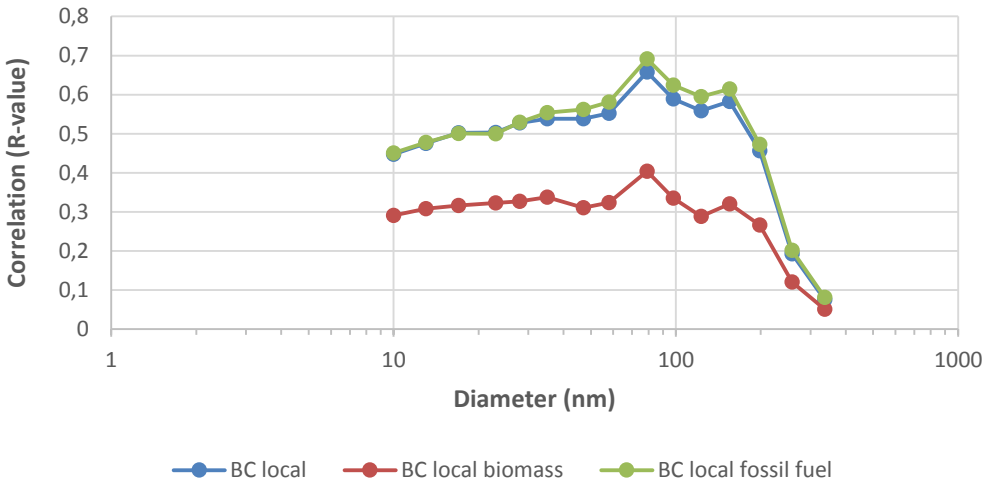

Fig. 21. *Correlation between local BC (blue line), BC_{WB} (red line) and local BC_{FF} (green line), and particle size during Monday to Thursday 6:00 AM to 18:00 PM for the time period of 121101 to 140601.*

Correlation between local BC particles and size reached a peak at about 80 nm with an R-value of 0.66. The correlation with particles below 80 nm are lower, indicating the importance of other processes than those affecting BC. The correlation between local BC and particles larger than 150 nm is much lower, indicating that most traffic related BC particles at Hornsgatan are in the size interval of 50-150 nm.

Measurements carried out in Lycksele, Northern Sweden, during winter 2005/2006 (Krecl et al., 2007) of the particle number size distribution and BC highly influenced by burning of biomass showed a correlation peak at 200 nm (R = 0.91). This shift towards larger particles can be explained by the differences in sources of BC, where Hornsgatan is an urban street site (with traffic as only BC source since the background is subtracted) and Lycksele is a small town with residential wood combustion as the dominant particle source. However, the correlation between BC mass concentration and particle number was larger than 0.60 even for nucleation particles and 0.87 for particles with a diameter of 80 nm, which is higher than Hornsgatan. Gramsch et al. (2014) studied the size distribution of particles and compared with BC in the urban area of Santiago de Chile in the winter of 2009. Two sites had a location similar to Hornsgatan with high traffic impact. They found a high correlation (R = 0.85) between BC and particles in the size range 175-700 nm, and a decrease in correlation with decreasing particle size (R = 0.40-0.52 for particles 10-39 nm). The higher correlation with the larger particle ranges were explained by influences of residential burning generating larger BC particles, while BC in this study (Hornsgatan) is from traffic only. Ning et al. (2013) measured BC particle size by tandem operation of a DMPS and a refined Aethalometer in different environments in Hong Kong. They found that the mass size distributions of BC from diesel engine tailpipe measurements peaked at 100-150 nm, similar to the results for Hornsgatan, while measurements further away from the source had peaks at larger diameters around 200 nm, showing the evolution of BC particles from source emissions to atmosphere and the influences of other sources than traffic.

Local BC_{FF} (green line) and local BC_{WB} (red line) in figure 21 is the BC fractions resulting from the source apportionment (Torkel subtracted from Hornsgatan) and should reflect the

amount of BC generated from local traffic at Hornsgatan (local BC_{FF}) and combustion of fuel that contains a higher amount of unburned hydrocarbons (local BC_{WB}) and therefore consist of molecules with a higher absorption capacity in the shortwave spectra giving a "biomass combustion fraction" of BC. At sites less affected by traffic, where combustion of biomass becomes a more contributing source to total BC (e.g. Torkel), BC_{WB} can be used as a more "true" marker for biomass combustion than at sites that are heavily affected by the local traffic. Since unburned fuel also consist of molecules more or less containing OC there will always be some absorbing differences between the wavelengths resulting in a "biomass combustion signal" even though there are no burning of biomass going on. For example stone minerals have the ability to absorb light in the UV spectra (EEA, 2013). The particles giving rise to BC_{WB} is assumed to be larger than vehicle exhaust particles, which can be used to investigate if there is a correlation between larger particles (> $PM_{2.5}$) and local BC_{WB}. This correlation was found to be higher (R = 0.57) for dry road conditions (i.e. high concentration of larger particles) compared to wet road conditions (R = 0.36), indicating the presence of larger UV absorbing particles (e.g. particles containing stone minerals).

The size distribution of local BC_{FF} follows, as expected, the same pattern as the local BC but with a slightly higher correlation for particles in the BC size fraction (50-150 nm), which can be explain by the local BC_{FF} being the local BC but without the contribution from BC_{WB}. BC_{WB} has significantly lower correlation for all particle sizes.

3.8 BC emission factors

As mention in section 2.3.4.3, four different approaches were used to calculate and evaluate EF's for BC.

1. Using TRANSPHORM absolute BC emission factors.
2. Using TRANSPHORM fraction BC emission factors (absolute BC emission factors calculated from the ratio BC/PM-exhaust, where PM-exhaust emission factors are from HBEFA).
3. Using the emission factor for NOx from HBEFA and scaling of the measured ratio in ambient air concentrations of local BC and local NOx at Hornsgatan (urban background at Torkel subtracted from the measurements at Hornsgatan).
4. Using local CO_2 measurements and emission factors for CO_2 from HBEFA and scaling according to the ratio of local BC/local CO_2.

3.8.1 Weighted EF's from road traffic at Hornsgatan (approach 1 and 2)

EF's (g/km) for BC, NOx and PM-exhaust were calculated for the different vehicle types and fuels dominating; BUS (diesel, ethanol, biogas), light duty vehicle (LDV/personal cars) (diesel, ethanol, biogas, gasoline), light duty truck (LDT) (diesel, gasoline) and heavy duty truck (HDT) (diesel). Two different approaches were used, one with absolute values for BC EF's given by TRANSPHORM (TRANSPHORM absolute BC EF's) and one with BC EF's calculated from the ratio BC/PM-exhaust (TRANSPHORM fraction BC EF's). The ratio BC/PM-exhaust was calculated using EF's from TRANSPHORM. This ratio was then applied to the EF's for PM-exhaust from HBEFA. The calculations were done with data from 2005 to 2015. Figure 22 show BC EF's for all vehicle types and fuels using approach 1 and 2.

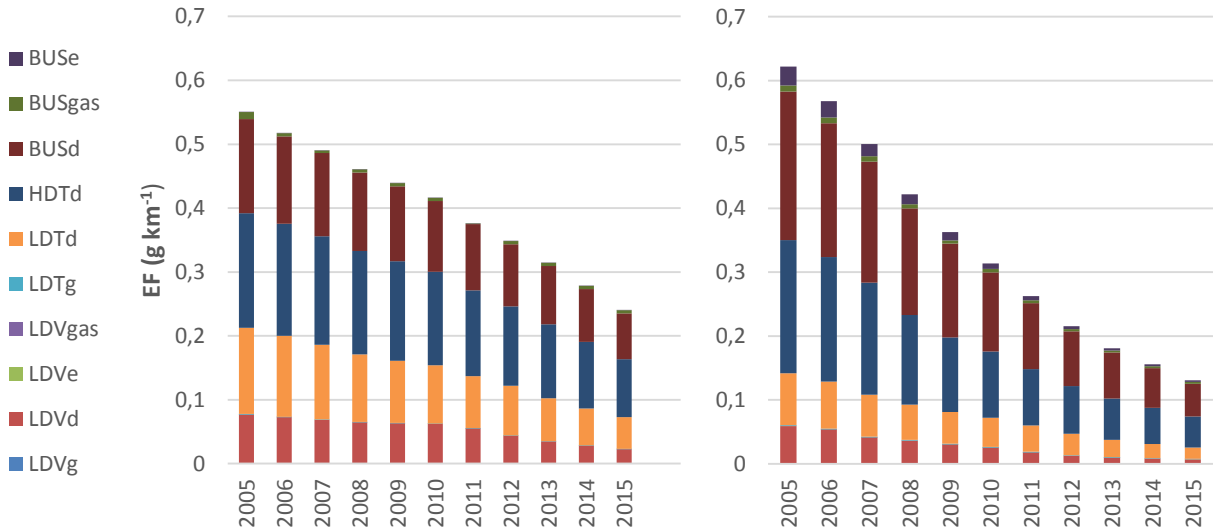

Fig. 22. *TRANSPHORM absolute BC EF's (g/km) (left) and TRANSPHORM fraction BC EF's (g/km) (right).*

Both the total time series and the individual composition for TRANSPHORM absolute and fraction BC EF's differ. The main explanation to this is that the ratio BC/PM-exhaust is based on simultaneously exhaust emission measurements of BC (giving TRANSPHORM absolute BC EF's) and PM-exhaust from the same vehicles, and then this ratio is applied to HBEFA PM-exhaust EF's, that are based on measurements from other vehicles, to obtain the TRANSPHORM fraction BC EF's. Therefore this approaches of deriving BC EF's will always differ. How much they differ is a function of several parameters, e.g. the number of vehicles and fuels that are tested, driving cycles that are used and after treatment technologies, like diesel particulate filters (DPF) that reduces the amount of emission particles. Since HBEFA has several subgroups to the different Euro classes, something that TRANSPHORM are missing, the implementation of new Euro classes will introduce differences between the approaches. Figure 23 show the differences of TRANSPHORM and HBEFA PM-exhaust EF's for different vehicles and fuels.

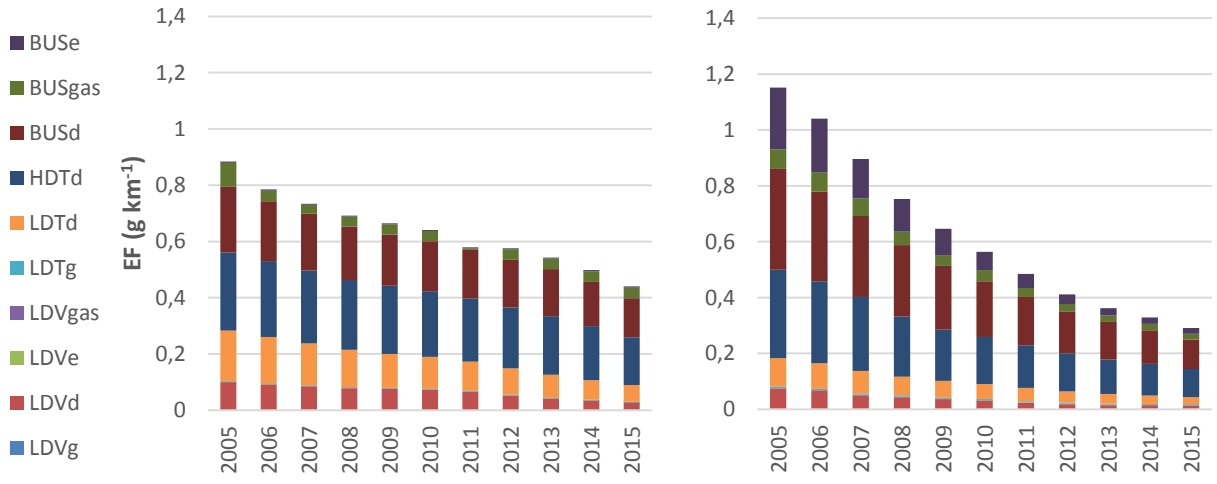

Fig. 23. *TRANSPHORM PM-exhaust EF's (g/km) (left) and HBEFA PM-exhaust EF's (g/km) (right).*

Even though HBEFA is supposed to provide more reliable EF's; more measurements, several subgroups of Euro classes and four levels of traffic service at Hornsgatan (compared to two for TRANSPHORM), the ratio BC/PM-exhaust can be assumed to be highly reliable since it is based on simultaneously measurements of the same vehicles. However, applying the ratios to HBEFA PM-exhaust EF's will result in a rather large difference in BC EF's due to the difference between TRANSPHORM and HBEFA PM-exhaust EF's, shown below in figure 24.

One way of evaluating the accuracy of the BC EF's derived using approach 1 and 2 is by comparisons with local ambient air measurements of BC. For that purpose a vehicle-km weighted EF for road traffic was finally calculated for BC and PM-exhaust, displayed in table 11. The vehicle-km weighted EF's are based on the assumption of a constant total vehicle-km (summing up the kilometres driven by all vehicles) but taking into account the development in fleet composition, according to table 10.

Table 10. *Development of the vehicle fleet composition at Hornsgatan for the years 2005 to 2015, given in percentage of the total vehicle fleet. This distribution is used for both TRANSPHORM and HBEFA.*

	2005	2006	2007	2008	2009	2010	2011	2012	2013	2014	2015
LDVg	75.76	69.57	61.07	53.22	49.38	44.40	40.72	36.62	34.68	30.29	29.43
LDVd	5.99	8.57	13.19	15.91	18.19	22.51	27.11	32.47	35.88	37.69	41.83
LDVe	1.41	4.27	6.79	11.95	13.00	11.96	9.53	7.21	6.12	6.82	5.57
LDVgas	1.37	2.13	2.13	1.83	2.43	3.59	4.51	5.00	4.63	6.15	3.74
LDTb	2.49	2.25	2.18	1.94	1.75	1.55	1.37	1.02	0.65	0.63	0.49
LDTd	9.76	9.85	11.46	12.02	12.25	12.83	13.42	14.21	14.58	14.91	15.36
HDTd	1.18	1.19	1.21	1.24	1.20	1.23	1.26	1.28	1.28	1.29	1.29
BUSd	0.27	0.27	0.30	0.29	0.28	0.29	0.34	0.37	0.38	0.41	0.43
BUSg	-	0.03	0.04	0.04	0.06	0.21	0.21	0.26	0.30	0.36	0.41
BUSe	1.77	1.87	1.62	1.57	1.47	1.42	1.53	1.55	1.50	1.47	1.45

Table 10 clearly illustrate the fuel shift from gasoline to diesel, mainly for LDVs and LDTs. Diesel LDVs (LDVd) is increasing with 117 % from 2005 to 2015 while gasoline LDVs (LDVg) is decreasing with 61 %. In the same time diesel LDTs (LDTd) increases with 57 % and gasoline LDTs (LDTg) decreases with 80 %. Table X displays TRANSPHORM absolute BC EF's that after 2006 are higher than HBEFA PM-exhaust EF's. This once again points out the differences between the different deriving approaches that TRANSPHORM and HBEFA uses (since BC can never exceed PM-exhaust).

Table 11. *Vehicle-km weighted EF's (g/km) for BC and PM-exhaust from road traffic at Hornsgatan for the years 2005 to 2015.*

	TRANSPHORM absolute BC EF	TRANSPHORM fraction BC EF	TRANSPHORM PM-exhaust EF	HBEFA PM-exhaust EF
2005	0.0207	0.0154	0.0293	0.0247
2006	0.0215	0.0155	0.0295	0.0240
2007	0.0251	0.0162	0.0333	0.0234
2008	0.0256	0.0151	0.0332	0.0212
2009	0.0258	0.0137	0.0329	0.0190
2010	0.0280	0.0135	0.0352	0.0181
2011	0.0280	0.0120	0.0357	0.0165
2012	0.0272	0.0102	0.0341	0.0148
2013	0.0242	0.0085	0.0304	0.0131
2014	0.0209	0.0073	0.0265	0.0121
2015	0.0190	0.0065	0.0236	0.0114

Figure 24 illustrates the annual mean vehicle-km weighted TRANSPHORM absolute and fraction BC EF's in comparison with the time series of local BC obtained from measurements at Hornsgatan and Torkel during the time period 2006 – 2015, using an aethalometer AE31.

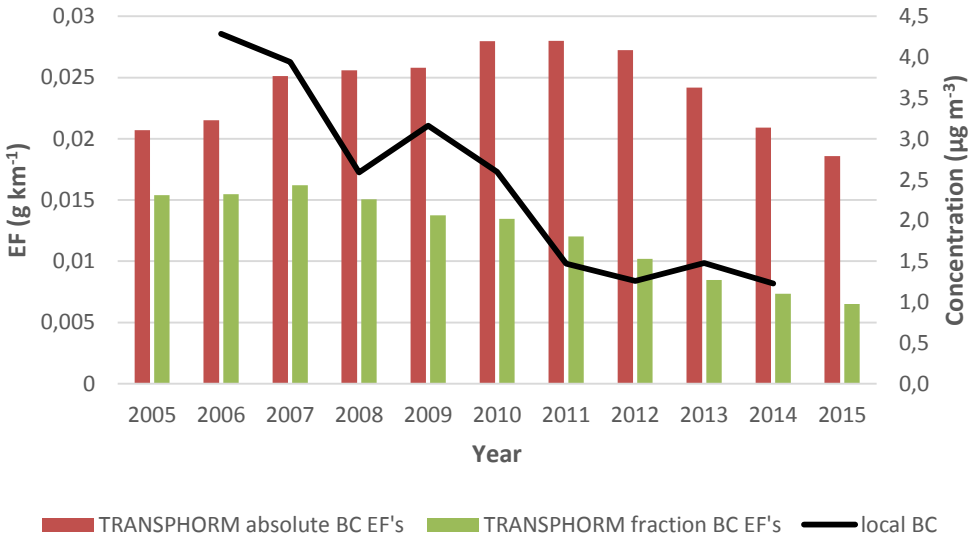

Fig. 24. *Annual mean vehicle-km weighted EF's (g/km) for TRANSPHORM absolute BC (directly given by TRANSPHORM) and TRANSPHORM fraction BC (absolute values calculated from the ratio BC/PM-exhaust (TRANSPHORM) with application to HBEFA PM-exhaust EF's). The black line show the time series of local BC concentration (µg m^{-3}) measured in ambient air during 2006 - 2014.*

The fuel shift, where diesel vehicles (having a high BC EF compared to gasoline) increasing very rapidly, will affect the vehicle-km weighted BC EF more or less depending on the approach used. TRANSPHORM absolute EF is increasing from 2005 to 2011, which is explained by the fact that the traffic load of diesel vehicles (i.e. diesel LDVs) is increasing faster than the absolute BC EF for diesel vehicles is decreasing. After 2011 the implementation of

higher Euro classes (especially those including the requirement of DPF) can be assumed to be sufficiently for the EF's to drop faster than the increase of diesel vehicles. Figure 25 show how many diesel vehicles in traffic at Hornsgatan that is of Euro 4 – 6, and therefore is obligated to have DPF, during the time period 2005 – 2015. Diesel HDTs show a fast increase with nearly 80 % Euro 4 – 6 in 2015, while only just above 30 % of diesel LDVs are Euro 4 – 6.

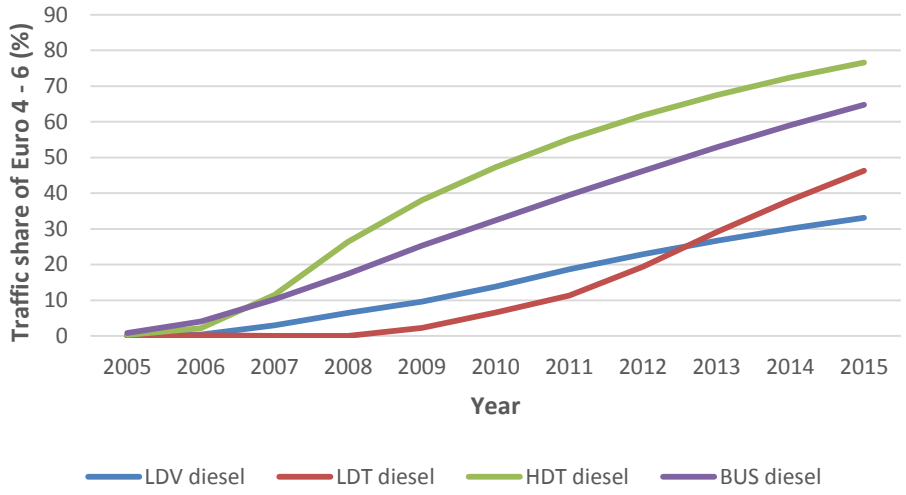

Fig. 25. *Traffic share of Euro class 4 – 6 (including requirements for DPF) at Hornsgatan from 2005 – 2015, obtained from HBEFA.*

The TRANSPHORM absolute BC EF (red bars in figure 24) show increased emissions of BC from local road traffic (30.2 %) between 2006 and 2011, which do not agree with the decreasing trend of 65.7 % in ambient air measurements of local BC during the same period (black line). The TRANSPHORM fraction BC EF (green bars), on the other hand, is decreasing with 22.6 %, which is more in line with the measured concentration trend. For the whole period 2006 to 2014 the TRANSPHORM absolute BC EF decrease with 2.8 % while the ambient air concentration decreases with 71.3 %. The TRANSPHORM fraction BC EF decreases with 52.9 %, once again showing a similar trend as local air measurements.

During three months in 2009 a camera automatically recorded the number plates of a large number of vehicles at Hornsgatan (SLB 7:2010). These recordings were used to calculate the contribution from different categories of vehicles to the emissions of NOx and ambient air concentrations of NOx and NO_2. The recordings can also be used to compare with the vehicle composition used for the TRANSPHORM absolute and fraction BC EF in 2009. This shows that the fleet composition used to calculate the TRANSPHORM absolute and relative BC EF was very consistent with the real-world vehicle measurements. The corrected TRANSPHORM absolute BC EF was calculated to be 0.0245 g/km instead of 0.0258 g/km, a decrease with 5.0 %, while the corrected TRANSPHORM fraction BC EF decreased from 0.0137 g/km to 0.0131 g/km, a decrease with 4.4 %.

Figure 27 show the emissions (kg/year) from the different vehicles and fuels using TRANSPHORM absolute BC EF's compared to TRANSPHORM fraction BC EF's. For the emission calculations the change in traffic load at Hornsgatan has been taken into consideration.

In 2006 a congestion tax was introduced for inner Stockholm and in 2010 the ban of using studded tires at Hornsgatan was conducted. Figure 26 show the time series for the amount of vehicles per day at Hornsgatan.

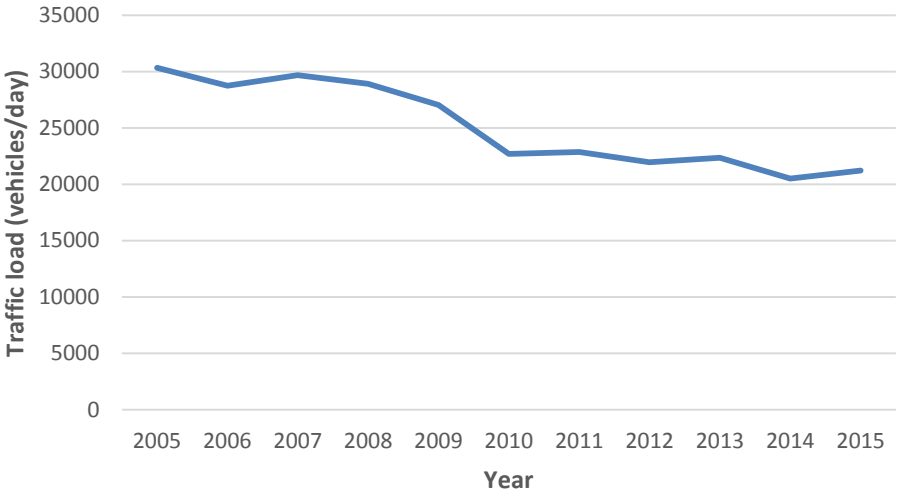

Fig. 26. *Time series of the traffic load (vehicles/day) at Hornsgatan from 2005 to 2015.*

It is obvious that diesel is the major contributor to the total emissions of BC (kg/year), regardless the choice of BC EF approach. However, the absolute values differs as already mentioned, and the time series has different appearances. The main contributors are diesel LDVs and LDTs, which in principal alone has stand for all BC emissions at Hornsgatan in resent years. The BC emission time trend based on TRANSPHORM fraction BC EF's once again show a pattern more like the trend of the real-world BC concentration measured in local ambient air, giving the overall conclusion that the TRANSPHORM fraction BC EF's is more correct to use.

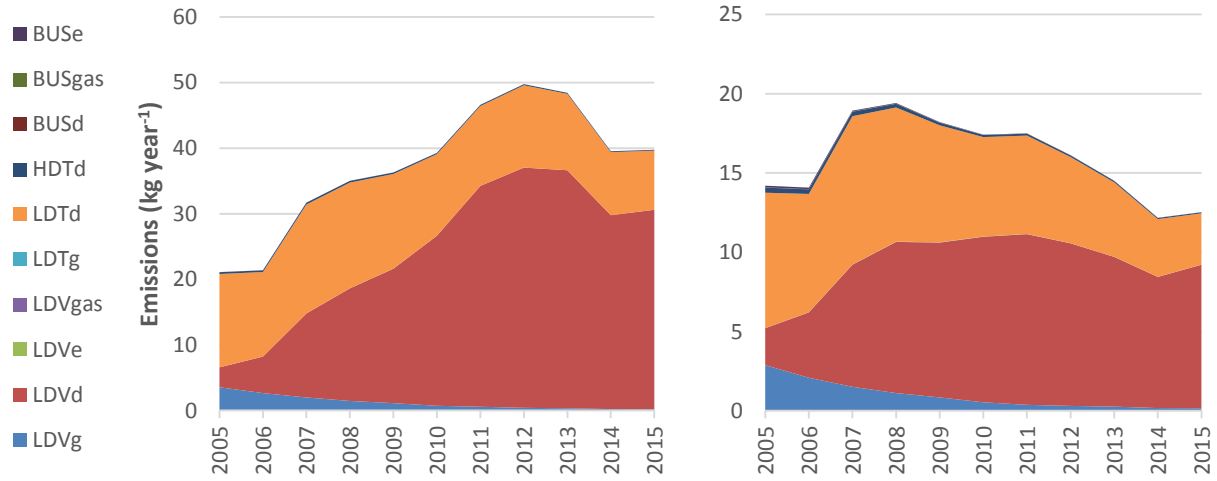

Fig. 27. *Emissions of BC (kg/year) at Hornsgatan from different vehicles and fuels using TRANSPHORM absolute BC EF's (left) and TRANSPHORM fraction BC EF's (right).*

3.8.2 EF's based on NOx together with measurements in ambient air (approach 3)

The aim with this approach was to find a way to estimate an EF for BC with lower uncertainty since NOx from traffic is a regulated pollutant according to the EU emission directive and therefore much more measured than BC, giving an EF for NOx with lower uncertainty. Both NOx and BC have been measured in ambient air at Hornsgatan and Torkel for several years giving a rather long time series to use for this approach. The measurements for simultaneously data for NOx and BC used for the further calculations are from April 14 2006 to June 26 2014, Monday to Thursday 6:00 AM to 18:00 PM. Both NOx and BC mass concentration are assumed having traffic as only source since the background values measured at Torkel are subtracted from the measurements at Hornsgatan (local NOx and local BC). The concentration trends (based on the annual median value) during this time period for the two pollutants are different, which are displayed with blue (local BC) and red (local NOx) lines in figure 28. The local BC/local NOx ratio time series is given by green bars showing how the decrease in local BC generate in a decreasing ratio trend. The error bars are the 25th and 75th percentile of the local BC/local NOx ratio. All data of the measured local BC and local NOx are given in T12 in appendix.

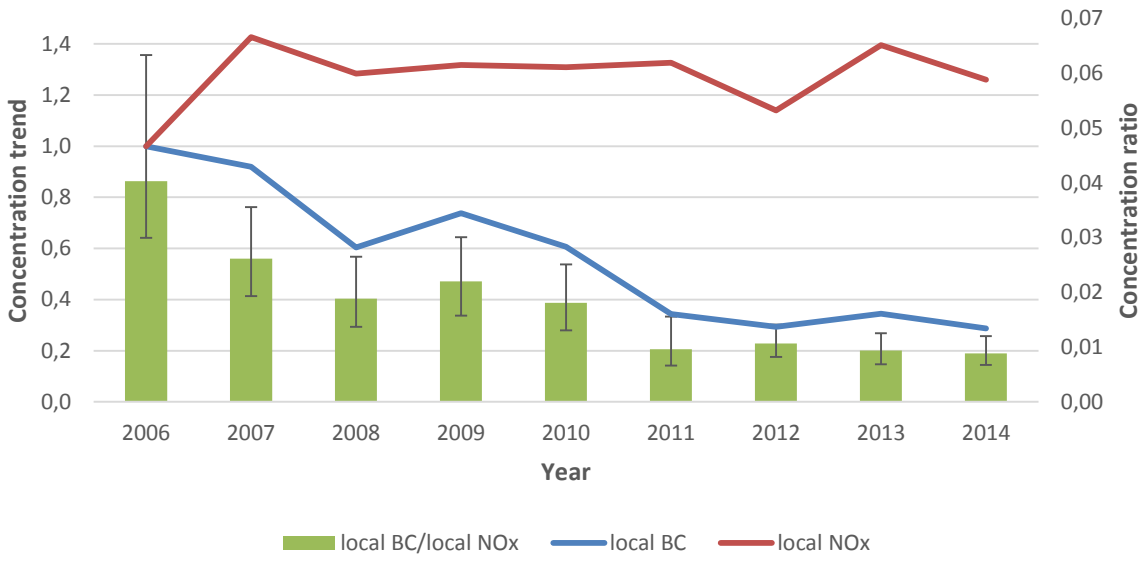

Fig. 28. *Time series of the concentration trend (based on the annual median value) (left axis) for local BC (blue line) and local NOx (red line). The local BC/local NOx ratio time series (green bars) (right axis), with error bars showing the 25th and 75th percentile of the local BC/local NOx ratio, are also displayed. All measurements are from April 14 2006 to June 26 2014, Monday to Thursday 6:00 AM to 18:00 PM.*

The local BC/local NOx ratio decreases with 78.0 % between 2006 and 2014, which is only due to the large decrease of 71.3 % in local BC. Local NOx show a time series with only very small changes.

Figure 29 illustrates HBEFA NOx EF's for the different vehicles in the fleet from 2006 to 2014. A decrease is observed for all vehicle categories and fuels.

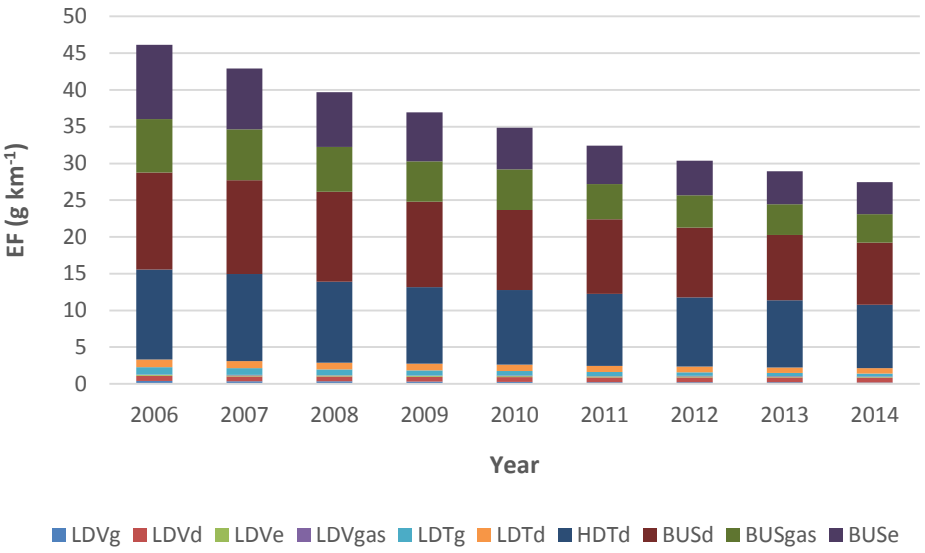

Fig. 29. *NOx EF using HBEFA for the different vehicle categories and fuels at Hornsgatan from 2006 to 2014.*

Using the same fleet composition development as before (table 10) and the assumption of a constant total vehicle-km for the whole fleet, a vehicle-km weighted NOx EF was calculated for the years 2006 – 2014, shown in table 12.

Table 12. *Vehicle-km weighted EF's (g/km) for NOx from road traffic at Hornsgatan for the years 2005 to 2015 using HBEFA.*

	2006	2007	2008	2009	2010	2011	2012	2013	2014
NOx EF	0.83	0.76	0.72	0.67	0.66	0.64	0.67	0.66	0.65

The annual vehicle-km weighted NOx EF's is shown in figure 30 (right) together with the NOx emissions (kg/year) (left) based on these EF's. Since diesel vehicle is known to emit a higher amount of NOx than gasoline vehicles the fuel shift is affecting the vehicle-km weighted NOx EF even though the individual EF's for each vehicle category and fuel is decreasing steadily from 2006 to 2014. However, there is a steady decreasing trend of the vehicle-km weighted NOx EF from 2006 to 2011. Contrary to the vehicle-km weighted TRANSPHORM absolute and fraction BC EF that decreased from 2011 and forward, a levelling off (and a small increase) is seen in the NOx EF after 2011. The same pattern is seen for the emissions of NOx. One explanation to this can be that the after treatment techniques used to decrease the emissions of NOx are not that effective as for BC. The modelled NOx EF has been found to be underestimated compared to the real-world NOx EF (Carslaw et al., 2011).

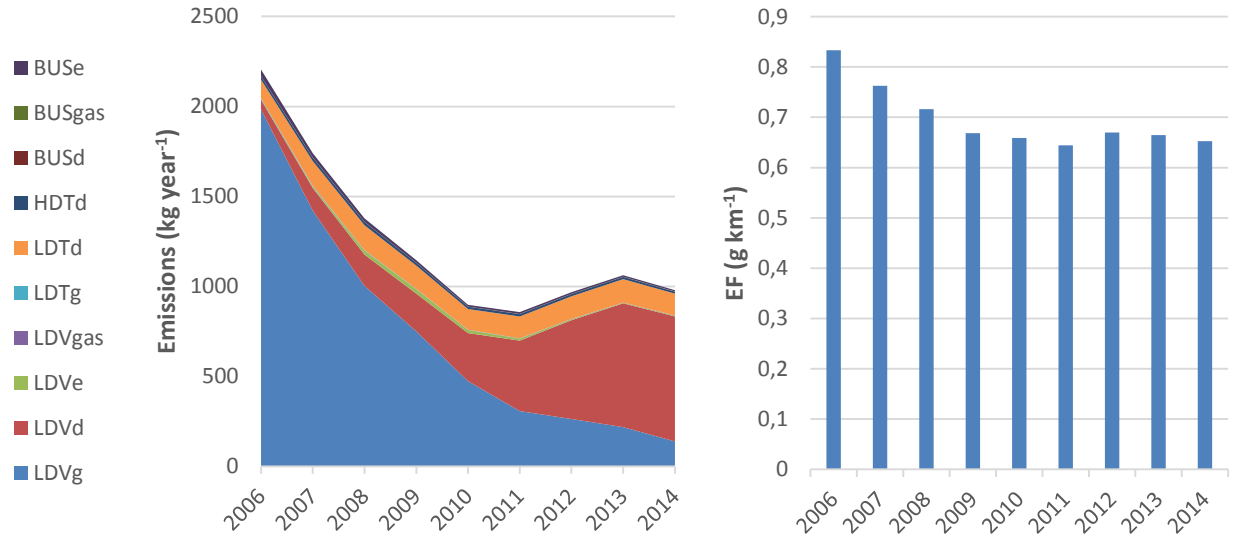

Fig. 30. *Emissions of NOx (kg/year) using HBEFA (left) and vehicle-km weighted NOx EF (g/km) using HBEFA (right).*

The vehicle-km weighted NOx EF has decreased between 2006 and 2011 with 22.7.0 %, while the measurements of local NOx in ambient air at Hornsgatan has increased with 25.9 %, indicating that the real-world NOx EF decrease less than the calculated (which also has been shown in several studies, e.g. Carslaw et al., 2011). However, the local NOx concentration in 2006 was unusually low and differed a lot from the value in 2007. Taking an average of 2006 and 2007 years median concentrations resulted in an increase of local NOx with 7.9 % between 2006/2007 and 2010, which indicates that the calculated NOx EF can be underestimated.

Looking at the whole time series (2006 – 2014) the decrease in the NOx EF is in total 21.7 % while the ambient air concentration increases with 3.8 % (using the mean value of 2006 and 2007). NOx emissions was in the past totally dominated by gasoline LDVs, but the decrease has been massive and after 2011 diesel LDVs has accounted for the dominating part of NOx emitted from local traffic at Hornsgatan (see figure 30, left).

To be able to compare with the vehicle-km weighted BC EF's from approach 1 and 2 (table 11), the median value of the local BC/local NOx ratio for 2006 to 2014 were multiplied with the vehicle-km weighted EF for NOx according to

$$\mathrm{EF\ (BC)_{year}} = \mathrm{EF\ (NOx)_{year}} \left(\frac{\text{local BC}}{\text{local NOx}}\right)_{\text{year}} \qquad (14)$$

The NOx based EF's together with the TRANSPHORM absolute and fraction BC EF's are displayed in figure 31. The error bars show the NOx based BC EF's calculated from the 25th and 75th percentile, while the purple line represents the time series for the concentration ratio of local BC/local NOx used to calculate the NOx based BC EF's.

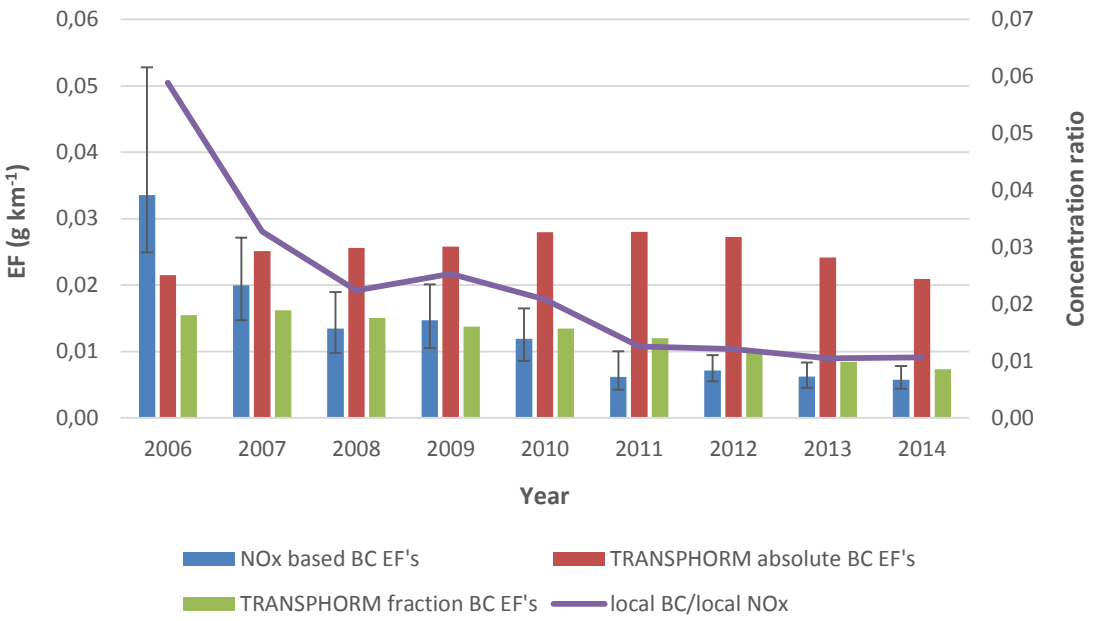

Fig. 31. *NOx based BC EF's (blue bars) together with the TRANSPHORM absolute (red bars) and fraction BC EF's (green bars) (g/km) (all EF's on the left axis). All NOx based EF's are calculated from data April 14 2006 to June 26 2014, Monday to Thursday 6:00 AM to 18:00 PM. The error bars show the NOx based BC EF's calculated from the 25th and 75th percentile of the local BC/local NOx ratio. The purple line represents the time series for the concentration ratio of local BC/local NOx used to calculate the NOx based BC EF's (right axis).*

The calculated NOx based BC EF's (blue bars) has a decrease from 2006 to 2014 of 82.8 %, which is in line with the decrease of local BC of 71.3 % in local ambient air. Since this EF calculation approach is based on the more certain NOx measurements in local ambient air, the uncertainties could be considered to be lower. The time series of TRANSPHORM fraction BC EF and the NOx based BC EF has a similar trend and are both following the trend for the concentration of local BC.

However, the approach is also based on the EF for NOx which might be underestimated. If the NOx EF instead is considered to increase according to the measurements of local NOx (3.8 % between 2006/2007 and 2014) and not decreasing according to HBEFA (21.7 %), the NOx based BC EF would increase to 0.0076 g/km for 2014 (an increase of 32.6 % compared to HBEFA). This additional increase in the NOx based BC EF would lead to a total decrease of 77.2 % (instead of 82.8 %), which means an even better agreement with ambient air measurements. But there is a further aspect to this, namely the levelling off of NOx EF from 2011 to present. Considering only the period 2011 – 2014, the HBEFA NOx EF is 1.3 % higher 2014 compared to 2011. The ambient air concentration of NOx decreases by 5.1 % during the same time, which once again indicates that there might be an underestimation of the NOx EF. Since the NOx based BC EF are calculated according to eq. 14 and proportional to the NOx EF, the NOx based BC EF will also be underestimated. However, the similarity between the trends of the NOx based BC EF and the ambient air concentration of BC indicates that the approach of a NOx based EF for BC can be a reasonable way of estimating BC EF's from local air measurements of BC and NOx, combined with HBEFA NOx EF.

In the same manner as for the "correction" of the TRANSPHORM absolute BC EF in 2009, the camera recordings of vehicle composition performed at Hornsgatan (SLB 7:2010) could be used to "correct" the NOx EF and ultimately the NOx based BC EF. This change was found to be a decrease of 9.1 %, a somewhat larger change than for the TRANSPHORM absolute and fraction BC EF.

3.8.3 EF's based on CO_2 together with measurements in ambient air (approach 4)

The same procedure as for the NOx based approach were used to calculate EF's for BC based on EF's for CO_2 and measurements of CO_2 and BC concentration in local ambient air. CO_2 at Hornsgatan has no other source than the traffic which make this an approach with high potential for EF's of BC associated with low uncertainties. The time series for CO_2 measurements at Hornsgatan and Torkel is only for a short period, 14 October 2014 to 11 May 2015, Mon – Thu 06-18, but this approach for deriving BC EF's are still of great interest to evaluate. The CO_2 based EF for this period was calculated to be 0.021 g/km (0.016 – 0.035 g/km based on the 25th and 75th percentile of the local BC/local CO_2 ratio). This can be compared to the TRANSPHORM absolute and fraction BC EF (for 2015), displayed in figure 32.

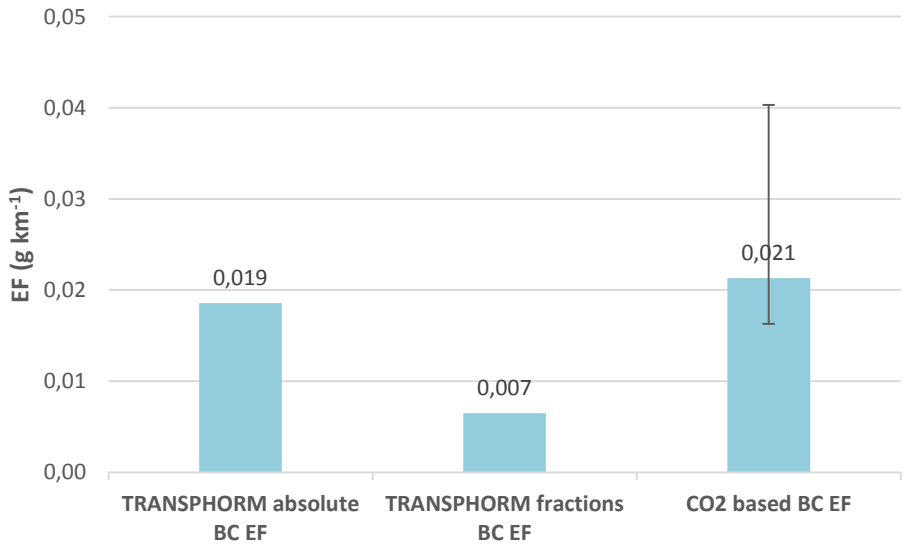

Fig. 32. *CO_2 based BC EF for the period 14 October 2014 to 11 May 2015, Mon – Thu 06-18. Displayed are also the TRANSPHORM absolute and fraction BC EF for comparison. The error bars show the CO_2 based BC EF calculated from the 25th and 75th percentile of the local BC/local CO_2 ratio.*

The CO_2 based BC EF is substantially higher, which can have several explanations. First, the vehicle-km weighted EF for CO_2, derived by dividing the emissions by the vehicle km's (data for Hornsgatan from the latest emission database (EDB) in the Airviro system, using HBEFA), calculated to be 299 g/km, might be too low or too high. A sensitivity analysis of the vehicle-km weighted EF for CO_2 with ± 100 g/km resulted in a variation of the CO_2 based BC EF between 0.014 and 0.028, which lies in the interval of the 25th and 75th percentile. The conclusion is therefore that the uncertainty in the vehicle-km weighted EF for CO_2 has only minor effect on the uncertainty in the EF for BC.

Another uncertainty comes from the mean value of the local BC/local CO_2 ratio. The background concentration of CO_2, measured at Torkel, is high which means that the difference between Hornsgatan and Torkel (local CO_2) is low and relatively sensitive to small changes (e.g. seasonal or meteorological variations). While this approach only have data provided for a limited time period the results may be affected by the seasonal, which is something that must be taken into account. The time series of local CO_2 (figure 33, green line) during this period reveals that this might be the case.

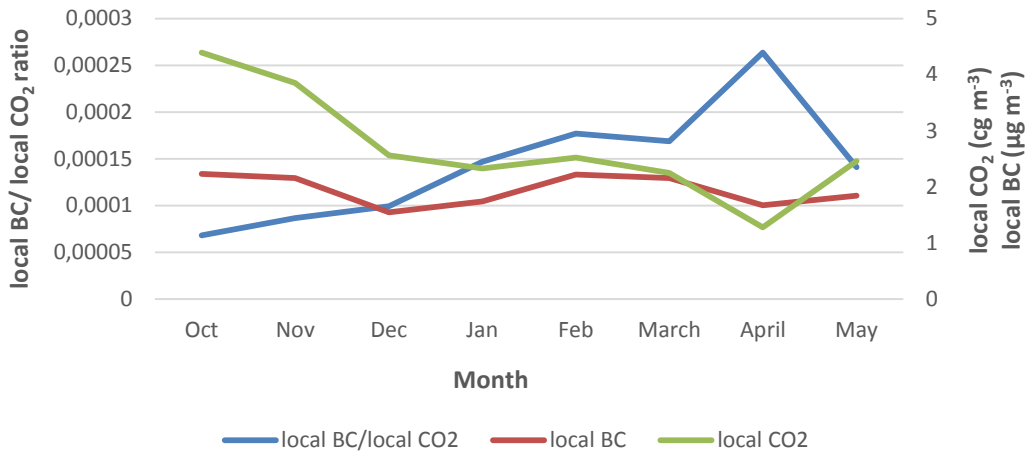

Fig. 33. *Time series of the local BC/local CO_2 ratio (left axis) and local CO_2 (cg m^{-3}) and local BC (µg m^{-3}) (right axis) for measurements at Torkel and Hornsgatan during the time period 14 October 2014 to 11 May 2015, Mon – Thu 06-18.*

Local BC (red line) has a more or less constant value during the period while local CO_2 (green line) decrease relatively much from Oct to April (70.8 %). This leads to a major increase in the local BC/local CO_2 ratio (blue line) of 286.4 %. This points out the limitation of using such a short period for this approach. A sensitivity analysis using the lowest value in Oct and the highest value in April gave a CO_2 based BC EF ranging from 0.020 to 0.079 g/km. This approach might have potential but it has to be further evaluated, especially by a longer time series for the determination of a more representative average value of the local BC/local CO_2 ratio.

3.8.4 Uncertainties regarding the calculation of emission factors at Hornsgatan

3.8.4.1 Slope of the road

Hornsgatan has a slope of about 3 % with an uphill westward and a downhill eastward. This means that the traffic travelling uphill is on the north side of the street and the traffic running downhill is on the south side. All measurements at Hornsgatan is done on the north side since the slope of the road can play a significant role for the amount of emissions from local road traffic.

Sensitivity analysis of Hornsgatan slope show that the weighted EF for NOx can be more than double as high for traffic travelling westward compared to eastward. The EF ratio W/E was found to be 2.35 and the ratio W/no slope was 1.34. However, it is assumed that the traffic load is about the same uphill and downhill but the slope can still play a significant role at special meteorological conditions, especially when the wind is blowing perpendicular to the street causing a street canyon effect with rising pollutant levels on the leeward side of the street. If this side is the same side as the uphill side, the higher EF's caused by the slope of the road will contribute much more to the levels in ambient air than if the uphill side pollutants were efficiently diluted. The slope effect may not be so important for the trend analysis. Also it is likely that BC emissions are also affected by the slope, making the ratio of BC to NOx somewhat less sensitive to the slope effect.

3.8.4.2 Level of service

The level of service is a measure used to relate the quality of traffic service by categorization of the traffic flow into four groups; free flow, heavy, saturated and stop and go, depending on the amount of vehicles. It is important for calculated emissions from road vehicles which level of service that is assumed for the road or area of interest and this can affect the EF's to a large extent. The maximum speed at Hornsgatan is 50 km/h. A sensitivity analysis of the importance of the level of service for the weighted NOx EF at Hornsgatan was done comparing the speeds 30, 40 and 50 km/h. As displayed in figure 34 the speed has a positive influence (decreasing EF's) on the different categories of service. The highest EF's is found for stop-and-go conditions and the lowest for free flow, as expected.

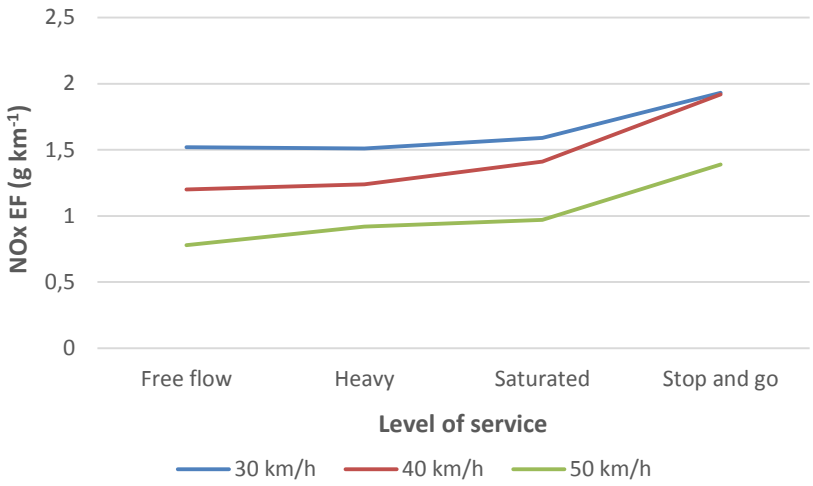

Fig. 34. *NOx EF's for local road traffic at Hornsgatan depending on level of service at different maximum speeds.*

However, the composition of the level of service at Hornsgatan is not constant. The assumed distribution of the level of service is based on measurements of the vehicle amount and speed during day and night that is averaged into hourly means. Depending on the splitting value between the groups the composition will be different. However, with splitting values of <1200 vehicles/h (free flow), 1200-1500 vehicles/h (heavy), 1500-1800 vehicles/h (saturated) and >1800 vehicles/h (stop-and-go) a typical level of service can be decided (for every hour) and used for the calculation of a weighted EF from the local traffic at Hornsgatan. The variance of the EF can be covered by assuming a maximum EF for only stop-and-go conditions and a minimum EF for only free flow conditions. The weighted NOx EF, with an hourly typical level of service, at Hornsgatan is displayed in figure 35, with error bars showing values for stop-and-go (maximum) and free flow (minimum).

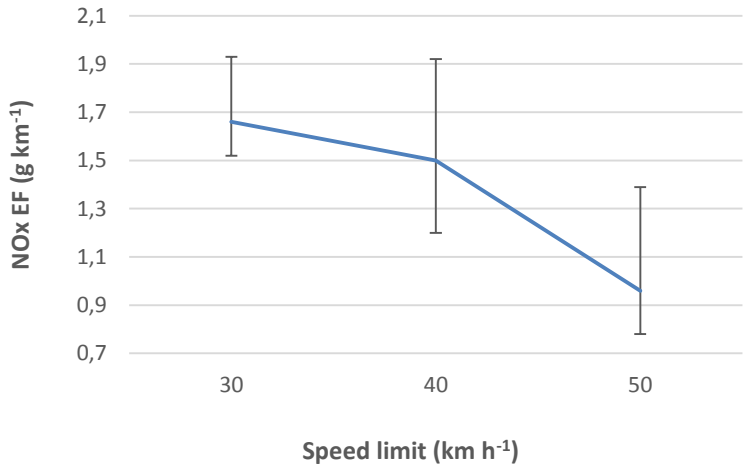

Fig. 35. *NOx EF for local road traffic at Hornsgatan assuming an hourly typical level of service at different speed limits. The error bars showing the maximum and minimum EF with only stop-and-go conditions or free flow conditions, respectively.*

The increase in the EF between free flow and stop-and-go conditions are 28, 60 and 78 % for 30, 40 and 50 km/h, respectively. The effect of level of service on BC is not known but likely to be important. However, the ratio of BC to NOx will be less sensitive in the same way as for the slope effect.

3.8.4.3 Other important factors

The criteria for vehicle selection is an important parameter since the EF can differ a lot depending on vehicle characteristics, emission control technology, fuel specifications and operating conditions like cold-starts and acceleration (Franco et al., 2013). At Hornsgatan cold starts is not a problem but it is possible with increased EF's due to acceleration after stopping at a red light or making a 90 degree turn.

Overall, the conclusion is that the above uncertainty factors can add or cancel each other out. A comparison with measurements provide information of the overall uncertainty of the calculated EF's. For Hornsgatan the trend analysis is assumed be rather unaffected by the above uncertainty factors since NOx, CO_2 and BC probably will be affected simultaneously, making the ratio of BC to NOx and BC to CO_2 less sensitive to external circumstances.

4 Conclusions

4.1 Conclusions of the conducted study

This study has utilized the wavelength dependence to distinguish between the contribution of BC from the major sources in Stockholm; traffic and residential biomass combustion. The optical attenuation method was applied to data collected from Nov 2012 to June 2014 at two measurement sites in Stockholm; Hornsgatan and Torkel. This was the first time in Sweden that the contributions of FF and WB emissions to BC were investigated using data from a multiple-wavelength aethalometer.

- At Hornsgatan, for the whole campaign period the contribution to the average BC mass concentration was 84 ± 6 % from FF and 16 ± 6 % from WB. In winter the contribution from WB increased to 20 ± 6 % while in summer it was half of that in winter (11 ± 7 %). At Torkel, the contribution from FF was 66 ± 6 % and from WB 34 ± 6 %. The contribution from WB during winter was 39 ± 6 % and during summer 25 ± 5 %. The absolute values of BC_{WB} are relatively similar at Hornsgatan and Torkel while BC_{FF} was 3.6, 4.1 and 2.8 times higher in total, in summer and in winter, respectively, at Hornsgatan compared to Torkel.
- The time series showed an annual pattern with higher contributions from WB during colder periods while warmer periods were characterized by higher contributions of FF.
- The contribution of BC_{FF} and BC_{WB} to $PM_{2.5}$ at Hornsgatan was found to be 17.9 and 2.9 %, respectively, during daytime (Mon-Thu 06-18) decreasing to 8.2 and 2.1 % at weekends (Sat-Sun). The contribution from BC_{WB} was found to be less than 3 % for all periods. At Torkel the contribution from BC_{WB} was about two times higher compared to Hornsgatan and around 4.5 % (highest during winter with 5.7 %).
- The diurnal variation showed a separation between BC_{FF} and BC_{WB} with clear differences between the two sources. The diurnal pattern for NOx was almost identical to BC_{FF} but differed from BC_{WB}, consistent with the fact that NOx is a good tracer for vehicle exhaust, not for biomass combustion.
- At Hornsgatan a high correlation was seen between BC_{FF} and NOx (R = 0.82) while BC_{WB} and NOx had lower correlation (R = 0.44). The correlation was also high between BC_{FF} and traffic at Hornsgatan (R = 0.61) while BC_{WB} and traffic showed a weaker correlation (R = 0.24).
- The method showed successful separation between the contribution from FF and WB during the bon fire events at April 30. Occasions of episodes with increased emissions from local sources and long range transportation of pollutants also showed a successful behaviour of the model.
- The overall uncertainty using this approach comprises several aspects where the most important are the choice of the Ångström exponent, α_{FF} and α_{WB}, together with the method used for determining mass absorption cross sections and the interpretation of enhanced absorbing properties in the UV-spectra by particles emitted by local traffic. Trying to determine the amount of these substances and how much they effect the source

apportionment is an important problem to solve to obtain a reliable source apportionment.

The trends in measured BC concentrations should reflect the trends in emissions from local road traffic at Hornsgatan. Since NOx and particle number concentration trends indicate a shifting relation, a possibility is that BC instead can be used as a good marker for combustion sources, especially for diesel exhaust, that has been classified as carcinogenic to humans.

- The particle number for exhaust particles at Hornsgatan showed a distribution shifted toward nucleation mode particles with a diameter around 25 nm, while the particle volume size distribution instead had coarse mode particles dominating (peak around 250 nm).
- Correlation between local BC particles and size reached a peak at about 80 nm (R = 0.66). The correlation with particles below 80 nm were lower and decreased drastically for particle sizes above 150 nm, indicating that most traffic related BC particles at Hornsgatan are in the size interval of 50-150 nm.
- Using the assumption of a mean density of 1.5 g/cm^3 for exhaust particles, 64 % of the total mass of exhaust particles in the size range 47-155 nm would be BC particles. Varying the density ± 0.3 g/cm^3 the BC amount would be 53 – 80 % in the BC size range 47 – 155 nm.
- The annual mean of EF's for BC using TRANSPHORM showed different values depending on how they were derived. TRANSPHORM absolute BC EF's increased between 2006 and 2011 with 30.2 % while measurements of local BC decreased with 65.7 %. For the whole period 2006 to 2014 the TRANSPHORM absolute BC EF decrease with 2.8 % while the ambient air concentration decreased with 71.3 %. For TRANSPHORM fraction BC EF's, based on the ratio BC/PM-exhaust, there was instead a decrease in the EF of 22.6 % between 2006 and 2011, which was more in line with the decreasing trend of measured BC concentration. The TRANSPHORM fraction BC EF decreased with 52.9 % for the whole period 2006 to 2014, once again showing a similar trend as local air measurements.
- Different comparisons pointed to an overestimation of the TRANSPHORM absolute BC EF's and the TRANSPHORM fraction BC EF's was found to be more correct to use.
- A NOx based BC EF, based on measurements of NOx and BC in ambient air together with HBEFA NOx EF, showed a decrease from 2006 to 2014 of 82.8 %, which was highly in line with the decrease of measured BC of 71.3 % in local ambient air.
- The CO_2 based BC EF was found to be substantially higher. This approach might have potential but it has to be further evaluated, especially by a longer time series for the determination of a more representative average value of the local BC/local CO_2 ratio.

The measurements of NOx concentration in ambient local air at Hornsgatan was found to decrease much less than expected from the calculated vehicle-km weighted HBEFA NOx EF, indicating that the EF for NOx is underestimated. The calculated NOx based BC EF might therefore also be uncertain since it is based on HBEFA NOx EF. However, the measured

concentration of NOx and BC in ambient local air indicates that BC is decreasing much faster than NOx, and more in line with both the NOx based BC EF and the TRANSPHORM fraction BC EF, than the TRANSPHORM absolute BC EF.

4.2 Recommendations for future studies

In order to propose effective mitigation strategies for BC emissions it is of importance to investigate geographical distributions and seasonal variations of BC emission sources. Source apportionment studies like this is a step on the way but still there are needs for further investigations and evaluations of different methods available for source apportionment calculations. Recommendations based on this study is to evaluate this model more properly by comparison with other methods and a side by side campaign with the newer model AE33. It would also be of interest to determine the variation in the site specific mass absorption cross section by a longer (or several) OC/EC campaign and to do parallel OC/EC measurements at Torkel and Hornsgatan (for the evaluation of using the same site specific mass absorption cross section). The ability of the model to separate BC from FF and WB can be further evaluated by episodes of known combustion of biomass (e.g. Russian wild fires) or by unique WB tracers like levoglucosan or potassium. The model also assumes the simplification of equal site specific mass absorption cross sections for FF and WB aerosols. To evaluate the effect of this for the source apportionment, it would be necessary to do OC/EC analyses in more closed environments (close to the source) where there are minimal mixing between BC particles from the different sources.

The work towards reliable BC EF's requires measures targeted on both the ability on making correct representations of the real-world vehicle fleet and fuels used, and development of measurements of emissions (direct or indirect). Since BC still is unregulated in exhaust emissions and ambient air it is not a priority to measure BC, resulting in unreliable EF's. The problem goes both ways; as long as BC is an unregulated pollutant the measurements will be few and a standard method for these measurements will not be established, leading to results that are difficult to use (due to different methods used making comparisons complicated) as a basis for implementation of limits and regulations.

5 Acknowledgments

I sincerely thank my supervisors Christer Johansson and Michael Norman for helping me gain knowledge and continue my work in the right direction during the time for this study. There has not been one moment where I have felt lack of support and commitment from Christer and Michael and I can truly recommend them in all forms of tutoring situations.

I will also thank all colleagues at SLB analys for helping me during my field work but also for teaching me and increasing my knowledge of air measurements and instruments used within this field. An extra thanks to Lars Burman helping me with several of the derived EF's and Hans Areskoug during the time for the OC/EC analysis.

Also thanks to Johan Martinsson, PhD Student at the Centre for Environmental and Climate research at Lund University, for helpful feedback and discussion in the beginning of the study.

6 References

Aethalometer handbook AE31, A.D.A. Hansen, Magee Scientific Company, Berkeley, California, USA, 2005.

Aethalometer Model AE33 User Manual, version 1.44, Magee Scientific, Aerosol d.o.o., Slovenia, 2014.

Andersson, A., Sheesley, R. J., Kruså, M., Johansson, C., and Gustafsson, Ö., 2011. ^{14}C-Based source assessment of soot aerosols in Stockholm and the Swedish EMEP-Aspvreten regional background site, Atm. Env., 45, 215 – 222.

Andreae, M. O. and Gelencsér, A., 2006. Black carbon or brown carbon? The nature of light absorbing carbonaceous aerosols, Atmospheric Chemistry and Physics, 6, p 3131-3148.

Areskoug, H., Johansson, C., Alesand, T., Hedberg, E., Ekengrena, T., Vesely, V., Wideqvist, U. and Hansson, H.-C., 2004. ITM-report 110: Concentrations and sources of PM10 and PM2.5 in Sweden, Institute of Applied Environmental Research, Stockholm University, Sweden.

Asmi, A., Wiedensohler, A., Laj, P., Fjaeraa, A.-M., Sellegri, K., Birmili, W., Weingartner, E., Baltensperger, U., Zdimal, V., Zikova, N., Putaud, J. P., Marinoni, A., Tunved, P., Hansson, H.-C., Fiebig, M., Kivekäs, N., Lihavainen, H., Asmi, E., Ulevicius, V., Aalto, P. P., Swietlicki, E., Kristensson, A., Mihalopoulos, N., Kalivitis, N., Kalapov, I., Kiss, G., de Leeuw, G., Henzing, B., Harrison, R. M., Beddows, D., O'Dowd, C., Jennings, S. G., Flentje, H., Weinhold, K., Meinhardt, F., Ries, L. and Kulmala, M., 2011. Number size distributions and seasonality of submicron particles in Europe 2008 – 2009. Atmospheric Chemistry and Physics, 11: 5505 – 5538.

Barregard, L., Sällsten, G., Gustafson, P., Andersson, L., Johansson, L., Basu, S. and Stigendal, L., 2006. Experimental Exposure to Wood-Smoke Particles in Healthy Humans: Effects on Markers of Inflammation, Coagulation, and Lipid Peroxidation. Inhal. Toxicol. 18;845 – 853.

Birch, M. E. and Cary, R. A., 1996. Elemental carbon-based method for monitoring occupational exposures to particulate diesel exhausted. Aerosol Science and Technology, 25(3) p 221 – 241.

Bond, T. C., 2001. Spectral dependence of visible light absorption by carbonaceous particles emitted from coal combustion. Geophys. Res. Lett. 28: 4075 – 4078.

Bond, T. C., Doherty, S. J., Fahey, D. W., Forster, P. M., Berntsen, T., DeAngelo, B. J., Flanner, M. G., Ghan, S., Kärcher, B., Koch, D., Kinne, S., Kondo, Y., Quinn, P. K., Sarofim, M. C., Schultz, M. G., Schulz, M., Venkataraman, C., Zhang, H., Zhang, S., Bellouin, N., Guttikunda, S. K., Hopke, P. K., Jacobson, M. Z., Kaiser, J. W., Klimont, Z., Lohmann, U., Schwarz, J. P., Shindell, D., Storelvmo, T., Warren, S. G. and Zender, C. S., 2013. Bounding the role of black carbon in the climate system: A scientific assessment, Journal of Geophysical Research Atmospheres, (118/11) 5380 – 5552.

Cavalli, F., Viana, M., Yttri, K. E., Genberg, J. and Putaud, J.-P., 2010. Toward a standardised thermal-optical protocol for measuring atmospheric organic and elemental carbon: the EUSAAR protocol. Atmospheric Measurment Techniques 3, p 79 – 89.

Chakrabarty, R. K., Moosmuller, H., Garro, M.A., Arnott, W. P., Walker, J. W., Susott, R. A., Babbitt, R. E., Wold C. E., Lincoln, E. N. and Hao, W. M., 2006. Emissions from the laboratory combustion of wildland fuels: Particle morphology and size. Journal of Geographic Research 111.

Chan, T. W., Huang, L., Leaitch, W. R., Sharma, S., Brook, J. R., Slowik, J. G., Abbatt, J. P. D., Brickell, P. C., Liggio, J., Li, S.-M. and Moosmüller, H., 2010. Observations of OM/OC and specific attenuation coefficients (SAC) in ambient fine PM at a rural site in central Ontario, Canada. Atmospheric Chemistry and Physics, 10, 2393 – 2411.

Day, D. E., Hand, J. L., Carrico, C. M., Engling, G., and Malm, W. C., 2006. Humidification factors from laboratory studies of fresh smoke from biomass fuels, Journal of Geophysical Research, 111, D22202.

EC, 2008, Directive 2008/50/EC of the European Parliament and of the Council of 21 May 2008 on ambient air quality and cleaner air for Europe (OJ L 152, 11.6.2008, p. 1 – 44) (http://eur-lex.europa.eu/LexUriServ.do?uri=OJ:L:2008:152:0001:0044:EN:PDF) accessed 14 October 2014.

EEA, 2013, EMEP/EEA emission inventory guidebook – 2009, EEA Technical report No 12/2013, European Environment Agency (http://www.eea.europa.eu/publications/emep-eea-guidebook-2013) accessed 14 April 2015.

EEA, 2013, European Environment Agency Technical report, No 18, Status of black carbon monitoring in ambient air in Europe, ISSN 1725 – 2237.

Eriksson, A., 2015. Physicochemical properties and atmospheric ageing of soot – Investigated through aerosol mass spectrometry, Doctoral Dissertation, the Faculty of Engineering, Lund University, Sweden.

Franco, V., Kousoulidou, M., Muntean, M., Ntziachristos, L., Hausberger, S. and Dilara, P., 2013. Road vehicle emission factors development: A review. Atmospheric Environment 70: 84 – 97.

Funasaka, K., Miyazaki, T., Kawaraya, T., Tsuruho, K. and Mizuno, T., 1998. Characteristics of particulates and gaseous pollutants in a highway tunnel, Environmental Pollution 102, 171 – 176.

Grahame, T. J., Klemm, R. and Schlesinger, R. B., 2014. Public health and components of particulate matter: The changing assessment of black carbon, Journal of the Air and Waste Management Association 64, 620 – 660.

Gramsch, E., Reyes, F., Oyola, P., Rubio, M. A., López, G., Pérez, P. and Martínez, R., 2014. Particle size distribution and its relationship to black carbon in two urban and one rural site in Santiago de Chile. Journal of the Air & Waste Management Association, 64(7): 785 – 796.

Hansen, A. D. A., Rosen, H., and Novakov, T., 1984. The aethalometer – An instrument for the real-time measurement of optical absorption by aerosol particles, Sci. Total Environ., 36, 191 – 196.

Herich, H., Hueglin, C., and Buchmann, B., 2011. A 2.5 year's source apportionment study of black carbon from wood burning and fossil fuel combustion at urban and rural sites in Switzerland, Atmos. Meas. Tech., 4, 1409 – 1420.

Horvath, H., Catalan, L. and Trier, A., 1997. A study of the aerosol of Santiago de Chile III: Light absorption measurements. Atmospheric Environment 31: 3737 – 3744.

Instruction Manual: Model 3010 Condensation Particle Counter, TSI Incorporated, St. Paul. MN, USA, 2002.

Jerret, M., Burnett, R. T., Ma, R. J., Pope, C. A., Krewski, D., Newbold, K. B., Thurston, G., Shi, Y. L., Finkelstein, N., Cale, E. E., and Thun M. J., 2005. Spatial analysis of air pollution and mortality in Los Angeles, Epidemiology, 16, 727 – 736.

Johansson, C., and Eneroth, K., 2007. Traffic Emissions, Socioeconomic valuation and Socioeconomic measures (TESS) part 1: Emissions and exposure of particles and NO_x in greater Stockholm, SLB analys, Stockholm Environment and Health Protection Administration.

Johansson, C. and Hansson, H. C., 2007. ITM-rapport 165: PM10 och sot i Sverige, Institutionen för tillämpad miljövetenskap, Stockholms Universitet; SLB analys, Miljöförvaltningen.

Jönsson, O., Andersson, C., Forsberg, B. and Johansson, C., 2013. Air pollution episodes in Stockholm regional background air due to sources in Europe and their effect on human population. Boreal Environ Res, 18: 280 – 302.

Kittelson, D., Watts, W. and Johnson, J., 2004. Nanoparticle emissions on Minnesota highways. Atmospheric Environment 38: 9 – 19.

Knutson, E. O. and Whitby, K. T., 1975. Aerosol classification by electric mobility: Apparatus, theory, and applications. Journal of Aerosol Science 6:443 – 451.

Kochbach, A., Li, Y., Yttri, K. E., Cassee, F. R., Schwarze, P. E., and Namork, E., 2006. Physicochemical characterisation of combustion particles from vehicle exhaust and residential wood smoke, Particle and Fibre Toxicology, 3:1.

Krecl, P., Ström, J. and Johansson, C., 2007. Carbon content of atmospheric aerosols in a residential area during the wood combustion season in Sweden. Atmospheric Environment 41, 6974 – 6985.

Kristensson, A., Rissler, J., Löndahl, J., Johansson, C. and Swietlicki, E., 2013. Size-resolved respiratory tract deposition of sub-micrometer aerosol particles in a residential area with wintertime wood combustion. Aerosol and Air Quality Research, 13: 24 – 35.

Lin, J. J. and Tai, H.-S., 2001. Concentrations and distributions of carbonaceous species in ambient particles in Kaohsiung City, Taiwan. Atmospheric Environment 35, 2627 – 2636.

Liousse, C., Cachier, C. and Jennings, S. G., 1993. Optical and thermal measurements of black carbon aerosol content in different environments: variations of the specific attenuation cross section, sigma (σ), Atmospheric Environment, 27A, p 1203 – 1211.

Na, K., Sawant, A. A., Song, C. and Cocker III, D. R., 2004. Primary and secondary carbonaceous in the atmosphere of Western Riverside County, California. Atmospheric Environment 38, 1345 – 1355.

Ning, Z., Chan, K. L., Wong, K. C., Westerdahl, D., Mocnik, G., Zhou, J. H. and Cheung, C. S., 2013. Black carbon mass size distributions of diesel exhaust and urban aerosols measured using differential mobility analyzer in tandem with Aethalometer. Atmospheric Environment 80: 31 – 40.

Pope, C. A., Burnett, R. T., Thun, M. J., Calle, E. E., Krewski, D., Ito, K., and Thurston, G. D., 2002. Lung cancer, cardiopulmonary mortality, and long-term exposure to fine particulate air pollution, J. Am. Med. Assoc., 287 (9), 1132 – 1141.

Ramanathan, V. and Carmichael, G., 2008. Global and regional climate changes due to black carbon. Nature Geoscience 1 (4): 221 – 227.

Sandradewi, J., Prévôt, A. S. H., Szidat, S., Perron, N., Alfarra, M. R., Lanz, V. A., Weingartner, E., and Baltensperger, U., 2008a. Using Aerosol Light Absorption Measurements for the Quantitative Determination of Wood Burning and Traffic Emission Contributions to Particulate Matter, Environ. Sci. Technol., 42, 3316 – 3323.

Sandradewi, J., Prévôt, A. S. H., Weingartner, E., Schmidhauser, R., Gysel, M., and Baltensperger, U., 2008b. A study of wood burning and traffic aerosols in an Alpine valley using a multi-wavelength Aethalometer, Atmospheric Environment, 42, 101 – 112.

Schnaiter, M., Linke, C., Möhler, O., Naumann, K.-H., Saafhoff, H., and Schöck, O. W., 2005. Absorption amplification of black carbon internally mixed with secondary organic aerosols, Journal of Geophysical Research, 110, D19204.

Schwarz , J. P., Gao, R. S., Spackman, J. R., Watts, L. A., Thomson, D. S., Fahey, D. W., Ryerson, T. B., Peischl, J., Holloway, J. S., Trainer, M., Frost, G. J., Baynard, T., Lack, D. A., de Gouw, J. A., Warneke, C. and Del Negro, L. A., 2008. Measurement of the mixing state, mass and optical size of individual black carbon particles in urban and biomass burning emissions. Geophysical Research Letters 35 (13).

Sehlstedt, M., Dove, R., Boman, C., Pagels, J., Swietlicki, E., Löndahl, J., Westerholm, R., Bosson, J., Rarath, S., Behndig, A. F., Pourazar, J., Sandström, T., Mudway, I. S. and Blomberg,

A., 2010. Antioxidant Airway Responses Following Experimental Exposure to Wood Smoke in Man. Part. Fibre Toxicol. 7:21.

SLB rapport 7:2010: Utsläpp och halter av kväveoxider och kvävedioxid på Hornsgatan. Analys av trafikmätningar under hösten 2009, Miljöförvaltningen, SLB-analys, 2010.

SLB årsrapport 2014: Luften i Stockholm År 2014, SLB-rapport 2:2015, Miljöförvaltningen, Stockholms Stad, 2015.

Standard Operating Procedures for thermal-optical analysis of atmospheric particulate organic and elemental carbon (SOP), EMEP Manual for OC/EC sampling and analysis. (http://www.nilu.no/projects/ccc/manual/) assessed 28 October 2014.

Targino, A. Krecl, P. and Johansson, C., 2012. Deterioration of air quality across Sweden due to transboundary agricultural burning emissions. Boreal Environ Res, 18: 19 – 36.

TRANSPHORM, 2013. Transport related Air Pollution and Health impacts – Integrated Methodologies for Assessing Particulate Matter, Deliverable D1.1.2: Methodology for the quantification of road transport PM-emissions, using emission factors or profiles.

Transport Analysis Vehicle Statistics: http://www.trafa.se/en/Statistics/Road-traffic/Vehicle-statistics/ (2005-2014) assessed 1 May 2015.

Turpin, B. J. and Huntzicker, J. J., 1995. Identification of secondary organic aerosol episodes and quantification of primary and secondary aerosol concentrations during SCAQS. Atmospheric Environment 29, p 3527 – 3544.

Törnqvist, H., Mills, N. L., Gonzalez, M., Miller, M. R., Robinson, S. D., Megson, I. L., MacNee, W., Donaldson, K., Soderberg, S., Newby, D. E., Sandstrom, T. and Blomberg, A., 2007. Persistent endothelial dysfunction in humans after diesel exhaust inhalation. American Journal of Respiratory and Critical Care Medicine 176(4): 395 – 400.

Wallén, A., 2011. Measuring Elemental Carbon in Occupational Environments, Doctoral Thesis in Applied Environmental Science, Stockholm University, Sweden.

Weingartner, E., Keller, C., Stahel, W. A., Burtscher, H. and Baltensperger, U., 1997. Aerosol emission in a road tunnel. Atmospheric environment 31, 451 – 462.

Weingartner, E., Saathof, H., Schnaiter, M., Streit, N., Bitnas, B., and Baltensperger, U., 2003. Absorption of light by soot particles: Determination of the absorption coefficient by means of Aethalometers, Journal of Aerosol Science, 34, 1445 – 1463.

Watson, J. G., Chow, J. C., and Chen, L.-W. A., 2005. Summary of Organic and Elemental Carbon/Black Carbon Analysis Methods and Intercomparisons, Aerosol and Air Quality Research, Vol. 5, No.1, 65 – 102.

WHO, 2012a, Health effects of black carbon, Joint WHO/UNECE Task Force on Health Aspects of Air Pollutants under UNECE's Long-Range Transboundary Air Pollution Convention (LRTAP), World Health Organization, Regional Office for Europe, Copenhagen

(http://www.unece.org/fileadmin/DAM/env/documents/2012/air/Health_Effects_of_Black_Carbon_report.pdf) accessed 28 September 2014.

WHO, 2012b, IARC: Diesel Engine Exhaust Carcinogenic (Press Release).

WHO, 2013, Review of evidence on health aspects of air pollution – REVIHAAP, Technical Report, World Health Organization, Regional Office for Europe, Copenhagen (http://www.euro.who.int/_data/assets/pdf_file/0004/193108/REVIHAAP-Final-technical-report.pdf) accessed 28 September 2014.

Wåhlin, P., Palmgren, F. and Van Dingenen, R., 2001. Experimental studies of ultrafine particles in streets and the relationship to traffic. Atmospheric Environment 35: 63 – 69.

Appendix

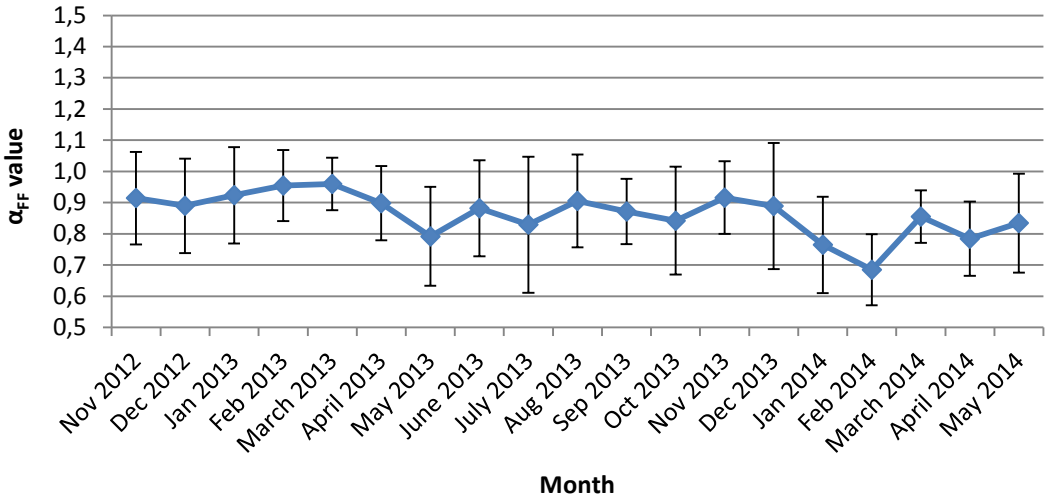

Fig. A1. *Time series of the monthly mean Ångström exponent α for the difference between Hornsgatan and Torkel (only traffic influence). Vertical lines indicate one standard deviation from the calculated mean values.*

Table T1. *Sensitivity analysis of α_{FF} (0.9 – 1.1) and α_{WB} (1.7 – 2.3) resulting in negative values of $b_{abs}(\lambda)_{FF}$ and $b_{abs}(\lambda)_{WB}$ from equation 9, at Hornsgatan and Torkel.*

		Hornsgatan		Torkel	
Ångström exponent		Negative values (%)			
α_{FF}	α_{WB}	$b_{abs}(\lambda)_{FF}$	$b_{abs}(\lambda)_{WB}$	$b_{abs}(\lambda)_{FF}$	$b_{abs}(\lambda)_{WB}$
0.9	1.7	8.0	5.3	2.3	4
0.9	1.8	8.0	5.1	2.3	3.5
0.9	1.9	8.0	4.9	2.3	3.2
0.9	2.0	8.0	4.8	2.3	3
0.9	2.1	8.0	4.7	2.3	2.8
0.9	2.2	8.0	4.6	2.3	2.7
0.9	2.3	8.0	4.5	2.3	2.7
1.0	1.7	27.7	5.2	5.1	4
1.0	1.8	27.7	5.0	5.1	3.4
1.0	1.9	27.7	4.9	5.1	3.2
1.0	2.0	27.7	4.8	5.1	3
1.0	2.1	27.7	4.7	5.1	2.8
1.0	2.2	27.7	4.6	5.1	2.7
1.0	2.3	27.7	4.5	5.1	2.7
1.1	1.7	60.4	5.2	12.6	4
1.1	1.8	60.4	5.0	12.6	3.4
1.1	1.9	60.4	4.9	12.6	3.1
1.1	2.0	60.4	4.8	12.6	3
1.1	2.1	60.4	4.7	12.6	2.8
1.1	2.2	60.4	4.6	12.6	2.7
1.1	2.3	60.4	4.5	12.6	2.7

Table T2. *OC/EC sampling at Torkel (mass concentration calculated using eq. 12). σ is an uncertainty given by the Thermal/Optical Carbon Aerosol Analyzer.*

Filter number	Sampling start (LT)	Sampling stop (LT)	OC (μg m^{-3})	σ	EC (μg m^{-3})	σ
1	2014-10-07 07:00	2014-10-07 19:00	4.95	0.33	1.08	0.14
2	2014-10-07 19:00	2014-10-08 07:00	5.61	0.36	1.02	0.13
3	2014-10-08 07:00	2014-10-08 19:00	2.54	0.21	0.63	0.12
4	2014-10-08 19:00	2014-10-09 07:00	1.73	0.17	0.25	0.10
5	2014-10-09 07:00	2014-10-09 19:00	3.99	0.28	0.93	0.13
6	2014-10-09 19:00	2014-10-10 07:00	2.55	0.21	0.39	0.10
7	2014-10-10 07:00	2014-10-10 19:00	3.03	0.23	0.51	0.11
8	2014-10-10 19:00	2014-10-11 07:00	1.61	0.16	0.21	0.10
9	2014-10-11 07:00	2014-10-11 19:00	2.54	0.21	0.36	0.10
10	2014-10-11 19:00	2014-10-12 07:00	3.72	0.27	0.59	0.11
11	2014-10-12 07:00	2014-10-12 19:00	1.79	0.17	0.35	0.10
12	2014-10-12 19:00	2014-10-13 07:00	1.50	0.16	0.26	0.10
13	2014-10-13 07:00	2014-10-13 19:00	2.25	0.20	0.30	0.10
14	2014-10-13 19:00	2014-10-14 07:00	2.20	0.19	0.42	0.10
No sampling between 2014-10-14 07:00 to 2014-10-17 07:00						
16	2014-10-17 07:00	2014-10-17 19:00	1.65	0.17	0.43	0.10
17	2014-10-17 19:00	2014-10-18 07:00	2.04	0.18	0.42	0.10
18	2014-10-18 07:00	2014-10-18 19:00	1.33	0.15	0.26	0.10
19	2014-10-18 19:00	2014-10-19 07:00	0.87	0.13	0.17	0.09
20	2014-10-19 07:00	2014-10-19 19:00	1.82	0.18	0.38	0.10
21	2014-10-19 19:00	2014-10-20 07:00	2.97	0.23	0.47	0.11
22	2014-10-20 07:00	2014-10-20 19:00	1.53	0.16	0.22	0.10
23	2014-10-20 19:00	2014-10-21 07:00	0.94	0.13	0.11	0.09
24	2014-10-21 07:00	2014-10-21 19:00	1.87	0.18	0.30	0.10
25	2014-10-21 19:00	2014-10-22 07:00	1.01	0.13	0.17	0.09
26	2014-10-22 07:00	2014-10-22 19:00	1.67	0.17	0.32	0.10
27	2014-10-22 19:00	2014-10-23 07:00	0.97	0.13	0.18	0.09
28	2014-10-23 07:00	2014-10-23 19:00	3.50	0.26	0.24	0.10
29	2014-10-23 19:00	2014-10-24 07:00	1.27	0.15	0.24	0.10
Mean day			2.46		0.50	
Mean night			2.07		0.35	
Mean			2.27		0.40	
75th percentile			2.86		0.46	
25th percentile			1.51		0.24	

Table T3. *Aerosol absorption coefficients, b_{abs} (λ) (Mm^{-1}), calculated using eq. 3, averaged into twelve-hour values to match the integrated OC and EC mass concentrations (M_{OC}, M_{EC}) obtained from the TOT analysis.*

Starting date and time	370 nm	470 nm	520 nm	590 nm	660 nm	880 nm	950 nm
141007 07:00	42.44	26.48	21.89	18.97	16.56	11.39	10.14
141007 19:00	45.44	27.96	22.95	19.77	17.16	11.55	10.21
141008 07:00	15.54	9.63	8.19	7.21	6.37	4.58	4.10
141008 19:00	13.31	7.28	6.12	5.35	4.68	3.29	2.93
141009 07:00	34.48	22.83	19.26	16.92	14.94	10.52	9.44
141009 19:00	18.05	10.44	8.73	7.62	6.71	4.72	4.25
141010 07:00	17.13	10.92	9.33	8.26	7.34	5.37	4.86
141010 19:00	11.99	6.35	5.36	4.67	4.08	2.90	2.58
141011 07:00	16.04	9.20	7.66	6.64	5.75	4.03	3.59
141011 19:00	34.95	18.22	14.45	12.18	10.51	7.02	6.24
141012 07:00	19.06	10.83	8.93	7.72	6.73	4.63	4.14
141012 19:00	9.43	5.22	4.47	3.95	3.50	2.53	2.28
141013 07:00	16.44	9.45	7.98	7.00	6.14	4.40	3.94
141013 19:00	28.57	16.78	13.83	11.93	10.34	7.17	6.38
141017 07:00	18.35	11.63	9.70	8.50	7.54	5.28	4.75
141017 19:00	23.22	12.44	10.15	8.70	7.57	5.12	4.56
141018 07:00	14.12	7.51	6.17	5.31	4.61	3.18	2.84
141018 19:00	9.29	3.59	3.07	2.70	2.37	1.70	1.52
141019 07:00	18.70	10.66	9.00	7.86	6.80	4.80	4.24
141019 19:00	15.59	10.65	8.97	7.83	6.77	4.80	4.25
141020 07:00	16.98	9.63	8.27	7.29	6.36	4.73	4.28
141020 19:00	6.55	2.82	2.37	2.05	1.77	1.26	1.13
141021 07:00	15.67	10.35	8.72	7.63	6.64	4.80	4.30
141021 19:00	4.64	3.65	3.06	2.65	2.26	1.57	1.39
141022 07:00	16.03	10.75	9.09	8.02	7.16	5.14	4.67
141022 19:00	8.60	4.51	3.73	3.21	2.81	1.92	1.72
141023 07:00	11.44	6.54	5.42	4.72	4.16	2.91	2.64
141023 19:00	9.52	5.41	4.40	3.77	3.28	2.21	1.97

Table T4. *Site specific mass absorption cross sections (MAC) σ_{abs} (λ) (m^2 g^{-1}), calculated using eq. 13.*

Starting date and time	370 nm	470 nm	520 nm	590 nm	660 nm	880 nm	950 nm
141007 07:00	39.1	24.4	20.2	17.5	15.3	10.5	9.3
141007 19:00	44.6	27.5	22.6	19.4	16.9	11.3	10.0
141008 07:00	24.5	15.2	12.9	11.4	10.0	7.2	6.5
141008 19:00	53.2	29.1	24.4	21.4	18.7	13.2	11.7
141009 07:00	37.1	24.5	20.7	18.2	16.1	11.3	10.1
141009 19:00	46.0	26.6	22.3	19.4	17.1	12.0	10.8
141010 07:00	33.4	21.3	18.2	16.1	14.3	10.5	9.5
141010 19:00	56.4	29.9	25.2	22.0	19.2	13.6	12.1
141011 07:00	44.7	25.7	21.3	18.5	16.0	11.2	10.0
141011 19:00	59.0	30.8	24.4	20.6	17.7	11.8	10.5
141012 07:00	54.4	30.9	25.5	22.0	19.2	13.2	11.8
141012 19:00	35.9	19.9	17.0	15.0	13.3	9.6	8.7
141013 07:00	54.0	31.0	26.2	23.0	20.2	14.4	12.9
141013 19:00	67.8	39.8	32.8	28.3	24.5	17.0	15.1
141017 07:00	42.7	27.1	22.6	19.8	17.6	12.3	11.0
141017 19:00	55.1	29.5	24.1	20.6	18.0	12.1	10.8
141018 07:00	54.6	29.0	23.9	20.5	17.8	12.3	11.0
141018 19:00	54.3	21.0	18.0	15.8	13.9	9.9	8.9
141019 07:00	49.8	28.4	24.0	20.9	18.1	12.8	11.3
141019 19:00	33.1	22.6	19.0	16.6	14.4	10.2	9.0
141020 07:00	76.8	43.5	37.4	33.0	28.8	21.4	19.3
141020 19:00	60.4	26.0	21.9	18.9	16.3	11.6	10.4
141021 07:00	51.5	34.0	28.6	25.1	21.8	15.8	14.1
141021 19:00	27.8	21.9	18.4	15.9	13.6	9.4	8.3
141022 07:00	49.9	33.5	28.3	25.0	22.3	16.0	14.5
141022 19:00	49.1	25.8	21.3	18.3	16.0	11.0	9.8
141023 07:00	48.1	27.5	22.8	19.8	17.5	12.3	11.1
141023 19:00	39.3	22.4	18.2	15.6	13.5	9.1	8.1
Mean	48.0	27.4	22.9	20.0	17.4	12.3	11.0
75th percentile	54.5	30.5	25.0	21.8	19.1	13.2	11.8
25th percentile	39.2	23.1	19.3	16.8	14.6	10.5	9.4

Table T5. *12-h integrated PM_{10} and $PM_{2.5}$ mass concentrations measured during the same period as the OC/EC campaign.*

Starting date and time	PM_{10} ($\mu g\ m^{-3}$)	$PM_{2.5}$ ($\mu g\ m^{-3}$)
141007 07:00	24.99	8.40
141007 19:00	28.01	24.77
141008 07:00	8.42	7.06
141008 19:00	11.03	9.37
141009 07:00	22.86	20.94
141009 19:00	14.16	11.87
141010 07:00	16.48	13.29
141010 19:00	12.75	10.81
141011 07:00	12.77	10.46
141011 19:00	16.44	14.05
141012 07:00	14.79	13.51
141012 19:00	4.85	4.34
141013 07:00	6.57	4.92
141013 19:00	9.31	7.31
141017 07:00	7.66	5.42
141017 19:00	8.29	6.87
141018 07:00	5.80	4.84
141018 19:00	3.96	3.75
141019 07:00	9.47	7.82
141019 19:00	12.46	10.19
141020 07:00	5.57	4.36
141020 19:00	2.09	1.79
141021 07:00	4.52	3.44
141021 19:00	3.59	3.37
141022 07:00	9.70	7.03
141022 19:00	5.16	4.49
141023 07:00	6.63	4.94
141023 19:00	6.62	5.66
Mean day	11.16	8.31
Mean night	9.91	8.47
Mean	10,53	8,39
75th percentile	13.82	10.72
25th percentile	5.63	4.58

Fig. A2 & A3. *Low-volume sampler Comde – Derenda (type PNS 16T-3.1, Germany).*
Fig. A4. *PM_{10} inlet.*
Fig. A5. *PM_{10} inlet treated with gel on the inside to prevent particles >10 µm to reach the sampling filters.*

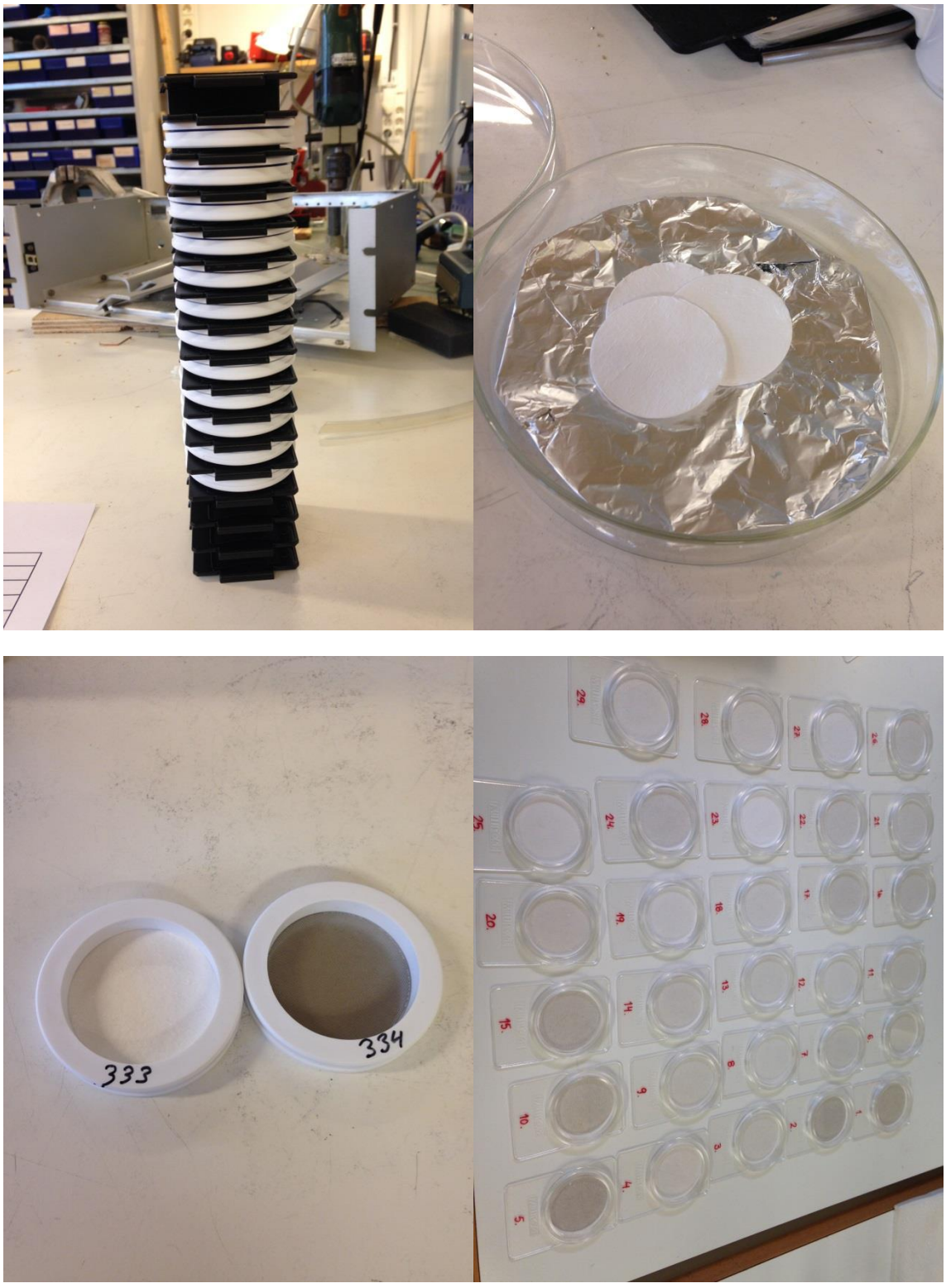

Fig. A6. *Filter holders placed in a magazine that could store 16 filter holders in total.*
Fig. A7. *Clean quartz fiber filters (T293, 47mm, Pall Corporation).*
Fig. A8. *Filter holders, 333 holding a clean filter, 334 empty.*
Fig. A9. *Loaded filters stored during analysis.*

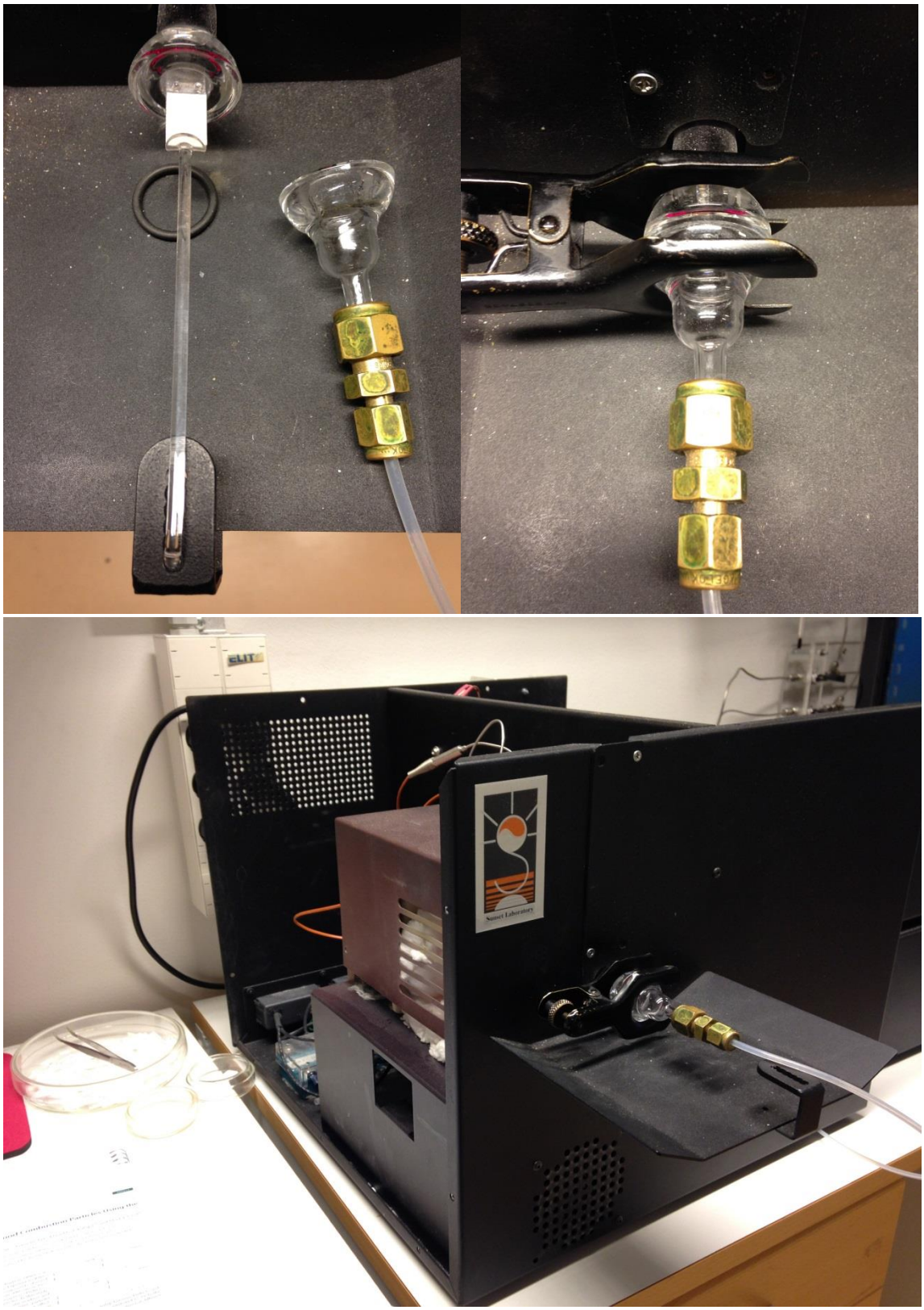

Fig. A10. *Analysis of 1.5 cm^2 punches of the loaded filters.*
Fig. A11. *Closing the opening before analysis starts.*
Fig. A12. *Thermal/Optical Carbon Aerosol Analyzer (Sunset Laboratory Inc., Forest Grove, USA).*

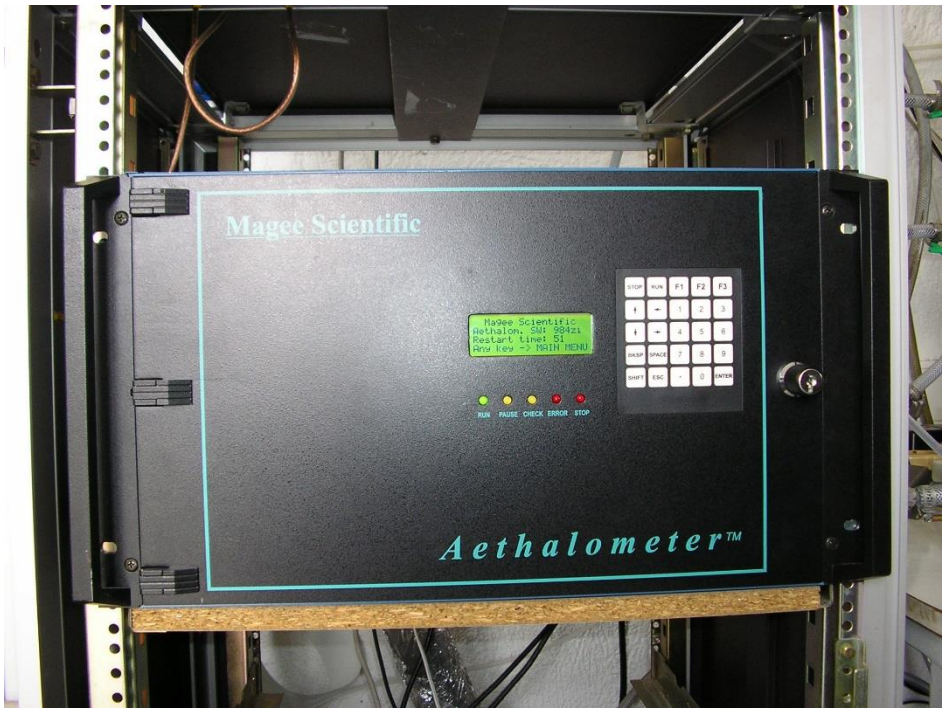

Fig. A13. *Aethalometer AE31, Magee Scientific, Berkeley, California, USA.*

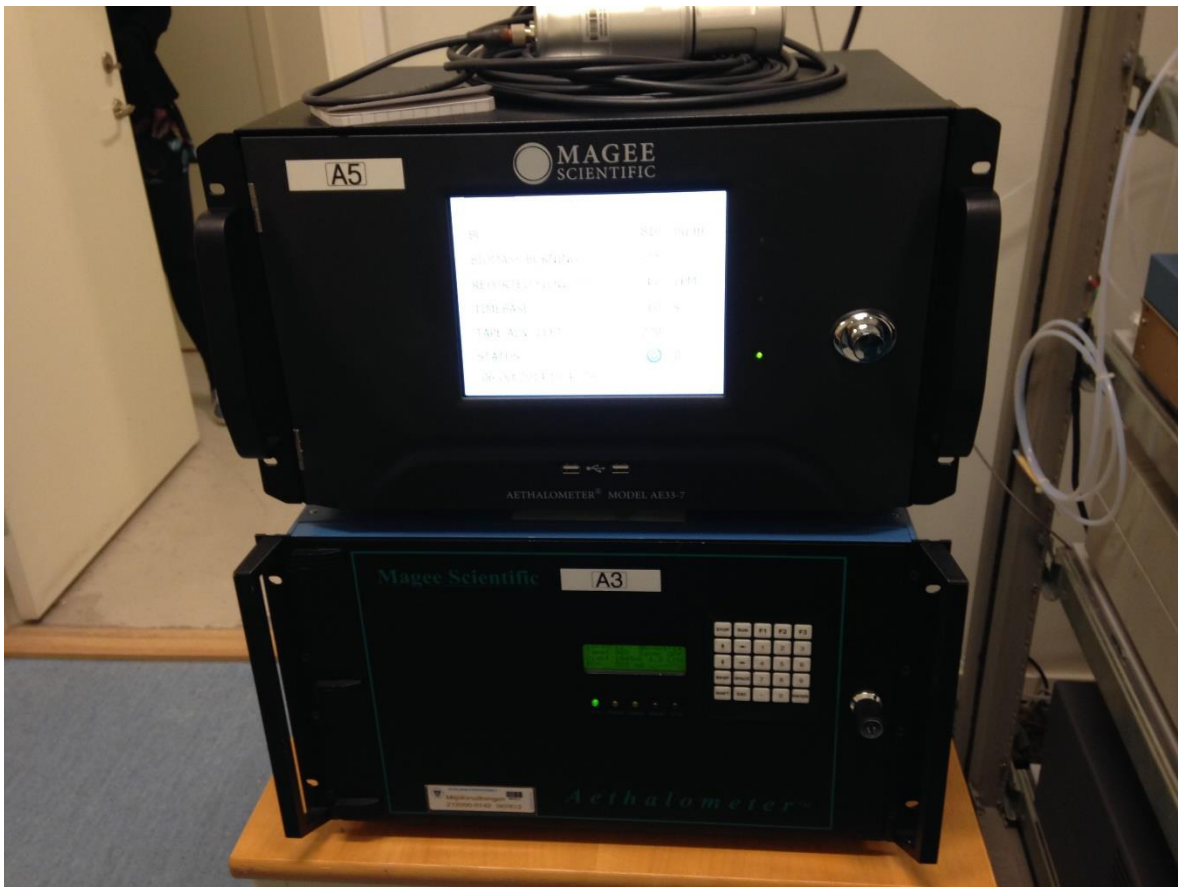

Fig. A14. *Aethalometer AE33, Magee Scientific, Slovenia (standing on the top of an AE31).*

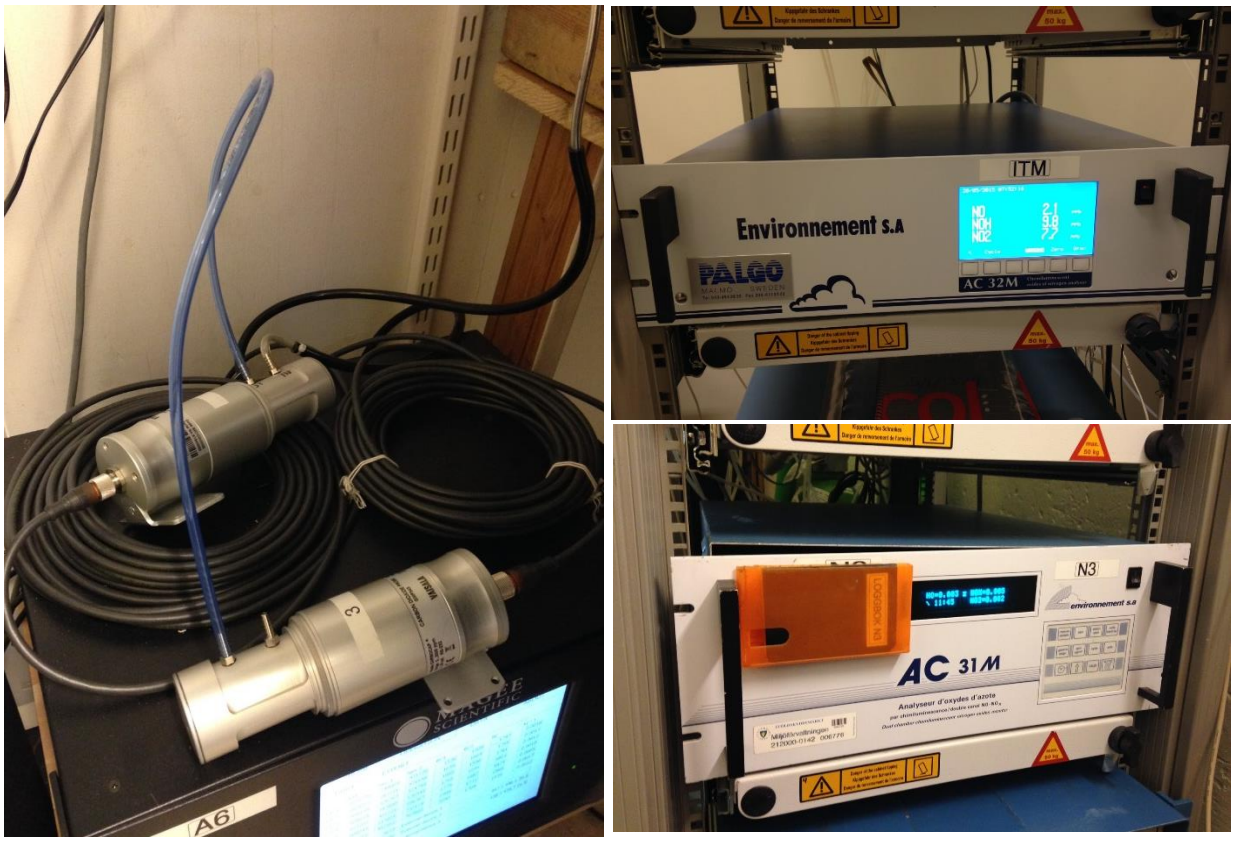

Fig. A15. *Carbon Dioxide Probe (linked to an AE33), model GMP343, Vaisala CARBOCAP, Helsinki, Finland.*

Fig. A16. *Chemiluminescence analyser measuring NOx at Torkel, model AC 32 M, Environment S.A, France.*

Fig. A17. *Chemiluminescence analyser measuring NOx at Hornsgatan, model AC 31 M, Environment S.A, France.*

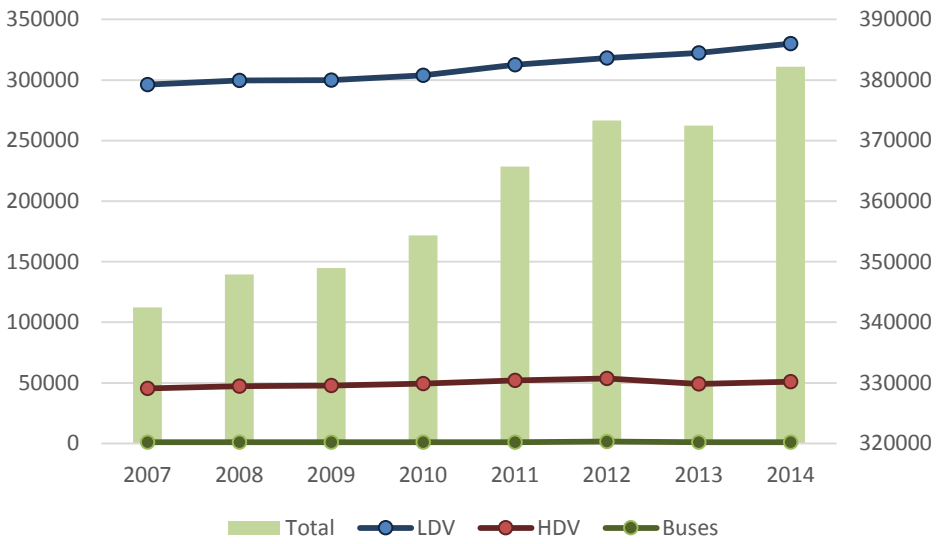

Fig. A18. *Total vehicle fleet number in inner Stockholm (vehicles registered in the Swedish Road Traffic Registry) from 2007 to 2014. The total number of vehicles is on the right axis and the vehicle types (LDV, HDV and buses) are on the left axis.*

Table T6. *Monthly mean BC mass concentrations (total, from biomass burning and from fossil fuel combustion) at Torkel. The percentage of WB and FF of total BC are also displayed.*

Time	Total (µg/m³)	WB (µg/m³)	FF (µg/m³)	WB (%)	FF (%)
Nov 2012	0.53	0.17	0.35	32.6	67.4
Dec 2012	0.67	0.24	0.44	35.1	64.9
Jan 2013	0.57	0.21	0.35	37.7	62.3
Feb 2013	0.56	0.20	0.36	36.2	63.8
Mars 2013	0.46	0.17	0.29	36.5	63.5
April 2013	0.44	0.16	0.28	36.9	63.1
May 2013	0.50	0.15	0.35	29.1	70.9
June 2013	0.37	0.09	0.27	25.3	74.7
July 2013	0.49	0.12	0.36	25.2	74.8
Aug 2013	0.50	0.13	0.38	25.0	75.0
Sep 2013	0.51	0.14	0.37	27.0	73.0
Oct 2013	0.56	0.19	0.36	34.9	65.1
Nov 2013	0.44	0.14	0.30	31.4	68.6
Dec 2013	0.47	0.18	0.29	38.4	61.6
Jan 2014	0.53	0.21	0.32	39.3	60.7
Feb 2014	1.03	0.46	0.57	44.4	55.6
Mars 2014	0.51	0.18	0.33	35.6	64.4
April 2014	0.42	0.16	0.26	37.3	62.7
May 2014	0.34	0.11	0.23	31.5	68.5
Winter (DJF)	0.64 ± 0.02	0.25	0.39	39 ± 6	61 ± 6
Summer (JJA)	0.45 ± 0.01	0.11	0.34	25 ± 5	75 ± 5
Total	0.52 ± 0.01	0.18	0.34	34 ± 6	66 ± 6

Table T7. *Monthly mean BC mass concentrations (total, from biomass burning and from fossil fuel combustion) at Hornsgatan. The percentage of WB and FF of total BC are also displayed.*

Time	Total (µg/m³)	WB (µg/m³)	FF (µg/m³)	WB (%)	FF (%)
Nov 2012	1.53	0.25	1.28	16.1	83.9
Dec 2012	1.57	0.29	1.28	18.4	81.6
Jan 2013	1.49	0.29	1.20	19.4	80.6
Feb 2013	1.56	0.29	1.27	18.4	81.6
Mars 2013	1.57	0.26	1.31	16.3	83.7
April 2013	1.42	0.22	1.20	15.6	84.4
May 2013	1.52	0.17	1.35	11.2	88.8
June 2013	1.49	0.16	1.33	11.0	89.0
July 2013	1.46	0.15	1.31	10.4	89.6
Aug 2013	1.68	0.18	1.50	11.0	89.0
Sep 2013	1.74	0.20	1.54	11.6	88.4
Oct 2013	1.62	0.25	1.37	15.3	84.7
Nov 2013	1.33	0.19	1.14	14.6	85.4
Dec 2013	1.01	0.20	0.81	19.7	80.3
Jan 2014	1.08	0.21	0.87	19.6	80.4
Feb 2014	1.55	0.41	1.14	26.3	73.7
Mars 2014	1.11	0.22	0.89	19.6	80.4
April 2014	1.25	0.20	1.05	15.7	84.3
May 2014	1.30	0.17	1.13	13.2	86.8
Winter (DJF)	1.38 ± 0.04	0.28	1.10	20 ± 6	80 ± 6
Summer (JJA)	1.54 ± 0.08	0.17	1.38	11 ± 7	89 ± 7
Total	1.44 ± 0.05	0.23	1.21	16 ± 6	84 ± 6

Table T8. *Sensitivity analysis of BC mass concentration from biomass burning and fossil fuel combustion (%) at Torkel, changing α_{WB} and α_{FF} ± 0.2 and ± 0.1, respectively.*

α_{FF}	α_{WB}	FF (%)	WB (%)	FF winter (%)	WB winter (%)	FF summer (%)	WB summer (%)
0.8	2.0	62	38	57	43	70	30
0.9	2.0	66	34	61	39	75	25
1.0	2.0	72	28	67	33	80	20
0.9	1.8	61	39	55	45	71	29
0.9	1.9	64	36	59	41	73	27
0.9	2.1	68	32	64	36	76	24
0.9	2.2	70	30	66	34	78	22

Table T9. *Sensitivity analysis of BC mass concentration from biomass burning and fossil fuel combustion (%) at Hornsgatan, changing α_{WB} and α_{FF} ± 0.2 and ± 0.1, respectively.*

α_{FF}	α_{WB}	FF (%)	WB (%)	FF winter (%)	WB winter (%)	FF summer (%)	WB summer (%)
0.8	2.0	78	22	74	26	82	18
0.9	2.0	84	16	80	20	89	11
1.0	2.0	90	10	86	14	95	5
0.9	1.8	80	20	76	24	88	12
0.9	1.9	83	17	78	22	88	12
0.9	2.1	85	15	81	19	90	10
0.9	2.2	86	14	82	18	90	10

Table T10. *Mass concentrations of $PM_{2.5}$, total BC, BC_{FF} and BC_{WB} ($\mu g\ m^{-3}$) and percentage of $PM_{2.5}$ at Hornsgatan.*

	PM2.5 ($\mu g\ m^{-3}$)	BC ($\mu g\ m^{-3}$)	BC_{FF} ($\mu g\ m^{-3}$)	BC_{WB} ($\mu g\ m^{-3}$)	BC (% of $PM_{2.5}$)	BC_{FF} (% of $PM_{2.5}$)	BC_{WB} (% of $PM_{2.5}$)
Whole week: Mon-Sun							
Mean	10.83	1.32	1.06	0.23	14.56	12.18	2.38
75th perc.	13.32	1.78	1.44	0.30	18.98	16.26	3.05
25th perc.	5.69	0.61	0.45	0.11	6.65	5.01	1.35
Working days: Mon-Thu							
Mean	10.70	1.47	1.20	0.24	16.12	13.64	2.48
75th perc.	12.97	2.04	1.70	0.31	21.65	18.64	3.20
25th perc.	5.67	0.66	0.48	0.12	7.20	5.55	1.42
Weekend: Sat-Sun							
Mean	10.39	0.95	0.71	0.21	10.36	8.24	2.11
75th perc.	12.57	1.21	0.92	0.27	12.75	10.39	2.62
25th perc.	6.22	0.62	0.45	0.11	6.26	4.64	1.38
Daytime: Mon-Thus 06-18							
Mean	11.58	1.93	1.64	0.28	20.76	17.91	2.86
75th perc.	14.14	2.52	2.17	0.36	28.17	24.49	3.74
25th perc.	6.36	1.17	0.95	0.16	10.67	8.97	1.63
Winter: DJF							
Mean	11.63	1.26	0.96	0.28	12.98	10.40	2.59
75th perc.	13.28	1.72	1.32	0.37	17.08	14.03	3.27
25th perc.	5.95	0.54	0.38	0.13	5.89	4.06	1.63

Table T11. *Mass concentrations of $PM_{2.5}$, total BC, BC_{FF} and BC_{WB} ($\mu g\ m^{-3}$) and percentage of $PM_{2.5}$ at Torkel.*

	PM2.5 ($\mu g\ m^{-3}$)	BC ($\mu g\ m^{-3}$)	BC_{FF} ($\mu g\ m^{-3}$)	BC_{WB} ($\mu g\ m^{-3}$)	BC (% of $PM_{2.5}$)	BC_{FF} (% of $PM_{2.5}$)	BC_{WB} (% of $PM_{2.5}$)
Whole week: Mon-Sun							
Mean	5.91	0.49	0.31	0.18	13.16	8.44	4.73
75th perc.	7.45	0.60	0.39	0.22	14.92	9.49	5.52
25th perc.	2.16	0.22	0.14	0.07	5.51	3.36	1.88
Working days: Mon-Thu							
Mean	5.80	0.50	0.32	0.18	13.86	9.14	4.71
75th perc.	7.21	0.62	0.40	0.22	15.86	10.30	5.52
25th perc.	2.15	0.23	0.15	0.07	5.71	3.53	1.91
Weekend: Sat-Sun							
Mean	5.26	0.44	0.25	0.19	12.36	7.24	5.12
75th perc.	6.89	0.56	0.33	0.24	14.93	8.27	6.46
25th perc.	2.04	0.23	0.13	0.08	5.66	3.38	2.02
Daytime: Mon-Thus 06-18							
Mean	6.92	0.74	0.55	0.20	16.39	11.81	4.58
75th perc.	9.13	0.90	0.63	0.26	19.73	14.81	5.37
25th perc.	2.53	0.31	0.21	0.09	7.15	4.57	1.90
Winter: DJF							
Mean	7.04	0.59	0.34	0.25	14.55	8.87	5.69
75th perc.	7.94	0.75	0.45	0.30	16.38	9.98	6.65
25th perc.	2.10	0.25	0.15	0.09	6.67	3.66	2.67

Table T12. *Median local BC and local NOx mass concentrations ($\mu g\ m^{-3}$), with values for 25th and 75th percentile together with the local BC/local NOx ratio for the time period 2006 to 2014, used for calculations of BC EF's using approach 3.*

	local BC ($\mu g\ m^{-3}$)	25th perc. ($\mu g\ m^{-3}$)	75th perc. ($\mu g\ m^{-3}$)	local NOx ($\mu g\ m^{-3}$)	25th perc. ($\mu g\ m^{-3}$)	75th perc. ($\mu g\ m^{-3}$)	local BC/ local NOx
2006	4.29	2.83	6.06	115.53	51.81	180.89	0.040
2007	3.94	2.11	6.42	164.81	77.88	251.16	0.026
2008	2.59	1.50	4.15	148.35	75.54	228.66	0.019
2009	3.16	1.57	4.92	152.27	81.95	223.61	0.022
2010	2.60	1.33	4.00	151.21	81.25	220.22	0.018
2011	1.47	0.75	2.58	153.29	95.41	221.62	0.010
2012	1.26	0.68	1.91	131.71	57.15	202.45	0.011
2013	1.48	0.86	2.16	161.14	91.88	236.82	0.009
2014	1.23	0.63	1.86	145.51	62.24	221.07	0.009

Table T13. *Data for Hornsgatan, from the latest emission database (EDB) in the Airviro system, used to calculate a vehicle-km weighted EF for CO_2 in 2015.*

Vehicle type	Emissions CO_2 (ton/year)	Vehicle km's (million km/year)	EF CO_2 (g/km)
Bus diesel	131.95	0.10	1268.78
Bus ethanol	60.33	0.05	1160.13
Bus biogas	52.14	0.04	1337.03
LDV diesel	694.75	3.41	203.92
LDV ethanol	268.07	0.78	345.90
LDV biogas	43.43	0.25	175.14
LDV gasoline	1479.17	5.79	255.47
LDT diesel	342.80	1.53	224.79
LDT gasoline	61.43	0.27	230.07
HDT diesel	673.23	0.52	1289.71

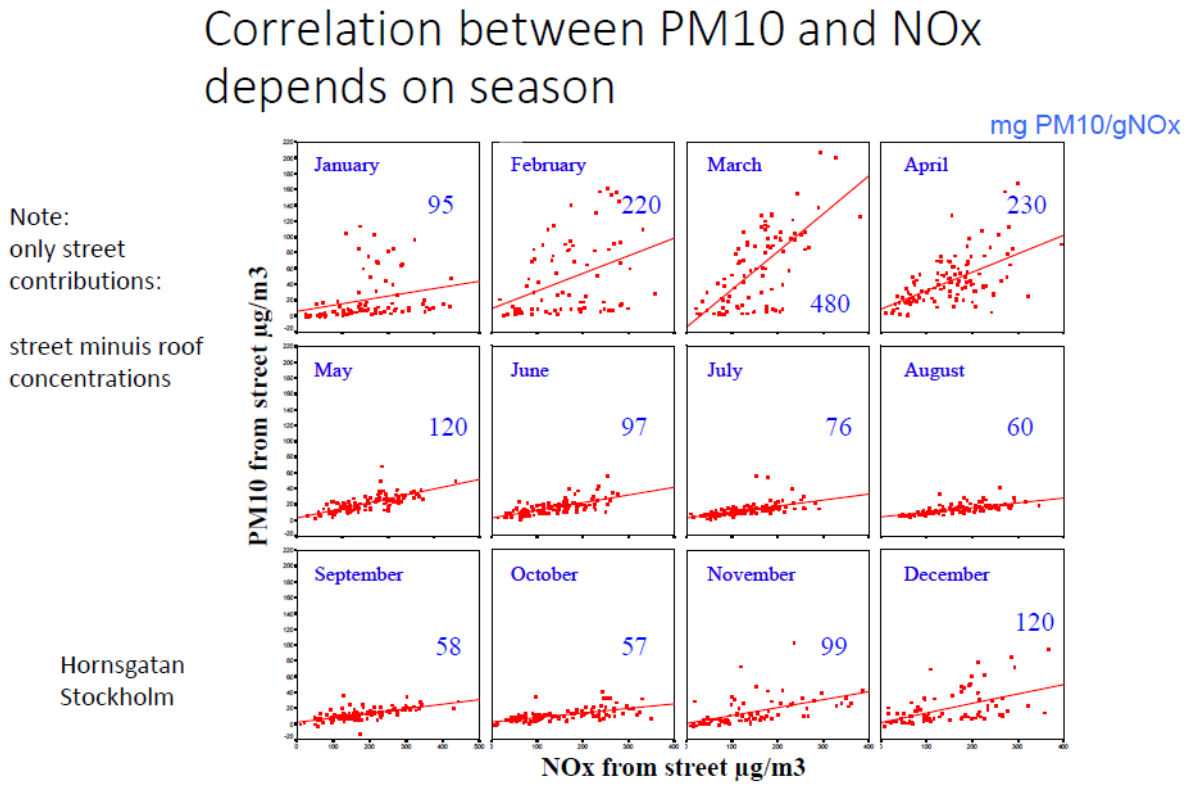

Fig. A19. *Linear correlation between NOx and PM_{10} showing the seasonal variation at Hornsgatan.*